WIND TUNNEL EXPERIMENTS ON A MODEL AUTOGYRO AT SMALL ANGLES OF INCIDENCE.

By C. N. H. Lock, M.A., and H. C. H. Townend, B.Sc.

Reports and Memoranda No. 1154.
(Ae. 319.)
March, 1928.

Summary.—Introductory.—A wooden scale model, 6 feet in diameter, of the original 4-bladed rotating wing unit of the Cierva Autogyro, has been tested in the Duplex tunnel at blade angles of 0°, 1°, 1·8°, 2·3° and 3°. It has also been tested as a 2-blader at a blade angle of 1·8°. The extreme range of incidence was from 2° to 20° and of rotational speed from 3 to 12 revolutions per second. It was found that the model would not rotate at all at a blade angle of 4° while at 3° blade angle it would only rotate at angles of incidence above 12°. In order to supplement the measurement of forces and rotational speed at zero torque, observations of forces and angular accelerations were made over a more limited range at varying rotational speed, by means of a chronograph and stroboscope. These observations were interpreted as giving the forces and torque in steady motion when the torque was not zero. Observations were also made of the angular motion of the blades in flapping about their hinges.

Results.—The greatest value of lift/drag ratio was observed on the screw with blade angle 1·8° at an incidence of 3°; this value, subject to considerable uncertainty on account of the large correction for drag of the boss, was 7·5 for the 4-blader and 8·0 for the 2-blader at 4° incidence. The scale effect was appreciable on lift coefficient at all angles of incidence but on other coefficients it was small except at the smallest incidence. The comparison between 2- and 4-blader was in good agreement with the simple Prandtl theory of interference given in R. & M. 1111, so that the results should apply to an autogyro of any intermediate solidity. The torque curves derived from the observations of angular acceleration confirm the remaining observations in showing that the results vary critically with change of blade angle. The observed flapping motion is in good qualitative agreement with theory, the second and higher harmonics being negligible on account of the high density of the model blades.

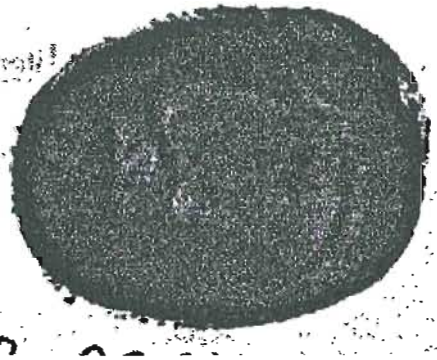

CONTENTS.

LIST OF SYMBOLS.

θ = Angle of pitch.

c = Chord of blades.

R = Radius of autogyro.

σ = Ratio of blade area to disc area (solidity ratio).

σ_4 = Solidity ratio for standard 4-blader.

V = Forward speed, feet per second.

Ω = Rotational speed in radians per sec.

n = Rotational speed in revolutions per sec.

i = Angle of incidence of Autogyro.

$\mu = \dfrac{V \cos i}{R\Omega}$

ψ = Angular position of blade in azimuth, measured from downwind position in an anti-clockwise direction looking downwards.

β = Angular displacement of blade about hinge, reckoned positive when measured upwards.

L = Lift.

D = Drag.

T = Thrust.

Y = Lateral force, reckoned positive when measured to starboard (i.e., towards blade moving upstream).

Q = Torque.

$L_V = L/\pi \rho R^2 V^2$.

$L_\Omega = L/\pi \rho R^4 \Omega^2$.

$Q_\Omega = Q/\pi \rho R^5 \Omega^2$.

$\left(\dfrac{D}{L}\right)' = \dfrac{D}{L} + \dfrac{Q\Omega}{LV}$

a_0, a_1, b_1, &c. = Coefficients in Fourier expansion of flapping angle β.

$\beta = a_0 - a_1 \cos \psi - b_1 \sin \psi$.

b_1 is positive when port wing is raised.

(33064) Wt. 51/6007/1607 375 11/28 Harrow G. 7/1

Foreword.—In view of the length of the present report it may be mentioned that more than half the text is occupied with description of the apparatus and methods of observation, the length of this part of the report being due to the novelty of many of the experimental methods required. For the benefit of those who wish to take the experimental methods as read, the following list is inserted of those sections of the report which deal with results :—§§ 1.0, 2.0, 3.3 to 3.43, 4.0, 4.4 to 4.42, 5.1 to end. Of the purely experimental part of the report, the method of obtaining rate of change of velocity from stroboscope observations described in 4·1 and of deducing the lift, drag and torque on the model may be of some general interest.

1.0. *Introduction.*—The Cierva autogyro is a windmill of low pitch whose plane is inclined at a small angle to the relative wind ; this windmill takes the place of the wing system of an ordinary aeroplane. Photographs of a scale model of 6 ft. diameter arranged for test in the Duplex wind tunnel are given in Figs. 1 and 2 ; the windmill rotates on a ball bearing A, Fig. 2, and each blade is hinged on a ball bearing B, Fig. 3, whose axis lies in the plane of rotation so that the blades are free to flap in a direction normal to this plane. In flight the windmill rotates freely under the influence of the relative wind caused by the forward or downward motion of the machine, while the blades are prevented from departing far from the plane of rotation by centrifugal force, but execute a slight flapping oscillation relative to the plane of rotation under the influence of the unsymmetrical aerodynamic forces.

When the first reports of the autogyro appeared in this country (in 1925) the only experimental data available on a screw of low pitch were those contained in R. & M. 885, " Some experiments on airscrews at zero torque " and in R. & M. 1014, " An extension of the Vortex Theory of Airscrews : Applications to airscrews of low pitch with experimental results." The experiments in these reports related to a two-bladed screw of 3 ft. diameter with its plane of rotation normal to the wind direction.

A few preliminary experiments were undertaken on this screw with its axis inclined to the wind, and it was found possible to apply the results to the autogyro with the aid of strip theory calculations. This screw failed, however, to give a reasonably high maximum lift/drag ; chiefly because it rotated with difficulty at angles of incidence below 20° and would not rotate at all below 10°. At this angle the lift/drag must be less than cotangent 10° or 5·5.

At the time it was supposed that the failure of this model to reproduce the high efficiency claimed for the Autogyro was due to differences in design, particularly in the following respects :—(*a*) freedom of the blades to flap, (*b*) difference between two and four blades, (*c*) difference of blade section. In the light of subsequent

[*To face page* 4.

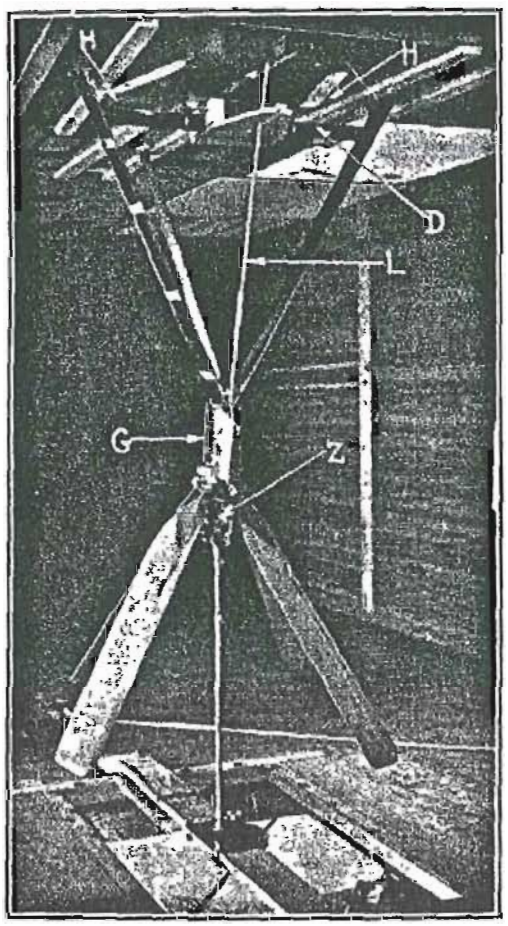

FIG. 1.

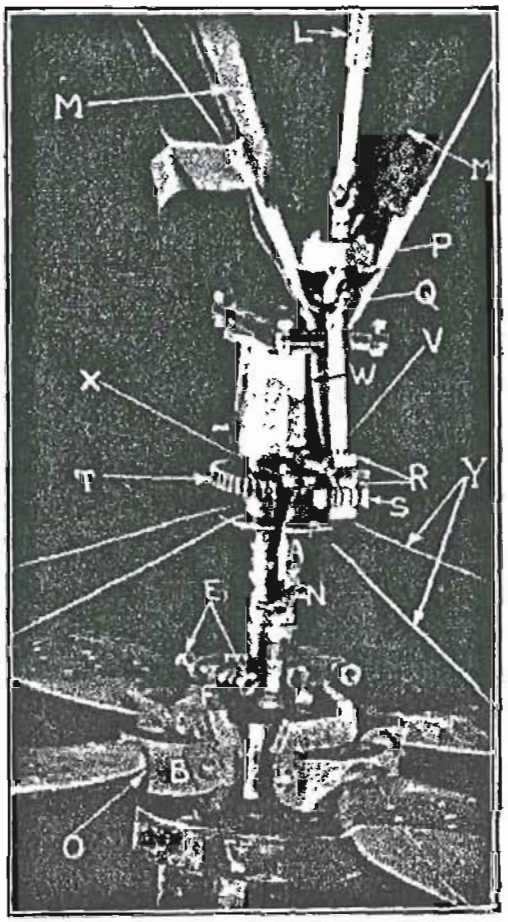

FIG. 3.

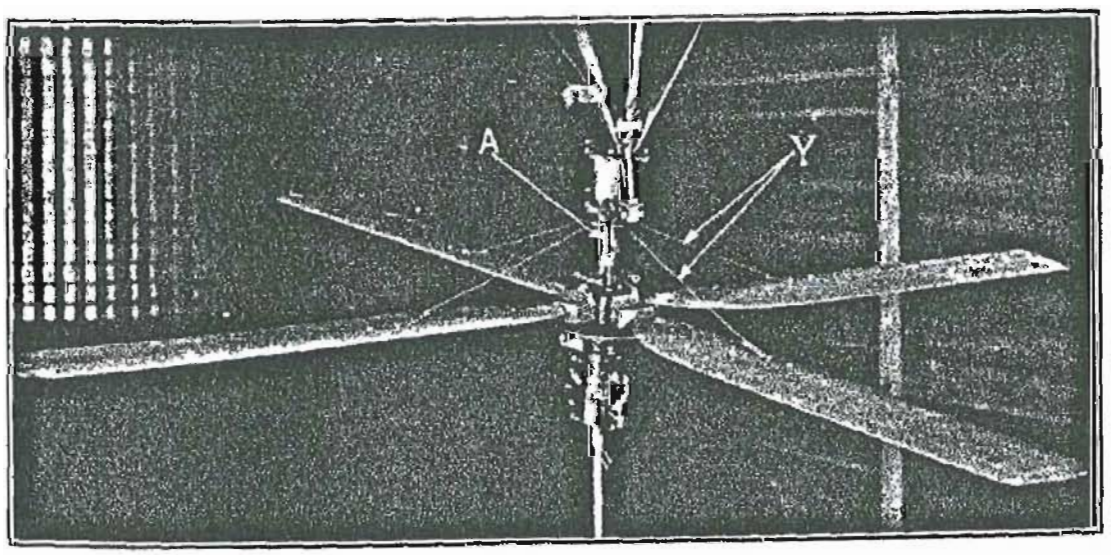

FIG. 2.

Photographs of 6 ft. diameter Model Autogyro in the Duplex Tunnel.

experiments, however, which suggest that the L/D of this screw should have been favoured by considerations (*a*) and (*b*), it seems more likely that the large boss was partly responsible for the low value obtained, whilst the failure to rotate at small angles was due to the low scale of the model in conjunction with cause (*a*).

It was therefore decided to make and test a 3 ft. diameter scale model of the autogyro wing unit, but it was found that the difficulty of obtaining rotation at small angles to the wind with this model was nearly or quite as great as with the airscrew of aerofoils while the highest lift/drag obtained was no greater. There was also experimental evidence of a considerable scale effect, especially on the rotational speed, e.g. the model would only rotate at small angles of incidence by the use of the very highest tunnel speed available.

In order to obtain the highest possible scale it was then decided to construct a model of 10 ft. diameter for test in the Duplex wind tunnel. It was realised that so large a model would experience a very large tunnel interference, but this effect would be least at the smallest angles of incidence corresponding to the highest lift/drag. In order to check the correction for tunnel interference and to bridge the gap in scale a set of wooden blades to make a 6 ft. diameter model was also to be constructed. The design and construction of these models was kindly undertaken by the R.A.E. It was decided to build up each blade of the 10 ft. model on a central steel tubular spar with wooden ribs covered with doped fabric, with the object of obtaining a model dynamically as well as geometrically similar to the full scale rotating wing unit which was of similar construction. In the model as originally designed the fabric was found to sag between the ribs so as to touch the central spar ; in order to improve the section the forward half of the blade between the leading edge and the main spar was reinforced with 3-ply wood ; this added to the weight as originally designed and the final value of the moment of the weight about the hinge divided by the fourth power of the diameter was about 2·2 times the full scale value.

Preliminary tests were made on this model in July, 1926. At the conclusion of the experiments the blades were measured up at several sections and it was found that owing to the method of construction it had been impossible to avoid sudden changes of curvature, especially at the edge of the 3-ply lining, of such a nature as might be expected to increase the drag of the sections appreciably. It was feared that these errors of shape might affect adversely the performance of the autogyro model.

Accordingly, a model aerofoil of 9 in. chord was constructed at the R.A.E. identical in the shape of section and method of construction with the 10 ft. autogyro model. This was tested for lift and drag in the usual manner on the roof balance of the 7 ft. tunnel No. 3 for

comparison with the previous tests in the duplex tunnel of a wooden aerofoil of similar symmetrical section and 18 in. chord described in R. & M. 1066.* The comparison showed that the fabric model was very adversely affected by slight errors in shape; the minimum drag was increased from 0·0054 to 0·0066 and the maximum lift decreased from 0·515 to 0·444 as compared with the wooden aerofoil at the corresponding scale. (VL = 67·5.) To put this in another way, the results for the fabric aerofoil corresponded roughly to those on the wooden aerofoil at only about one third the corresponding scale. Measurement of the 10 ft. model also showed that the sections had developed an appreciable camber.

When the opportunity arrived (in July, 1927) to resume the tests on a model autogyro in the Duplex tunnel it was therefore decided to concentrate first on the 6 ft. diameter model with wooden blades which had not been previously tested. This model was made by the R.A.E. at the same time as the 10 ft. model, with the principal object of checking the tunnel interference on the 10 ft. model and of bridging the gap in scale between the 10 ft. and 3 ft. models. The results of the tests on the 6 ft. model, here described, amply support the conclusion that the performance of the 10 ft. fabric model was adversely affected by errors of shape, since a maximum value of L/D of 6·0 was attained as compared with 4·25 on the 10 ft. model, the corresponding values being 7·5 and 4·6 after correcting for the drag of the boss and blade centres. The high value of the correction for the 6 ft. model was partly due to the use of the boss of the 10 ft. model and partly to the addition of a locking device for the blade angles; in every other respect the 6 ft. model was entirely satisfactory.

The special object of designing the 10 ft. model to be similar in density distribution to the full scale machine was to obtain an exact imitation of the flapping motion. As mentioned above exact dynamical similarity was not attained with the 10 ft. model; for the 6 ft. model the moment of the weight of the blade about its hinge ($\div D^4$) was increased from 2·2 to 4·0 times the full scale value. More recent developments in the theory of the flapping† have indicated, however, that the difference in flapping motion is unlikely to be of importance at any rate when the blades are straight as in the 6 ft. wooden model and the present full scale machine; the blades of the 10 ft. model were curved to imitate those of the original machine.

A complete description of the 6 ft. model and of the method of supporting it for force measurements is given below in § 2.0. The original programme of tests included as principal items the measurement of lift and drag, rotational and forward speed over a suitable

* R. & M. 1066.—Wind tunnel experiments on a symmetrical aerofoil (Göttingen 429 Section). By C. N. H. Lock, H.C.H. Townend and A. G. Gadd.

† R. & M. 1127.—Further development of Autogyro Theory, Part II. A general treatment of the flapping motion. By C. N. H. Lock.

range, subsidiary tests being the observation of the details of the flapping motion and the measurement of the lateral (horizontal) component force. The range of incidence was from 20° (the largest attainable with the apparatus) to the lowest incidence at which the model would rotate (2°). The limit of rotational speed considered safe was 12 revolutions per second, but at small angles of incidence the speed was limited by the highest tunnel speed available (100 ft. per sec.).

The original intention was to test the 4-bladed model at a sufficient series of blade angles from 0° up to the largest positive angle at which the model would rotate. The blade angle is defined to be positive when the component of relative wind parallel to the axle strikes the trailing edge of the blade before the leading edge, i.e. the pitch is of the same sense as that of a helicopter. The model was first tested at a blade angle 1·8° agreeing closely with the value 1° 45′ for the original full scale machine.* The blade angle was then increased to 4° and somewhat unexpectedly it was found that the model would not autorotate at any angle of incidence even when initially speeded up to 12 r.p.s. With a blade angle of 3° the model would only autorotate at angles of incidence greater than 12°. The standard measurements were finally made at the following series of blade angles :—0°, 1°, 1·8°, 2·3° and 3° (from 12° to 20° incidence in the last case).

In order to study more closely the nature of the breakdown at large blade angles, an attempt was made to develop apparatus to observe lift, drag and rotational speed while the model was rotating freely but the rotational speed was changing. Observations were made with this apparatus at certain angles of incidence at a number of blade angles, and in particular with a blade angle of 3° at angles of incidence below 12° at which the model decelerated at any tunnel speed. The results of these tests, though somewhat crude, are of great interest especially as they define in certain cases the maximum frictional torque against which the model would rotate, and the minimum rotational speed from which it would accelerate up to its steady speed.

2.0. *Description of 6 ft. diameter model.*—The blades of the 6 ft. diameter model were of wood, of constant chord and section, and without twist ; the shape of section is given in Table I being the symmetrical section Göttingen 429 modified to give a thicker trailing edge. The chord was 5·36 in. The boss and blade roots were considerably more bulky than those of the full scale machine on account of the necessity of varying the blade angle and of the fact that the centre was designed for the 10 ft. diameter model. The

* T.2155. (Unpublished.)

normal direction of rotation of the autogyro model was counter-clockwise looking downwards, as in the full scale machine, and the pitch that of a right-handed screw for positive blade angles.

For the purpose of attaching the blades to the centre and of altering the blade angles, the inner end of the blade root inside the hinge bearing was screwed into the boss as shown in Fig. 3 and was originally held in place by a simple lock nut. As the result of an accident to the 10 ft. diameter model caused by the lock nut slacking off and the blade altering its angle during a run, it was decided to provide a more positive locking device. The arrangement shown in Fig. 3 was designed and fitted by the Royal Aircraft Establishment; the tangent screws EE grip between them the radial piece F attached to the blade and allow an accurate adjustment of blade angle between the limits $-2°$ to $+6°$. This device was perfectly satisfactory in combining ease of setting with security. The method of setting the blade angle is described below in § 2.121.

2.1. *Description of Autogyro Balance.*—Owing to the size and motion of the model the wire suspension ordinarily used for force measurements on model aeroplanes and aerofoils was replaced by a more rigid mode of support. The arrangement actually used is shown in Fig. 4. EFGH is a frame in the form of an inverted tetrahedron of rigid rods, of which the apex E carries the spindle on which the model rotates; the frame FGH is horizontal and above the roof of the tunnel, the members EF, EG, EH passing through the holes in the roof. The frame carries steel points F_1, G_1 and H_1 attached to it near F, G and H, by which it is supported from the standard lift and vertical force balances.* For the present purpose these balances may be considered as three independent weigh beams which determine independently the vertical components of the reactions at F_1, G_1 and H_1. Actually the two beams of the lift balance which support F and G can be linked together so as to measure either the sum or difference of the vertical component reactions at F_1 and G_1. The link for measuring the difference is not shown in Fig. 4. To support the points at F_1 and G_1 the pulleys of the lift balances were replaced by steel cups. The point on the frame at H_1 is supported directly by the cup on the balance weigh-beam, and to avoid redundant constraints the point at G_1 is supported through a straight vertical strut, while at F_1 there is a pair of points in the line F_1G_1 resting in a cup and groove of the triangular strut K whose lower point rests in the cup on the lift balance arm, and whose plane is normal to the wind.

2.101. *Method of altering the angle of incidence.*—The spindle of the autogyro model is rigidly attached to the arms EF, EG of the frame, which are hinged at F and G about the axis FG. The arm

* R. & M. 823. Description of lift, vertical force and drag balances for the roof of the Duplex wind tunnel. Fewster.

EH is hinged at E and slides through a clamp at H connected to the rigid triangle FGH. By sliding the arm through the clamp the inclination of the plane EFG to the vertical, which is equal to the incidence of the autogyro model, can be varied between the limits 0° and 20°. A scale attached to the arm EH moves past a pointer attached to the main frame and the scale reading is calibrated against angle of incidence so that it can be set while the tunnel is running. The method of calibrating the scale is given below in § 2.122.

2.102. *Guard Tubes.*—The arms EF, EG, EH which are inside the tunnel, were constructed of streamline tube in order to reduce the parasitic drag as much as possible, but as a result of a direct measurement of the drag of the frame alone it was decided to construct guard tubes to shield the frame from the wind. These guard tubes (Fig. 1) were pivoted about the axis FG and about a point near E so that they could move with the frame when changing incidence.

Modifications to balance introduced after the preliminary tests :—

2.111. *Raising the balance in the Tunnel.*—In the original balance the centre of the autogyro was 10 inches below the centre line of the tunnel for 0° incidence and 5 inches for 20° incidence, the height being chosen so that the centre of the circle described by the wing tips of the original 10 ft. model would be in the centre of the tunnel at 20° incidence on the assumption that the mean upward inclination of the blades (" coning " angle) was about 5° as in the full scale machine. As the actual " coning " angle of the 10 ft. model was found to be about 0° the blade tips were always about 5 inches lower than they were designed to be. It was therefore decided to raise the model 8 inches for which purpose it was necessary to raise both balances by this amount on steel girders and to cut away a portion of the main roof beams to clear the arms EF and EG. In its final position the centre was 2·2 inches below the centre line at 0° and 2·8 inches above the centre line at 20° ; as the mean flapping angle of the 6 ft. model was approximately zero this adjustment was satisfactory.

2.112. *Stiffening the Frame.*—In the preliminary experiments trouble was experienced with vibrations of the spindle. It was therefore decided to stiffen the triangle EFG by inserting a strut inside the guard tube D (Fig. 1) and bracing wires H passing through the roof of the tunnel. In the present experiments the vibration was not large except at a critical speed of about 11 revolutions per sec.

2.113. *Starter Gear.*—As a result of the preliminary tests it was considered essential to construct a power drive for the autogyro model which could rotate it up to its maximum speed and then be completely disengaged so as to leave the model free to rotate on its

ball bearing, and the main frame free to oscillate on its points for the purpose of force measurements. The drive was provided by a one h.p. electric motor on the roof of the tunnel whose power was transmitted through a rod L (Fig. 3). This rod had a universal joint at each end and a telescopic portion in the middle to allow of the change of incidence of the model. Its lower bearing P was attached to the guard tubes M which shielded the arms of the main tetrahedral frame from the wind. Below this bearing the drive was transmitted through a universal joint Q to the pinion S which could be engaged with the pinion T attached to the rotating hub of the autogyro. The bearing R of the pinion S was a brass block sliding fore and aft about the centre Q in a guide V attached to the guard, and was kept in its disengaged position by a spring W. The block had a key which engaged in a slot in a piece X attached to the fixed axle of the autogyro. The key and slot were so designed that so long as S drove T the key remained in the slot but as soon as T started to drive S, the block was forced from left to right until the key disengaged and the spring W forced the pinion S out of engagement with the pinion T. In this position the driving gear and pinion were supported by the guard and entirely detached from the main frame supporting the model. Thus the model could be driven up to a high speed by means of the gear, which could then be disengaged by retarding the starting motor; or if the autogyro overran its drive under the effect of aerodynamic force, the gear automatically disengaged itself.

2.114. *New timing gear.*—In the original design, the gear for timing the revolutions of the model consisted of an electric contact on the axle of a 5 toothed star wheel of the ordinary cyclometer type driven by a pin near the circumference of the pinion T. The device therefore made contact once every 5 revolutions. Owing to the comparatively large diameter of the pinion, and the large amount of friction required to prevent the star wheel over-running it was thought that the retarding effect on the model might not be quite negligible. For the present experiments it was replaced by a pair of platinum contacts shown at N actuated by a roller working on a cam sweated to the surface of the tubular spindle A of the model. This device made contact once per revolution and actuated an electrical relay which reduced the number of contacts 15 times. The relay was constructed from the movement of a clock, the escapement lever of which was actuated by an electro-magnet in the make and break circuit; the escape wheel of 15 teeth then rotated through one turn in 15 revolutions of the model and a contact on its spindle was used for timing the revolutions with a stop watch.

2.115. *Additional Guards.*—As a result of preliminary experiments it was found that the flexible wires inserted in the 10 ft. model to limit the flapping motion of the blades could be dispensed with on the 6 ft. model as the blades could be allowed to come down to a

nearly vertical position without touching the floor, small springs being inserted to stop the blades at about 20° to the vertical (*see* Fig. 1). It was therefore possible to insert "guards" to protect the spindle of the autogyro from the wind. The lower guard Z was supported on a spindle from the tunnel floor, adjustable horizontally and vertically as the incidence of the model was varied. In Fig. 2 the blades are shown extended by means of steel wires YY which were inserted when it was required to take zeros on the roof balances so that the centre of gravity of the model might be roughly in its running position. When preparing to run the model the wires YY were removed and an upper guard (G Fig. 1) attached, which was similar to the lower guard and was fitted to the main guard tubes so as to shield the pinion T and the upper part of the autogyro spindle. It was desirable to shield as much as possible of the centre as the main and flapping bearings were relatively much more bulky than in the full scale machine.

2.12. *Details of Calibration.*

2.121. *Method of setting blade angle.*—Since the blade section was symmetrical, a straight edge of the form shown in Fig. 5 was used for setting the blade angles. The two blocks *c* and *d* were pushed towards each other so as to grip the two sides of the leading and trailing edges symmetrically. The surface *b* was designed to be parallel to the chord of the section under these circumstances. For the experiments on the 6 ft. model, an Army pattern clinometer was available for setting the angles. This consisted of a brass quadrant *a* at the centre of which was pivoted a radial arm *e* carrying a sensitive bubble which could be adjusted at a given angle to the straight base of the instrument. The radial arm carried a vernier graduated to 3 minutes so that it could be set by estimation to about 1 minute. In making the setting, the axle of the autogyro was first adjusted to be accurately vertical by means of the clinometer. The clinometer set to the required blade angle was then placed on the surface *b* of the straight edge, the blade being supported horizontally by a retort stand; the blade angle was adjusted by means of the tangent screws and lock nuts until the clinometer bubble was central. The accuracy of construction of the straight edge was checked by reversing it and placing the clinometer on the surface *ff*. Actually, it was found that the weight of the clinometer was sufficient to twist the blade slightly. This effect was eliminated by the use of a light sensitive bubble which was attached directly to the blade close to the straight edge by means of plasticine. The accuracy of setting the axle vertical could easily be checked by repeating the setting with the model rotated through two right-angles. The final relative accuracy of setting the blade angles (i.e., apart from possible want of symmetry of the sections) is probably less than 2′.

2.122. *Method of setting incidence.*—The clinometer also proved very convenient for calibrating the incidence scale. For a given setting on the scale it was only necessary to rest the clinometer on a wooden frame fixed to the rotating spindle so that its plane was vertical and its zero line was roughly parallel to the plane of the autogyro and to take maximum and minimum readings of the clinometer as the autogyro was rotated about its spindle.

It is suggested that the use of the clinometer in other experiments for setting incidence would be an improvement both in convenience and accuracy over the standard method of sighting on a protractor on the tunnel wall. For models designed for a smaller tunnel than the Duplex the deflection due to the weight of the clinometer might be too great.

2.123. *Centre of pressure for aerodynamic forces.*—The apparatus for measuring forces on the model was designed on the assumption that the resultant aerodynamic force passed through the centre of the spindle.

A displacement of the position of the centre of pressure from the centre of the autogyro is equivalent to a moment of the resultant aerodynamic force about an axis through this point. The existence of a pitching moment about the centre of the model would be most serious since it would cause an error in the determination of drag. It is necessary to consider separately the possibility of the transmission of such a moment by the blade in its different positions round the circle.

(1) For the blades instantaneously up or down stream a resultant moment of this type can only be due to a difference of the component forces at the hinges parallel to the axle between opposite blades. This effect must be very small because the instantaneous velocity of the air relative to these two opposite blades is approximately the same, while the moment due to this difference acting on a leverage of $4\frac{1}{2}$ in. appears as an error on the drag acting at a leverage of 78 inches.

(2) For the pair of blades instantaneously across stream the required moment will be equivalent to the moment of the aerodynamic forces about the line in the blade through the hinge, and will be zero if this line passes through the centres of pressure of all the sections of the blade. Actually the model was designed so that this might be the case as the line through the hinge lay at one quarter of the chord from the leading edge of all the sections, and this position is known to agree accurately with the centre of pressure of the section at all angles of incidence below the stalling angle. As the proportion of the sections beyond the stall is always of very small importance it follows that this contribution to the moment is also negligible.

It may therefore be concluded that it is sufficiently accurate to assume that the centre of pressure coincides with the centre of the autogyro.

2.124. *Setting of the blades for taking zeros on the balances.*—When the spindle of the autogyro is inclined to the vertical at an angle i, an angular displacement of all the four blades about their hinges causes a displacement x of the centre of gravity of the model along the spindle which will give a horizontal displacement of the centre of gravity, $x \sin i$, and this will affect the readings of both balances. It is therefore desirable that when taking zeros on the balances the blades should be supported approximately at the mean of their positions when in motion. This was affected by inserting the hooked steel wires Y (Figs. 2 and 3) whose length was accurately adjusted to give a flapping angle of 0°. It will be seen in §5.11 below that this was sufficiently near to the mean angle in all cases.

2.125. *Calibration of the Balances. The force components (lift and drag) in the plane of symmetry.*—In general both lift and drag are functions of both balance readings. Let L be the vertical component (lift) and D the horizontal component (drag), and let l be the reading of the lift balance, which is proportional to the sum of the vertical reactions at F_1 and G_1, and d be the reading of the drag balance giving the vertical reaction at H_1. From the construction of the balance it was considered that deflection was negligible, and consequently the force components would be linear functions of the balance readings. Write therefore

$$L = A_1 l - B_1 d \quad \ldots \quad (1)$$

$$D = A_2 l + B_2 d \quad \ldots \quad (2)$$

(l is reckoned positive when the sum of the reactions at F_1 and G_1 is upwards, and d is positive when the reaction at H_1 is downwards). Alternatively

$$l = a_1 L + b_1 D \quad \ldots \quad (3)$$

$$d = -a_2 L + b_2 D \quad \ldots \quad (4)$$

The constants a_1, b_1, a_2, b_2 were determined by direct calibration at a series of angles of incidence by applying known lift and drag forces separately and taking readings of both balances. The values of A_1, B_1, A_2, B_2 which are the constants actually required in analysing the observations were then deduced from the formulae:

$$A_1 = b_2/\delta, \quad B_1 = b_1/\delta, \quad A_2 = a_2/\delta, \quad B_2 = a_1/\delta, \quad \delta = a_1 b_2 + a_2 b_1$$

A_1 and B_1 are independent of the incidence since $A_1 l$ is the upward reaction at $F_1 G_1$ and $B_1 d$ is the downward reaction at H_1. This was verified by the calibration. A_2 and B_2 which vary with incidence were plotted against incidence from calibrations at a sufficient number of different angles of incidence.

2.126. *Balancing of the autogyro about its centre.*—In order to reduce vibration it was necessary to adjust the centre of gravity of the rotating model to lie accurately on the axis of rotation. A convenient method of determining whether the model was in balance was to take readings of the drag balance with the model rotated into 4 equidistant positions. It was found that balance weights of about ½ oz. were required on two consecutive blades and these were inserted in the wood near the tips; a final adjustment was made by smearing plasticine on the blade tips.

2.127. *Calibration of lateral force.*—The centre of pressure for lateral force as well as for drag was assumed to coincide with the centre of the model. The arguments already given in the case of the drag may be applied to the lateral force though with less certainty, but the importance of the lateral force is also less.

The balance was calibrated for lateral force by applying a known horizontal component force across tunnel by a string attached to the centre of the model and passing over a pulley. The calibration was taken at one angle of incidence only as the variation of the calibration factor with incidence was small and could be calculated with sufficient accuracy from the geometrical constants of the balance. As previously explained the lateral force was determined as the reading of the lift balance, when rigged to measure the differences of the vertical reactions at the two points F_1 and G_1. If the geometrical construction of the balance were perfect, this reading should be independent of both lift and drag forces. The independence of the lift was checked when the balance was previously set up by hanging a weight from the centre of the model and noting that the balance reading was zero. On replacing the balance for the present tests it was considered sufficient to verify that the bar FG was horizontal and the axle of the autogyro vertical (at 0° incidence) each within 2 or 3 minutes of angle.

3.0. *Range of Force Measurements.*—For the initial measurements of forces the blade angle was adjusted to the value 1·8° corresponding roughly to the blade angle 1° 45′ of the original full scale machine as recorded in T. 2155.* This blade angle was ultimately found to give the highest value of L/D. For this blade angle the observations were taken at angles of incidence ranging by steps of 2° from 20° (the highest angle which the apparatus would permit) down to 8°, and then by steps of 1° down to 3°.

The highest rotational speed was in general limited by considerations of strength of the model, to 12 revolutions per second, corresponding to a tip speed 226 ft./sec., roughly equal to the tip speed of the original full scale machine. The lower limit was in general 5 revolutions a second though a few observations were taken as low as 3 revolutions a second.

---

*T.2155 *loc cit.*

At angles of incidence below 5° the rotational speed was limited by the maximum tunnel speed available, 100 ft./second. As the maximum value of L/D occurs in this range, the limitation of rotational speed to 12 revolutions a second was not of great importance. Observations at the same blade angle were repeated at the end of all the experiments and a solitary observation was taken at an incidence of 2° in which it was found that the model would not rotate for a tunnel speed of less than 90 ft./second. At 1° incidence the model would not rotate at all and an accident occurred in attempting to make it do so. Owing to failure to shut down the tunnel with sufficient rapidity the rotational speed of the model fell until one of the blades hit the supports. Fortunately the only damage consisted in the splitting of the trailing edge of one of the blades which was found to be repairable.

It was originally intended to test a series of blade angles ranging from 0° up to the highest value at which the model would rotate. After completing the preliminary tests at 1·8°, the blade angle was set to + 4° and somewhat unexpectedly it was found that the model would not autorotate at any angle of incidence. The blade angle was then reset to 3° and autorotation was obtained at large angles of incidence. In attempting to reduce the incidence it was found necessary to modify the gear ratio of the starting motor so that it would rotate the model at its maximum safe speed of 12 revolutions a second. With this modification autorotation was obtained at 12° incidence at 10 or 12 revolutions a second, but at 10° incidence the model would not autorotate. Observations were made of the approximate lowest speeds at which the model would rotate at each angle of incidence above 10° which are given in the following Table.

Table of critical speeds for blade angle 3°.

Incidence (uncorrected).	11°	12°	14°	16°	18°
n (revs. per sec.) at which the model will just rotate	above 12	8·5 ?	6·7	5·3*	4·2

While the blade angle was still set at 3° the method of making observations on the model when accelerating or decelerating was developed, as mentioned in the introduction and described in detail in Section 4 below. Force measurements were then made with the blade angle set at 0° and also at 1°. No difficulty was experienced with these experiments, which call for no special comment. On analysing the results it was found that the maximum L/D for a blade angle of 1°

* This value was confirmed by the observations at varying rotational speeds, *see* below § 4.4.

was appreciably less than for 1·8°. It was therefore decided to test an additional blade angle (2·3°) intermediate between 1·8° and 3°. This again gave a lower maximum L/D and the results at the smaller angles of incidence were very critical, but no case of actual failure to rotate was observed at rotational speeds above 5 revolutions a second. Finally, as mentioned above, some repeat tests were made at a blade angle of 1·8° and the results were found to be in satisfactory agreement with the original tests.

In view of the success of the Autogyro Company in flying a 2-bladed autogyro, it was decided to test the present model as a 2-blader by removing two of the blades. The experiment was conveniently made after the accident to the model in which one blade was damaged. The experiments showed no special features except that as expected there was greatly increased vibration due to the periodic variation of the drag which necessitated additional damping in the drag balance. This vibration increased rapidly with decreasing incidence and the lowest incidence attained was 4°, which was hardly low enough to establish the maximum L/D.

3.01. *Lateral Force.*—Observations of the lateral force component Y, were made in conjunction with the observations of flapping described below in § 5 for the blade angle setting 1·8° only, at angles of incidence from 4° to 16°.

3.1. *Method of Reduction.*—As compared with an aerofoil an autogyro has in addition to the ordinary variables—velocity, incidence and the two components of resultant force—a fifth variable, the rotational velocity. There is therefore a rather large variety of types of non-dimensional coefficients by which to describe the results. For the practical purpose of determining the merits of the autogyro as a flying machine it is convenient to resolve the resultant force in the plane of symmetry into the components lift L and drag D, while the rotational speed is unimportant. The coefficients which are important in this connection are the lift coefficient on velocity $L/\pi R^2 \rho V^2$, here denoted by L_v, and the ratio D/L. The incidence is of secondary importance so that it is convenient to plot D/L against L_v, and L_v against incidence. From the point of view of the theory of the autogyro, the force components T, the thrust parallel to the axle, H, the longitudinal force, normal to the axle, and the rotational speed are fundamental. Within the range of incidence covered by the present report (2° to 22°) the thrust does not differ greatly from the lift L and the thrust coefficient $T/\pi R^4 \rho \Omega^2$ may be replaced by the lift coefficient $L/\pi R^4 \rho \Omega^2$ here denoted by L_Ω. This coefficient has the additional advantage that it defines the rotational speed of the full scale machine in horizontal flight. In the more recent developments of the theory of the autogyro, the longitudinal force component has been superseded by the coefficient D/L deduced from considerations of energy loss.

The four non-dimensional quantities L_V, D/L, L_Ω and the incidence i are actually sufficient to describe the results completely but it is convenient to record also the additional coefficient $V \cos i/R\Omega$, denoted by μ, which is of fundamental importance in the theory.

When the torque Q is not zero it must be included as a sixth variable. The form of torque coefficient which appears most convenient is $Q/\pi R^5 \rho\Omega^2$ which will be denoted by Q_Ω. Its relation to the standard torque coefficient k_Q of airscrew theory is

$$k_Q = \frac{1}{8}\pi^3 Q_\Omega.$$

The lateral component force Y is conveniently recorded in the form Y/L, the value of this ratio being expressed in degrees for convenience of comparison with the flapping angle. The lateral force is reckoned positive when measured to starboard (i.e. towards the blade which is moving up stream). The results of the measurement of Y are discussed below in § 5.13 in conjunction with the observations of the flapping motion.

3.2. *Corrections.*—It is necessary to apply the following corrections to some of the quantities observed in the tunnel.

3.21. *Velocity.*—Towards the close of the experiments some observations were made with a standard Pitot tube of the velocity in a line across the tunnel through the centre of the autogyro at a point 2 ft. from the wall. At the larger angles of incidence the velocity at this point was found to be appreciably increased by what may be considered as a blocking effect of the model. The maximum increase observed was 4 per cent. on V^2 for the 4-bladed autogyro at 1·8° blade angle and 20° incidence. It was decided to take the velocity at this point as being the equivalent free air speed ; as the variation of this velocity was small, only a limited number of observations were taken and the observations were analysed on the assumption that the increase of velocity was a function of the drag coefficient, $D/\pi R^2 \rho V^2$ only, this assumption being found to agree sufficiently well with the observations. On this basis corrections were applied to the velocity and to the coefficients L_V and μ, in which it occurs.

3.22. *Air Density.*—The temperature and barometric pressure were observed each day and the rotational speed was reduced to standard air density by the method customary in all wind tunnel experiments on air screws.

3.23. *Correction for tunnel interference.**—The ordinary formula for the Prandtl correction for tunnel interference on an aerofoil

* All observations throughout the report were made at an exact number of degrees incidence (uncorrected). In general when an angle of incidence is mentioned in discussing the results the uncorrected incidence is meant.

contains only the velocity V, the total lift L on the aerofoil, and the breadth and height of the wind tunnel. For an aerofoil horizontal in the Duplex tunnel the formula is

$$\Delta i = 0{\cdot}274\ L/\rho\ V^2\ C$$

where C is the cross sectional area of the rectangular channel and Δi is the increase of the incidence i (in radians). This formula can be applied at once to the autogyro; an argument in favour of its correctness is the fact that the calculation of the interference velocity on the assumption that the general flow pattern is the same as that round an elliptic wing having equal lift and a span equal to the diameter of the autogyro, gives results in fair agreement with experiment. In applying the above formula to the autogyro it was assumed that the relative values of four of the five variables, viz., V, Ω, T and H were unaffected by the presence of the tunnel walls while the incidence i was increased according to the last equation. For the present purpose it is sufficiently accurate, since the correction is fairly small, to assume that L instead of T is unaltered and that there is a correction on the drag as in the case of the aerofoil given by the equation

$$\Delta D = L\ \Delta i.$$

Of the coefficients here recorded the only ones affected are i and D/L and the magnitudes of the corrections are

$$\Delta i = 4{\cdot}525\ L_v \text{ degrees}$$
$$\Delta (D/L) = \Delta i \text{ in radians}$$
$$= 0{\cdot}0790\ L_v$$

3.24. *Correction for drag of boss and blade roots.*—It was unfortunate that the drag of the boss and blade roots of this model was relatively of much greater importance than that of the full scale machine. This was due firstly to the fact that the boss was designed for a 10 ft. model and secondly to the necessity for means of varying and locking the blade angle described in § 2.0 above. As mentioned in the same section it was possible owing to the omission of the safety wires to design guards which shielded a much greater proportion of the boss than in the case of the 10 ft. model. A number of observations of forces were made before these guards were completed. At the end of all the experiments after the blades had been removed, observations of drag were made with the spindle alone and also with wooden dummies of the blade roots as far as the point 0 of Fig. 3. The observations were repeated with and without additional guards in place. By taking the difference of the drag of the complete model with and without guards we obtain the drag of the parts of the centre shielded by the guards and subjected to the interference flow of the autogyro blades. Comparison with the corresponding observations on the dummy boss and blade roots

showed generally good agreement and suggested that the interference of the blades on the boss was of small importance. On the basis of this result it was assumed that the drag of the dummy boss and blade centres with the guards in place represented the correction which should be applied to the observed drag of the complete model with guards in place in order to obtain the drag of the blades alone. The accepted value of this correction was $0{\cdot}0013/L_v$ on D/L. Unfortunately this correction still represents a very large percentage of the drag of the blades at small angles of incidence; in particular the correction increases the highest maximum L/D of the 4-bladed model at 1·8° blade angle from 6·1 to 7·5, and of the 2-bladed model from 5·6 to 7·8. The maximum values of L/D for the blades alone are therefore somewhat uncertain. In order to obtain a correction suitable for the 2-blader the dummy boss was also tested with two blade roots only, set across stream and also along stream. The drag in the former case was quite as great as that of the four blade roots. Accordingly it was finally assumed that the correction for drag of boss and blade roots to be applied to the 2-blader was equal to that of the 4-blader and the relative importance of the correction was therefore twice as great. Further evidence for the accuracy of these corrections is obtained below in § 3.43 in discussing the comparison between the results for 2- and 4-bladers.

3.3. *Reduction to zero solidity ratio.*—For the purpose of comparison between the two bladed and four bladed models it is convenient to make use of the conception of an ideal autogyro of zero "solidity ratio." This corresponds to the reduction of aerofoil data to infinite aspect ratio as a basis of comparison between aerofoils of different aspect ratio. For the present purpose it is proposed to make use of Glauert's assumption of R. & M. 1111* as to the interference flow:—that the total interference velocity is parallel to the axle of the autogyro and constant over the disc, and that it is equal to the velocity of downwash of an aerofoil with elliptic loading and of a span equal to the diameter of the autogyro. Writing i_0 for the incidence and D_0 for the drag of the autogyro of zero solidity ratio, the formula for i_0 may be derived from formula (22) of R. & M. 1127 in the form (neglecting $(x/\mu)^2$)

$$\tan i_0 = \tan i - \frac{1}{2} T/\pi R^2 \rho V^2 \cos^2 i$$

$$= \tan i - \frac{1}{2} L_v \{1 + (D/L) \tan i\} \sec i$$

the formula of D_0/L may be similarly derived from formula (30) of R. & M. 1127.

$$D_0/L = D/L + \frac{1}{2} L_v \{1 + (D/L) \tan i\} \sec i.$$

* R. & M. 1111.—A general theory of the Autogyro. By H. Glauert.

In order that the force coefficients L_Ω and L_V may be independent of the solidity, σ, it is necessary to refer them to the total blade area instead of to the disc area, i.e. to use $(1/\sigma)\,L_\Omega$ and $(1/\sigma)\,L_V$ in place of L_Ω and L_V. As the majority of the results refer to the 4-bladed autogyro, it is convenient to take its solidity σ_4 as standard and to work out $(\sigma_4/\sigma)\,L_\Omega\ (=2\,L_\Omega)$ and $(\sigma_4/\sigma)\,L_V\ (=2\,L_V)$ for the 2-bladed autogyro. Accordingly values of i_0, D_0/L, $(\sigma_4/\sigma)\,L_\Omega$, and $(\sigma_4/\sigma)\,L_V$ have been worked out for the 2-bladed and 4-bladed autogyro at 1·8° blade angle. (Fig. 11.)

3.41. *Discussion of Results. Force Measurements. Effect of change of blade angle.*—Fig. 6 shows values of D/L corrected for drag of boss plotted against lift coefficient L_V for all blade angles tested. The results correspond to a rotational speed of 10 revolutions a second, i.e. a scale value $\Omega R\,c = 84{\cdot}2$ ft.²/sec. The most obvious conclusion from this as from all the results is that the performance of the model is extremely sensitive to changes of blade angle. From 0° blade angle up to 1·8° there is a steady decrease of D/L with blade angle for given lift coefficient over the whole range. At large values of lift coefficient this decrease continues up to 3° blade angle but at small values of lift coefficient the value of D/L has started to increase at 2·3° blade angle while at 3° blade angle the model will not rotate. Thus the change from highest maximum efficiency (lowest D/L) to the condition of failure to rotate corresponds to a change of blade angle of probably less than 1°. The failure of the model to rotate is undoubtedly connected with the stalling of the blade elements of the retreating blade. This point is considered more in detail below in connection with the results of tests at varying rotational speeds. It is evident that as the blade angle increases, the effect of stalling becomes important with great suddenness; apart from this effect the results verify the conclusion of R. & M. 1127 that the efficiency increases with blade angle.

On the same diagram Fig. 6 are plotted the corresponding results for a monoplane aerofoil of aspect ratio 6 having the same section as the autogyro wing. For the purpose of comparison, the lift coefficient of the aerofoil is calculated on the basis of the area of the circle on the span as diameter, so that the span of the aerofoil corresponds to the diameter of the autogyro. This basis of comparison has the further advantage that the approximate value of the induced drag, shown by the dotted straight line is the same for both. The comparison shows clearly the distinguishing qualities of the aerofoil and autogyro, the superior efficiency of the former at high speed, and the absence of sudden stall with increasing flying incidence of the latter. The remaining Figs. 7 and 8 show respectively the lift coefficients L_V and L_Ω plotted against incidence. The first figure does not call for special comment; Fig. 8 shows that the coefficient L_Ω is very nearly independent of incidence down to fairly small values in all cases, the only exception being the case of blade angle 2·3° at small angles of incidence and

blade angle 3° for which the results are known to be very critical. The values of L_Ω shown in Fig. 8 are sufficiently regular to provide a useful check on the relative accuracy of the setting of the blade angles. It is interesting to notice that over a considerable range the values of L_Ω decrease slightly with decreasing incidence in accordance with the theory of R. & M. 1127 and also, it is understood, with the full scale observation that the rate of rotation increases slightly with increasing forward speed.

3.42. *Effect of change of Reynolds Number.*—A selection of the coefficients is shown plotted against the rotational speed n* as follows :—D/L in Fig. 9 and L_v in Fig. 10, while the scale effect on L_Ω is shown in Fig. 8. The most striking result is the large scale effect on L_v in comparison with the other coefficients for large values of n, large values of incidence and small blade angles, these being the conditions in which the scale effect on the remaining quantities is least. This implies that the ratios of rotational speed, lift and drag are more nearly independent of Reynolds number than their ratios to the forward speed V required to produce rotation ; this again may be interpreted as a scale effect on torque coefficient since the rotational speed is determined by the condition of zero torque. It is to be expected on theoretical grounds (*see* R. & M. 1127, Part II) that the greatest scale effect will be found on the torque coefficient and the energy loss due to profile drag ; the effect of the latter on the value of D/L at large incidences is masked by the fact that the drag is the sum of the Prandtl induced drag, and the energy loss due to profile drag ; the former part (relatively most important at large incidence) depends on L_v and therefore increases with increase of Reynolds number while the latter part decreases.

The scale effect on the coefficient L_v alone shows no tendency to diminish with increase of scale, the curves against n being sensibly straight lines on the average at angles of incidence greater than 10°. The average increase from $n = 10$ to $n = 12$ is from 3 to 4 per cent. It is impossible to predict full scale values of this quantity with any accuracy except to say that the full scale machine will have considerable advantage over the model in this respect. The remaining coefficients L_Ω and D/L appear to have settled down to sensibly constant values at the highest Reynolds number reached and little alteration is to be anticipated up to full scale values.

All coefficients tend to vary in a critical manner at speeds approaching that at which the autogyro will not rotate ; this suggests that model experiments are of little value when the blade angle is close to the critical value, e.g. for a 6 ft. diameter model the blade angle should not exceed 2°, for a 3 ft. model it should not exceed 1·5°.

3.43. *Effect of change of solidity.*—The coefficients for the 2-bladed and 4-bladed autogyro at blade angle 1·8° have been

* Which is proportional to the Reynolds number at the tip = tip speed × chord ($R\Omega c$) = $8{\cdot}42\,n$ ft²/sec.

reduced to zero solidity by the method already described, and are plotted against i_0 in Fig. 11 in the form $(\sigma_4/\sigma)\, L_V D_0/L$ and $(\sigma_4/\sigma)\, L_\Omega$ The agreement between 2-blader and 4-blader is good over the whole range and may be taken as evidence that the performance of an autogyro of any solidity less than that of the standard 4-blader and of any blade angle within the range over which the 4-blader was tested, may be calculated by the formulæ of § 3.3 which may be written in the form

$$L_V = (\sigma/\sigma_4)\, L_{V4}$$

$$L_\Omega = (\sigma/\sigma_4)\, L_{\Omega 4}$$

$$i = i_4 - \frac{1}{2} T'_{V4} + \frac{1}{2} T'_V$$

$$D/L = D_4/L_4 - \frac{1}{2} T'_{V4} + \frac{1}{2} T'_V$$

where $T'_V = L_V (1 + (D/L) \tan i) \sec i$, and suffix 4 denotes values for the standard 4-blader.

The agreement of D/L for the 2- and 4-bladers also tends to confirm the accuracy of the correction for the drag of the autogyro boss.

4.0. *Observations at varying rotational speed.*—On discovering that the autogyro model would not rotate with the blades set at + 3° at angles of incidence below 12°, it seemed desirable to extend the range of experiments by taking observations when the torque was no longer zero. The application of a small driving torque would make it possible to extend the observations at + 3° blade angle to small angles of incidence, while observations over a range of rotational speeds for a given tunnel speed involving small positive or negative values of the torque would be of considerable interest. This extension of the number of variables would be of assistance in comparing the observations with the result of strip theory calculations; it should also be of some practical importance in a comparison between model and full scale. The experiments indicate that the most important scale effect is on the rotational speed for zero torque, or alternatively, on the torque for given rotational speed; this suggests that it may be possible to obtain results corresponding more closely to full scale by applying a torque to the model. In particular, it is probable that the full scale autogyro will autorotate at a somewhat larger blade angle than the model; experiments at the corresponding blade angle could be made only by applying a driving torque to the model.

In considering possible experimental methods for the 6 ft. model it was thought undesirable to attempt to design new apparatus for the purpose; the existing starting gear was not suitable as its use

interfered with the readings of the lift and drag balances and it would only exert a positive torque. In addition there was no simple means available for its measurement. As a simple preliminary method requiring scarcely any additional apparatus, observations were attempted when the rotational speed of the model was varying. The instantaneous angular velocity of the model was measured directly by means of a stroboscope so that the acceleration or deceleration could be deduced from a single differentiation of the resulting observations. In a number of cases instantaneous readings were also taken of the lift and drag balances and these were correlated with the readings of angular velocity by means of a chronograph.

In the normal case the autogyro has a definite stable speed of rotation A, (Figs. 12 and 13) at which the torque changes sign from negative to positive as the rotational speed increases. It is to be expected that in general the torque will again change sign at some lower rotational speed corresponding to a possible unstable steady motion B. There are then three possible types of motion, illustrated in Figs. 12 and 13, according to the particular speed at which the autogyro is started. (*a*) If it is started at a speed above A, the speed falls to the steady speed (A); (*b*) if it is started at a rotational speed slightly greater than B, the speed rises to the steady speed A; (*c*) if it is started at a speed slightly below B, the speed falls indefinitely. The curves shown in Fig. 12 were those actually obtained in a test at blade angle 3°, incidence (uncorrected) 16° and tunnel speed 32.0 feet per second; the zero of the time scale of Fig. 12 is of course purely arbitrary. The 3 branches marked (*a*), (*b*) and (*c*), in Fig. 12 correspond to the 3 portions of the corresponding curve of torque coefficient in Fig. 13; on particular occasions the speed remained close to the unstable speed B for many seconds before any indication was discernable as to whether the speed would rise or fall. This uncertainty added to the excitement of the experiments, since if the speed fell it was necessary to take as many observations as possible before vibration became excessive, and then to shut down the tunnel promptly enough to prevent possible damage being caused to the model. In cases when the autogyro would not autorotate at all (run steadily) the torque was always positive as at (*d*) and the speed always fell continuously.

4.1. *Details of apparatus and method of observation.*—The instantaneous angular velocity of the autogyro was observed by means of a stroboscope disc rotating on a vertical axis, mounted just above a glass window in the roof of the tunnel. On the floor of the tunnel was placed a white sheet on which a sharply defined shadow of the autogyro was cast by a "Pointolite" lamp. The motion of the shadow was observed successively through concentric rings of holes pierced in the disc of the stroboscope which was driven at a constant speed through a reduction gear of $8\frac{1}{2}$ to 1 (afterwards 7 to 1) by a

small electric motor. The rotational speed of the disc was varied between the extreme limits 3·4 to 1·7 revolutions per second by varying the armature voltage and by the use of field resistances. The concentric rings had the following numbers of holes starting from the outer ring:—14, 13, 25 ($= 2 \times 12{\cdot}5$), 12, 11, 10, 19 ($= 2 \times 9{\cdot}5$), 9, 8, 7. The motor driving the stroboscope was provided with a make and break contact by means of which an intermittent current was supplied to an alternating current frequency meter, of the vibrating reed type. This arrangement enabled the stroboscope to be maintained at a predetermined steady speed. The meter contained reeds responding to every $\frac{1}{2}$ cycle from 30 to 50 cycles and the wave form produced by the contact breaker was such as to cause all those reeds to vibrate which corresponded to a complete series of harmonics up to the 6th according to the speed. Advantage was taken of this circumstance to use the meter over a range of speeds otherwise outside its limits. Difficulties at first experienced in obtaining steady running of the disc were traced to imperfections in the original reduction gear which caused the speed to oscillate about its mean value, and a number of observations were rendered useless from this cause. On substituting a new gear this trouble was eliminated.

The chronograph was kindly lent by the Engineering Department; it was provided with four electrically operated pens marking a $\frac{1}{2}$ in. paper tape which was fed at a constant rate by an electric motor. To provide a time scale, one pen was operated by a mercury contact attached to the lever of a clock, the hairspring and balance wheel of which had been adjusted to beat exact seconds.

The remaining three pens were controlled by tapping keys of which one was operated by the observer on the stroboscope and the other two by observers on the lift and drag balances.

The object of the experiment was to determine the instants relative to a common time zero at which the rotational speed and balance readings attained definite predetermined values. The procedure in a typical experiment was as follows:—Case (*d*) in which the autogyro decelerates indefinitely. The tunnel was run at a given constant speed and the autogyro rotated by means of the starter at a given initial speed under the control of the observer on the stroboscope. The stroboscope speed was adjusted so that the time of passage of one hole in the outer ring of 14 holes past the eye of the observer was slightly greater than the time taken by the 4 bladed autogyro to make a quarter turn. Under these circumstances the image of the autogyro appeared to have the normal number of blades and to rotate slowly backwards. To commence the experiment the stroboscope observer pulled out the switch of the starting motor leaving the model rotating freely so that it at once started to decelerate and its image in the ring of 14 holes appeared to come to rest at an instant which was recorded by pressing the key, and was

taken as the arbitrary time zero. Afterwards the instants at which the image appeared to come to rest when seen through the remaining rings of holes were successively recorded on the chronograph and corresponded to rotational speeds of (13/14) n_0, (12/14) n_0, etc., where n_0 is the speed corresponding to the outer ring. At the instant the image appeared at rest in the innermost ring, the speed had the value (7/14) $n_0 = 1/2\ n_0$; in favourable circumstances the observations could be continued beyond this point, since, at the same instant, the image re-appeared at rest in the outer ring of 14 holes but with 8 blades; afterwards it appeared at rest in the next ring of 13 holes when the rotational speed had dropped to $\frac{1}{2}$ (13/14) n_0, and so on. Ultimately it was necessary to shut down the tunnel before the rotational speed became so low as to cause excessive vibration due to increased flapping.

The use of the extra rings of 25 and 19 holes was as follows. At some instant between those at which the image with 4 blades appeared at rest in the rings of 13 holes and 12 holes, an image with 8 blades came to rest in the ring of 25 holes and was recorded at the instant appropriate to 12·5 holes. The appearance of these images with 8 blades was useful in making it possible to obtain a greater number of points to define the curve of rotational speed against time. They also helped the observer to avoid mistakes as to which ring of holes he was looking through. For the former purpose it was sufficient to take two successive runs for which the stroboscope speeds were in the ratio say 12 to 12·5 so that the rotational speed corresponding to the ring 12 in the first run was equal to the rotational speed corresponding to the ring 12·5 in the second run. It was then possible to adjust the time zero for the two runs by making these two points coincide, whilst the remaining points of the two runs occurred alternately at equal intervals.

In a limited number of cases, observations of lift and drag were made simultaneously with observations of rotational speed. For this purpose it was necessary to determine first by trial the approximate range through which the balance reading would vary in the time during which the model was decelerating. A suitable number of balance readings were chosen beforehand, at intervals of say 1lb. or 2 lbs. in the case of the lift. At the commencement of a run the weights were adjusted to a reading corresponding to a rotational speed which would be passed through shortly after the commencement; after cutting out the starter the index of the balance was watched until it passed through its position of balance, at which instant a record was made on the chronograph by means of the tapping key. The observer immediately reduced or increased his weights by the predetermined amount and then waited until the index again passed through its balanced position. It was necessary to make the difference between successive readings great enough to allow sufficient time for the observer to change weights and for the

balance to settle down, but in favourable cases it was found possible to take as many as 10 readings in a single run at intervals of about 5 secs. Where necessary readings bracketing the previous readings were taken in additional runs. In actual fact the observations of forces were made in only a small proportion of these tests on account of the number of observers required and the time necessary in the preliminary trials to determine the range of forces. In the earliest experiments with blade angle 3° at 16° incidence the range of the drag balance reading was so small that it was found impossible to obtain satisfactory readings, and it was considered sufficient to take readings on the lift balance only as the reading of the drag balance affected the lift only slightly. Peculiar difficulties were experienced in the later experiments at fairly small blade angles where the acceleration of the model reached large values so that there was a tendency for the starting pinion to be thrown out of gear before the tunnel speed could be adjusted to its steady value. In this case it was necessary to throw the starter out of gear when the rotational speed was quite small and to allow the model to accelerate freely as the tunnel speed rose starting the observations as soon as the observer signalled that the tunnel speed had attained its steady value.

4.11. *Method of Reduction.*—A complete set of observations consists of the time points on the chronograph tape corresponding to a series of known values of the rotational speed and of known balance readings. The first operation is to plot the rotational speed and balance readings separately against the time referred to an arbitrary zero which is usually taken as the nearest second before the first recorded rotational speed. In general, there will be from 2 to 5 separate runs under identical conditions to be correlated with one another. For this purpose the time zeros of all the runs except one are altered by definite amounts and adjusted to make the values of rotational speed against time lie as closely as possible on a single smooth curve. The kind of accuracy with which this can be done is shown in Fig. 12. The same zero adjustments are then applied to the readings of the lift and drag balances plotted against time and should serve to throw these points also on to single smooth curves. The smoothness of the curve is of greatest importance in the case of rotational speed since it is necessary to differentiate this to obtain the torque. The next step is to obtain from the smooth curves values of dn/dt, l and d as functions of n. From the values of l and d the values of lift and drag can be obtained from the standard formulae of § 2.125, and from them the ordinary coefficients can be deduced. The angular acceleration was interpreted as giving the torque which would be required to maintain the autogyro at the corresponding steady rotational speed by means of the formula

$$Q = I \frac{d\Omega}{dt}$$

where I is the moment of inertia of the autogyro about its axle, as determined subsequently by the method described in § 4.3 below. The torque coefficient Q_Ω was then deduced by the formula

$$Q_\Omega = \frac{Q}{\pi \rho R^5 \Omega^2}.$$

It appears that the quantity required in determining the torque coefficient is $(1/n^2)\ (dn/dt)$ which is equal to $-\ d/dt\ (1/n)$. It was therefore found more convenient to plot $1/n$ instead of n against t as in Fig. 12 before measuring the slope of the curve.

Among the force coefficients deduced from the observations the value of the ratio D/L was included. It may be remarked that from the point of view of energy loss, the observed value of D/L when the torque is always positive, as in the case of the blade angle 3°, incidence 10° or less, is not strictly comparable with value of D/L at zero torque for smaller blade angles, since in order to obtain constant rotational speed, energy must be supplied to the autogyro. It therefore seems more reasonable to use for purposes of comparison a coefficient which will be denoted by $(D/L)'$ defined so as to include the whole of the energy required to propel the rotating unit of the autogyro. The part of the power required to overcome the drag of the autogyro is DV while the power expended to produce steady rotation is $Q\Omega$. We shall therefore define $(D/L)'$ as equal to $(DV + Q\Omega)/LV$ or

$$\left(\frac{D}{L}\right)' = \frac{D}{L} + \frac{Q\Omega}{LV}$$

$$= \frac{D}{L} + \frac{Q_\Omega}{\mu L_\Omega}$$

approximately.

4.12. *Range of Observations.*—The observations at varying rotational speed are recorded in Table 3 and covered the following cases. The earliest tests were made with the blade angle set at 3° at an angle of incidence 16° and cover all the four cases denoted by (*a*), (*b*), (*c*), (*d*) in Figs. 12 and 13. They also cover four different tunnel speeds and seven independent runs (about 30 runs in all). The majority of these include readings of the lift balance but not of the drag balance. The observations were then repeated at angles of incidence of 10°, 8° and 6° (Figs. 14 and 15). In these cases the torque was always positive, type (*d*); three values of the tunnel speed were taken at each angle of incidence (two at 8°). Observations of both lift and drag were taken at all three angles of incidence. As the blade angles were changed, observations were taken at 16° incidence in all cases except 0° blade angle and in the range (*b*) only. These observations were taken at two different tunnel speeds at each of the blade angles 2·3°, 1·8° and 1·0°. The experiments were limited by the necessity of completing the whole

of the experiments by a given date ; the tests at varying rotational speed being considered less important were sacrificed to the standard force measurements. No balance readings were taken in any of these later tests at varying rotational speed. Additional tests were made at 1·8° blade angle at angles of incidence of 10° and 6°, and at 1·0° blade angle at incidence 10°.

4.2. *Static Deceleration Test.*—With the blade angle set at 3° a single deceleration test was made with the tunnel at rest to obtain the static torque coefficient of the autogyro model.

4.3. *Measurement of Moment of Inertia of the model, about its centre.*—This measurement was made by two independent methods of which the results were in satisfactory agreement. The first method consisted in determining the amount of inertia of each blade separately by swinging it as a pendulum about the actual ball-bearing upon which it ran, making an allowance for the moment of inertia of the hub, which was determined very roughly, being only about 1 per cent. of the whole.

The second method was simpler and more satisfactory. The complete model was extended in its normal running position by means of light strings and was swung from knife edges attached to a chosen point in one blade, the axis of oscillation being normal to the plane of the model. The point of suspension was so chosen (on the basis of a previous rough estimate of the moment of inertia) that its distance from the centre of the model was only required very roughly, the only additional data required being the time of oscillation and the total weight of the model.

If I is the moment of inertia of the whole model about its centre and h the distance of the centre of oscillation from the centre of the model, the periodic time of oscillation T is given by

$$T = \frac{4\pi^2}{W h}\{I + W h^2/g\}.$$

This formula shows that the time of oscillation has a maximum value when h is equal to the radius of gyration of the model and for neighbouring values of h the relation between I and T is sensibly independent of the exact measurement of h. The accepted value of I deduced from these experiments was

$$I = 0{\cdot}630 \text{ slugs feet}^2.$$

4.31. *Moment of Inertia of a Blade about its Hinge.*—This quantity, together with the moment of gravity about the hinge, which is of importance in the theory of the flapping motion, was measured by swinging the blade as a pendulum, at the time of the experiments on the 10 ft. model in 1926, and the values obtained were :—

Moment of blade about hinge = 2·177 lbs. ft.

Moment of inertia = 0·118 slugs feet^2.

4.4. *Tests at Varying Rotational Speed. Discussion of Results, Torque Coefficients.*—A fairly complete set of observations of rate of change of angular velocity are available for a series of blade angles and of velocities for the case of 16° incidence. The values of torque coefficient deduced from these observations are plotted in Fig. 13 against $\mu (= V \cos) (i/R\Omega)$; the results appear to be very fairly consistent and confirm the accuracy of the method of observation.* At values of μ below 0·22 the curves are all roughly straight and parallel, the variation with scale and blade angle being fairly small. The points at which the curves cut the axis correspond to the ordinary stable speed of the model and are in good agreement with the values obtained in the course of the ordinary force measurements at constant rotational speed. As the value of μ increases, the slope of the curves changes abruptly at values of μ which vary considerably both with blade angle and with scale. This sudden change of curvature evidently corresponds to the stalling of an important part of the blade section, the larger values of μ corresponding to the stalled condition. In the stalled region the curves for different blade angles diverge from each other to a surprising degree; a result of this is that the difference between the stable and unstable rotational speeds increases very rapidly as the blade angle diminishes. Thus for 3° blade angle at a tunnel speed of 40 ft. per second, the unstable rotational speed is 0·72 of the stable speed; for a blade angle of 1·8° it was found impossible to reach the unstable speed, the torque being still negative at $\mu = 0{\cdot}59$ corresponding to one third of the stable rotational speed. The unstable speed corresponds to the critical speed of starting up the autogyro, such that if it is started above this speed it will accelerate until it attains the stable speed. The maximum negative value of the torque coefficient given by the curves of Fig. 13 determines the maximum frictional torque against which the model would maintain its rotation and shows how this quantity varies with blade angle and scale.

As regards scale effect the curves of Fig. 13 all correspond to constant forward speed but if a sufficient number of observations at different tunnel speeds were available the curves could be cross-plotted to give results for constant rotational speed, i.e. constant Reynolds number. At blade angle 3° and incidence 16°, for which there are results at four different tunnel speeds, points at a series of definite values of rotational speed are marked on the curves and from these points the general course of the curves for constant rotational speed could easily be deduced.

Corresponding results at the smaller angles of incidence 6°, 8° and 10° are shown in Figs. 14 and 15. These results are less extensive

* The observations at one tunnel speed (35·8 ft./sec.) out of five for blade angle 3° were found to be inconsistent with each other and with the observations at the remaining speeds. The discrepancy was not discovered till the blade angle was changed and its cause is uncertain but was probably due to unsteadiness of speed of the stroboscope disc.

and somewhat less consistent. The results for 3° blade angle show a gradual increase of the minimum retarding torque for a given rotational speed as the incidence decreases. For 1·8° blade angle the torque coefficient has no maximum negative value but the negative value continues to increase with increase of μ up to the limits of observation. In general as the incidence decreases, the torque, though still varying critically with blade angle, varies less critically with rotational speed. At small angles of incidence and low rotational speeds the difference of drag of the blade sections working in the neighbourhood of 0° and 180° incidence must contribute an appreciable negative torque; this possibly accounts for the change from positive slope for large values of μ at 16° incidence to negative slope at 6° incidence for 1·8° blade angle. This is consistent with the possibility of starting up the full scale autogyro fairly easily from rest at a small angle of incidence.

4.41. *Tests at varying rotational speed. Force measurements. Lift coefficients.*—In Fig. 16 the lift coefficient L_Ω ($= L/\pi R^4 \rho\Omega^2$) is plotted against μ for a given incidence. Force measurements were taken for 3° blade angle only. The results at 16° incidence are subject to the uncertainty due to the absence of readings of the drag balance mentioned above. The curves for this incidence represent the result of observations in the three different ranges (*a*), (*b*) and (*c*); it will be seen that the results for the three ranges lie accurately on a continuous curve. The range of variation of tunnel speed for which the points lie accurately on the same smooth curve is also sufficient to show that there is very little scale effect on the lift coefficient for given μ. Such scale effect as exists on L_Ω at zero torque is therefore due chiefly to the scale effect on the value of μ for given torque. On the same diagram, Fig. 16, are plotted points showing the values of L_Ω deduced from the standard force measurements at zero torque for all the different blade angles, at the same angle of incidence; the extension of these curves is due entirely to the scale effect on μ at zero torque. The results, especially at the smaller angles of incidence appear very consistent and show no tendency to a critical change of lift coefficient for given μ within the present range of blade angle. This consistency further provides an important verification of the accuracy of the measurements of lift at varying velocity while the curves indicate the type of change of lift coefficient with μ for given incidence.

4.411. *Drag coefficients.*—The only observations of drag at varying velocity relate to blade angle 3° at incidences of 6°, 8° and 10°. For comparison with other blade angles the quantity $(D/L)'$ defined in section 4.11 as representing the total energy required to maintain the autogyro in its steady condition is plotted against μ in Fig. 17. The observed results are not very consistent and suggest what appeared probable when taking the observations, viz., that the readings of the drag balance were more uncertain than those of the lift. Apart from this inconsistency the curves appear higher than would be

expected from the corresponding observations at the smaller blade angles at zero torque, plotted on the same diagram. This may possibly be due purely to observational errors in reading the drag balance in the case of variable velocity, but there is another possible source of error which involves a general discussion of the basis of the present experimental method.

It is tacitly assumed in interpreting results of the tests at variable velocity that the forces involved, including the torque, are functions of the velocities (rotational and translational) only, i.e. that the effect of the acceleration derivatives is negligible. This is probably true as regards aerodynamic acceleration derivatives because the accelerations observed were always very small owing to the large amount of inertia of the model and the small torque coefficient. In the actual model, however, the blades were free to flap, and it is by no means certain that the instantaneous flapping motion will be the same when the angular velocity is varying as when it is constant. In the particular experiments just referred to, the model was decelerating and the amplitude of the flapping motion must have been increasing, that is, the inclination of the plane in which the blades move to the plane normal to the axle must have changed by a considerable amount during a run. This change of inclination must require the application of external forces (apart from aerodynamic forces) and this would be equivalent to an additional loss of energy in steady motion.

4.42. *Static deceleration test.*—The results of the static deceleration test are given in the following Table and do not call for special comment. They should be of interest, however, in connection with the analysis of results by strip theory as giving a determination of the mean profile drag coefficient of the section in a specially simple case.

TABLE.

4-Bladed Autogyro at Static. Blade angle 3°, axle vertical.

n	10	8	5	4	3
$10^4 \times Q_\Omega$	3·01	3·02	3·04	3·14	3·37

5.0. *Observations of the flapping of the blades.*—In order to measure the angular motion of the blades about their hinges, a small concave mirror was attached to the under-surface of one blade close to the hinge. Light from a 100 c.p. "Pointolite" lamp, about 7 ft. below the autogyro passed upwards through a large plate-glass window in the floor of the tunnel, was reflected at the concave mirror back through the window and came to a focus at the surface of a sheet of paper on a drawing board close to the lamp. As the model rotated and the blade flapped, this spot of light described a closed curve on the surface of the paper which could be traced in pencil. The blade

had two degrees of freedom (*see* Fig. 2); the first corresponding to rotation of the model about its main bearing, is represented by the angle ψ through which the model has rotated in its normal direction of rotation, from the position in which the blade is down wind; the second corresponding to the rotation of the blade about its hinge is represented by the flapping angle β which is taken to be zero when the blade is at right angles to the axis, and positive when the blade is inclined upwards.

For the purpose of explanation we shall assume for simplicity that both lamp and mirror lie on the axis of rotation of the autogyro and that the mirror is adjusted so that its axis is parallel to the axis of rotation when β is zero. The reflected beam thus strikes the paper on the axis of rotation when β is zero for all values of ψ; taking this point as origin of polar co-ordinates r, θ, the scale of r and the origin of θ can be chosen so that $r = \beta^*$ and $\theta = \psi$.

The results show that to a good approximation the tips of the blades move in a plane whose normal may be slightly inclined to the axis of rotation and which passes near the centre of the model. This is equivalent to a motion in which the value of β varies harmonically about a mean value β_0 the period being equal to the period of rotation; the equation of the motion is therefore

$$\beta = \beta_0 + \beta_1 \cos(\psi - \psi_1)$$

and the equation of the curve traced out by the spot of light is

$$r = \beta_0 + \beta_1 \cos(\theta - \psi_1)$$

which is the equation of a limaçon. The resemblance of the curve actually obtained to this form is obvious (Fig. 18). This formula represents the curve actually observed sufficiently closely to illustrate such modifications of the ideal adjustments as are necessary in practice. In the first place the mirror was situated at a radius of 3 inches from the axis and the lamp had to be set outside the surface of the drawing board. Both these divergencies could be sufficiently compensated by altering the angular adjustment of the mirror.

Owing to the limitation of the area of the glass window in the floor of the tunnel it was impossible to take observations at angles of incidence greater than 16°. In the later experiments the system was therefore modified by placing the lamp on the floor inside the tunnel and reflecting its beam upwards by means of a plane mirror. Even with this arrangement the reflected beam becomes increasingly oblique for angles of incidence of 16° and upwards, and the results at these angles are therefore perhaps somewhat less accurate.

From equation (1) it appears that if β_0 is zero the limaçon reduces to two coincident circles passing through the origin. The two branches of the curve can always be kept distinct by altering

* To a sufficient approximation since the greatest value of β observed was just over 10° (negative).

the adjustment of the mirror so that the origin corresponds to a value of β different from zero. It is convenient in practice to keep the two branches fairly close together but distinct. It is further necessary to identify the values of ψ corresponding to each loop of the curve which would otherwise be liable to an ambiguity of 180°. For this purpose a small piece of plane mirror was so placed on the drawing board that in describing one of the loops the spot of light crossed its surface. As it did so the rotating mirror (when viewed by reflection in this fixed mirror) flashed brightly, appearing dark for the remainder of the revolution, and its position in azimuth at the moment of flashing was easily located by the eye. The value of ψ becomes indeterminate at the two points where the curve passes through the origin but this does not cause serious difficulty in practice when the whole curve is traced. In certain cases it was considered sufficient to determine the value of β corresponding to $\psi = 0°$, 90°, 180° and 270° only, and it was then desirable to adjust the mirror so that the indeterminate points did not occur at these values of ψ.

The scale of the radius vector of the spot of light on the drawing board was about 3 inches for a variation of 1° and the image of the spot was about $\frac{1}{8}$ inch in diameter. It was therefore considered quite sufficiently accurate to sketch the path in pencil by hand, and it was found that the path was usually sufficiently steady to make this a comparatively easy operation. Where the path varied slightly, it was possible, after marking one position on the path, to wait until the spot again passed through this point before marking further points. It is considered that the relative accuracy obtainable in this way was well inside 0·1° on β.

The diagram of the path of the spot of light was calibrated as follows. The blade carrying the mirror was set at a given value of β ($-2°$, $-1°$, 0°, etc.) by means of a wire of adjustable length supporting the weight of the blade. For this purpose the clinometer proved convenient and accurate. It was set up along the surface of the blade for $\psi = 0$ or 180° so that the clinometer reading was equal to $i + \beta$ or $i - \beta$ where i is the known value of the incidence. The autogyro was then rotated about its axle and the circle described by the spot of light marked on the diagram. The autogyro was then set in four different positions in azimuth corresponding to ($\psi = 0°$, 90°, 180° and 270°), and the blade was rotated on its hinge, the straight line described by the path of the spot being marked on the diagram. The four paths thus marked should coincide in pairs at right angles to each other and intersect in the origin O. The circles on the diagram then provide a scale and a zero for the determination of β while the straight lines provide a zero and origin for the determination of ψ.

The time required for calibration was the chief drawback to the method, as the calibration had to be repeated at each angle of incidence and required distinctly more time than the actual making of the records.

5.01. *Flapping Observations. Range of Observations.*—The earliest observations of flapping were made at the original blade angle of 1·8° and covered the usual range of rotational speed (up to 10 revolutions per second) and of angle of incidence from 4° to 16°. These observations were made with every possible precaution to obtain the maximum accuracy of which the method was capable. Subsequently, observations were made at blade angles 3·0° and 1·0° over a similar range with a single observation at 2·3°. In these observations attention was directed to securing the greatest economy of time consistent with good accuracy. In particular in many cases the position of the path of the spot of light was marked at the four quadrants only ($\psi = 0°, 90°, 180°, 270°$) the remainder of the curve being roughly sketched or omitted. For the method of analysis described below this should cause no appreciable loss of accuracy.

With the blade angle set at 3° a limited number of observations of flapping were made at 12° and 10° incidence with the model driven by the electric starter. The results of these observations are included at the end of Table 4, but are not plotted in the figures as they do not correspond to the results at zero torque.

5.02. *Method of reduction.*—From the flapping diagrams the values of β and ψ were obtained by direct measurement from the calibration circles as already described. For the case of blade angle 1·8° the results were obtained for 24 equidistant values of ψ, and results for 12 values of ψ at 30° intervals are given in Table 4. A few specimen curves of β against ψ are shown in Fig. 19. The analysis of the observations is based on the expansion of β as a Fouriers series in ψ in the form

$$\beta = a_0 - a_1 \cos \psi - b_1 \sin \psi - a_2 \cos 2\psi - b_2 \sin 2\psi \ldots$$

The values of the coefficients a_0 a_1 and b_1 have been worked out in all cases by the following approximate formulæ. Writing β_a, β_b, β_c, β_d for the values of β at $\psi = 0°$, 90°, 180° and 270° respectively, it is easy to verify that, neglecting harmonic terms of the 4th and higher orders—

$$a_0 = \frac{1}{4}(\beta_a + \beta_b + \beta_c + \beta_d);$$

neglecting harmonic terms of the 3rd and higher orders—

$$a_1 = \frac{1}{2}(\beta_a - \beta_c)$$

$$b_1 = \frac{1}{2}(\beta_b - \beta_d).$$

In the case of observations at 0° and 3° blade angles, values of β were taken off at the four equidistant values of ψ only, but the above formulæ still remain applicable.

5.1. *Discussion of Results. General.*—To verify the accuracy of the simplified method of analysis curves have been recalculated from the first three terms of the expansion (a_0, a_1, b_1) only, and are shown in Fig. 19 for comparison with the observed curves. The closeness of the agreement suggests that the higher order harmonics are of small importance and the analysis has therefore been carried no further.

5.11. *The mean flapping angle* a_0.—To a first approximation the value of a_0 is determined by :—(*a*) the moment of gravity about the hinge (due to the weight of the blade), (*b*) the moment of the centrifugal force and (*c*) the moment of the thrust. Of these (*b*) is exactly and (*c*) approximately proportional to Ω^2 and independent of the incidence, while (*a*) is approximately constant. It follows that β_0 is a function of Ω of the form

$$\beta_0 = A - \frac{G_1}{I_1 \Omega^2}$$

where A is approximately constant ; G_1 is the moment of gravity about the hinge of a single blade and I_1 the corresponding moment of inertia. Accordingly, in Fig. 20, a_0 has been plotted against $1/n^2$ (proportional to $1/\Omega^2$) and it is found that all observations for a given blade angle lie fairly closely on a single straight line. On the same figure is shown the theoretical slope $G_1/I_1\Omega^2$ deduced from the observed values of G_1 and I_1 for this blade, viz., $G_1 = 2{\cdot}17$ lbs. feet, $I_1 = 0{\cdot}118$ slugs feet^2. The slopes of the observed straight lines differ from each other rather more than might be expected, but the theoretical slope constitutes a satisfactory mean value.

5.12. *Principal component* a_1 *of the flapping motion.*—The observed coefficient a_1 of $\cos\psi$ represents the semi-amplitude of the component oscillation in the plane of symmetry ; in Fig. 21 it is plotted against μ and shows the expected increase with increase of blade angle and with increase of μ. There is also a large and rapidly increasing scale effect for given incidence but much less scale effect for given μ. The present results lie fairly well on smooth curves and are reasonably self consistent.

5.13. *Lateral component* b_1 *of the flapping motion, and lateral force,* Y.—It is convenient to discuss the coefficient b_1 (representing the lateral inclination of the circle in which the blade tips move) and the lateral force Y together for the following reasons. It appears that on the assumptions of R. & M. 1111 * and R. & M. 1127 *, both b_1 and Y are exactly zero for the case of infinitely heavy straight blades neglecting gravity. It appears from R. & M. 1111 and R. & M. 1127 that the vanishing of b_1 and Y for straight blades depends to a high approximation on the vanishing of the " coning " angle a_0

* *loc. cit.*

only. This result depends on the original assumption that the interference velocity is constant over the autogyro disc, but in § 10 of R. & M. 1111 Mr. Glauert has suggested that the curvature of the stream will also give rise to terms in b_1 and Y, and he obtains formulæ on the assumption that the interference velocity varies linearly with the co-ordinate of position in the direction of forward motion. For the 6 foot wooden model it has been shown that the variation of the relative effect of gravity and centrifugal force produces an important variation of a_0 with rotational speed n, i.e. a fictitious " scale effect." This " scale effect " will appear in b_1 and Y in so far as they depend on the " coning " angle a_0; as regards their dependence on the curvature of the stream there should be no appreciable scale effect. These considerations both point to the importance of separating the two effects in discussing the observed values of b_1 and Y and suggest a method of doing so.

The observed values of b_1 and Y/L for each blade angle and incidence were first plotted against a_0 (*see* Fig. 22) for the case of blade angle 1·8°. These points lie fairly well on straight lines whose slopes indicate the dependence of the variables on a_0; the values of the slopes have been plotted in Fig. 22 against μ. The results for b_1 though very irregular show no systematic variation with blade angle. The continuous curve was calculated from the equation on page 12 of R. & M. 1127 neglecting the term in a_2.

$$b_1 = \frac{\frac{4}{3}\mu a_0}{1 + \frac{1}{2}\mu^2}$$

The observation points lie somewhat above this curve especially for large values of μ.

For Y/L observations are only available for the one blade angle $\theta = 1{\cdot}8°$. The theoretical formula of R. & M. 1111 equation (33) contains a factor depending on x and θ which vanishes for $\theta = 1{\cdot}6°$ and is positive for $\theta = 1{\cdot}8°$, while the value corresponding to the observed slope is negative. Accordingly a mean straight line has been drawn through the observed points.

To obtain the term in b_1 depending on the curvature of the stream, a value of a_0 has been chosen for each blade angle corresponding roughly to the result at the highest value of Reynolds number and the observed values of b_1 corresponding to these values of a_0 corrected to zero a_0 by means of the theoretical curve of slopes of Fig. 22. The values of a_0 chosen were

Blade angle	a_0
0°	0·8°
1·8°	1·4°
3·0°	2·0°

According to the assumptions of R. & M. 1111 § 10 the corrected values of b_1 should satisfy the relation

$$b_1 = \frac{v_1}{v} \cdot \frac{1}{2} \mu L_V$$

where v_1 is the difference between the velocity of downwash at the extreme front and rear of the autogyro. In the calculations of R. & M. 1111 Mr. Glauert assumes $v_1 = v$ and it is to be expected at any rate that v_1/v will be a constant. Accordingly in Fig. 22d the corrected values of b_1 have been plotted against μL_V. It appears that the observation points lie on straight lines of the same slope with an accuracy which can scarcely be accidental, but these straight lines fall below the origin by considerable amounts which also vary considerably with the blade angle. The diagram suggests that the large increase of b_1 with L_V is due to curvature of the stream but it is difficult to reconcile the observations with any probable law of variation of curvature with L_V and blade angle.

The lateral force ratio Y/L has been corrected in a similar way by means of the empirical straight line of Fig. 22c. The curve shows that Y/L is from 1° to 1·5° more negative than b_1. It may be remarked that the observations indicate that an increase of the "coning" angle a_0 will make both b_1 and Y/L more positive. The greater "coning" angle for the full scale machine due to the lower density of the blades would therefore agree with a change of Y/L from negative (force to port) in the model to positive (force to starboard) in the full scale machine over a part of the range, which is believed to be consistent with the full scale observations.

6.0. *Conclusions.*—The most important result of the present experiments is that they have revealed an appreciably higher value of L/D than have been recorded in any previous experiments on the autogyro in this country. The final maximum values of 7·5 for the 4-blader and 8·0 for the 2-blader (for blades only) are subject to some uncertainty on account of the large boss correction but they certainly give the correct order of magnitude. The order of magnitude of scale effect shown on the model makes it unlikely that the values for the corresponding full-scale autogyro are appreciably higher. It is true that the boss effect on the full scale machine is probably fairly small but the lower density of the blades, which gives an increased "coning" angle, is likely to counterbalance the aerodynamic scale effect tending to increase the L/D. Fig. 10 shows that the scale effect on the lift coefficient L_V is considerable and is to the advantage of the full scale machine.

An important application of the present series of tests is to supply a means of interpreting observations on a smaller scale model. The results of the present tests fully explain the difficulty of obtaining consistent results with a 3 ft. model whose blade angle was in the

neighbourhood of 2°, since such a model at 90 ft./sec. is well in the critical range where the stalling effect is important. The results of the present experiments indicate that the importance of the stalling effect increases very rapidly with increasing blade angle and only begins to be of importance when the blade angle differs by less than 1° from that at which the model ceases to autorotate. There is good reason to believe that the existing strip theory is competent to predict the effect of change of blade angle on the assumption that stalling does not occur. It should therefore, for example, be capable of predicting from experiments on a 3 ft. model made over a small range of blade angles below 1° the performance of the full scale machine at the largest blade angle at which stalling is unimportant. The present tests may be taken to indicate that the full scale machine will stall seriously at a blade angle of perhaps 1·5° greater than would a 3 ft. model. It is therefore suggested that any future experiments that may be required on the effect of varying the blade angle from root to tip and the shape and chord of the section should be made on a 3 ft. model over a small range of angle settings up to the largest blade angle at which the model appears efficient, and that for the purpose of prediction to full scale a blade angle of say 1° greater should be assumed as the most efficient, the results being deduced by theory from the model observations at the smaller blade angle. This suggestion is put forward provisionally as it still requires testing by means of the present results. It seems likely that the chief practical difficulty would be to make a 3 ft. model of which the boss drag is not too much greater than that of the full scale machine.

Estimate of probable performance of an autogyro.—Mr. Glauert* estimates theoretically the probable performance of a complete autogyro by assuming a drag coefficient of 0·015 on wing area corresponding to 0·0048 on disc area, for the standard Avro structure, and a curve of thrust power available, suitably modified to allow for the efficiency of the airscrew. From the curves of D/L against L_v given in the present report and the thrust power curves referred to above, performance curves have been calculated for autogyros having different diameters of rotating wings. The same body drag and body weight have been used in each case. In estimating the weight of a wing it was thought that to assume the weight to be proportional to the cube of the radius would unduly prejudice the larger diameters. For a given weight of machine it is probable that the wing spars would not have to be very much stouter and that the variation of weight would lie between the cube and the square. The latter power has been assumed here, so that the comparison is likely to favour the performance of the autogyro. Since the weight to be supported is constant the centrifugal force will not vary appreciably, and the weight of the shaft has been taken to be the same throughout.

* T.2144.—(Unpublished).

The results of these calculations are given in Fig. 23 which shows the horse power required for given speed with various diameters of rotor, in terms of the diameter ($D_0 = 35{\cdot}5$ ft.) of the standard machine. In the case of the 4-bladed autogyro it appears that a considerable improvement would be obtained by increasing the diameter to $D1{\cdot}2_0$, specially at the low speed end, but this result depends critically on the assumed law of increase of weight ; with the cube law no improvement would be obtained. The improvement in the 2-blader continues to increase with diameter even when D/D_0 is 1·5, though it is very unlikely that use could be made of such a large rotor especially with only two blades. The most useful improvement is in the surplus power available for climbing.

These results may be compared with the performance of an Avro biplane 504K, fitted with a 110 h.p. Le Rhone engine given in Martlesham Health report M.268a. The top speed obtained with this machine was 88 m.p.h. and the maximum rate of climb was 650 ft./min. at 60 m.p.h. In the tests made on the full scale autogyro given in T.2155 a rate of climb of 160 ft./min. and a maximum speed of 67 m.p.h. were attained, though it was thought that the engine was not developing its full power at the time. The maximum rate of climb deduced from the curves of Fig. 23 with 100 b.h.p. is 145 ft./min. and the speed range is from 40 to 70 m.p.h.* ; these are in fair agreement with the full scale figures.

A noticeable feature of the comparison is that the autogyro would be able to make greater use of a variable pitch airscrew if available, than would the aeroplane, since the " power available " curve could be raised at its low speed end by this means which would give the autogyro the ability to fly at still lower speeds and to increase its climbing power considerably while the stalling of the aeroplane would preclude use being made of the increase of available power consequent upon a change of airscrew pitch.

Although there is little real evidence available it seems unlikely that changes of section or twist of the blades will produce a very great increase of L/D, and we may conclude that in this respect the best value for the autogyro is not likely to exceed 1/2 of the best value for the corresponding aerofoil of normal aspect ratio.

In conclusion the authors wish to record their appreciation of the assistance at various times of Messrs. Nixon and Walker in the experimental work and of Miss Yeatman in reducing the observations.

* The Stalling speed lies between 25 and 30 m.p.h.

TABLE 1.

6 ft. diameter wooden autogyro model.

Dimensions of blade section.

Göttingen 429 modified : symmetrical section : chord = 5·36″.

Dimensions in multiples of chord length.

Distance from L.E.	Half thickness.
Radius at L.E.	0·022$_5$
0·05	0·034$_5$
0·10	0·047$_5$
0·15	0·052
0·20	0·055
0·25	0·057
0·30	0·056
0·40	0·052
0·50	0·045
0·60	0·038
0·70	0·031
0·80	0·023$_5$
0·90	0·014
Radius at T.E	0·005$_5$

TABLE 2.

Force Measurements. Blade Angle $\theta = 0°$.

Incidence i (degrees).		V	n,	$L_\Omega = \frac{L}{\pi \rho R^4 \Omega^2}$	$L_V = \frac{L}{\pi \rho R^2 V^2}$	D/L	$\mu = \frac{V \cos i}{R \Omega}$
Uncorrected.	Corrected.						
5	5·12	55·6	5·15	0·00846	0·026	0·166	0·573
	5·12	55·7	5·22	0·00858	0·027	0·163	0·566
	5·13	76·6	7·52	0·00814	0·028	0·163$_5$	0·541
	5·13	76·6	7·57	0·00811	0·028	0·162	0·537
	5·14	97·2	10·11	0·00784	0·030	0·161	0·509
6	6·16	47·6	5·20	0·00842	0·036	0·173	0·483
	6·18	62·1	7·39	0·00802	0·040	0·169	0·443
	6·20	78·9	9·84	0·00775	0·043	0·169	0·423
	6·21	92·0	11·77	0·00774	0·045	0·168	0·412
7	7·22	34·7	4·37	0·00841	0·047$_5$	0·181	0·420
	7·25	52·1	7·30	0·00783	0·055	0·181$_5$	0·378
	7·27	69·9	10·22	0·00773	0·059	0·180	0·362
	7·28	82·1	12·20	0·00778	0·061	0·180	0·356
8	8·32	48·6	7·60	0·00797	0·069	0·194	0·338
	8·33	59·8	9·68	0·00784	0·073	0·194	0·325
	8·35	66·9	11·0	0·00781	0·075	0·196	0·319
	8·35	72·3	11·91	0·00785	0·076	0·197	0·319
10	10·45	39·7	7·38	0·00801	0·097	0·224$_5$	0·281
	10·46	52·3	10·07	0·00793	0·101	0·225	0·271
	10·49	56·9	11·08	0·00785	0·106	0·226	0·268

TABLE 2 (*continued*).

Force Measurements. Blade Angle $\theta = 0°$ (*continued*).

Incidence i (degrees).		V	n	$L_\Omega = \frac{L}{\pi \rho R^4 \Omega^2}$	$L_V = \frac{L}{\pi \rho R^2 V^2}$	D/L	$\mu = \frac{V \cos i}{R \Omega}$
Uncorrected.	Corrected.						
14	14·69	32·3	7·50	0·00786	0·151	0·291	0·222
	14·71	32·3	7·56	0·00793	0·154	0·290	0·220
	14·79	40·8	10·07	0·00794	0·172	$0·291_5$	0·208
	14·81	45·9	11·43	0·00799	0·176	$0·292_5$	0·207
18*	19·02	26·8	7·46	0·00805	0·221	0·363	0·181
	19·01	33·7	9·30	0·00812	0·219	0·365	0·183
	19·03	33·7	9·56	0·00787	0·223	0·368	0·178
	19·09	38·8	11·14	0·00805	0·235	0·367	$0·175_5$
	19·14	38·8	11·47	0·00794	0·246	0·367	0·171
20	21·21	19·6	5·90	0·00806	0·261	0·407	0·165
	21·23	24·0	7·65	0·00796	0·287	0·409	0·157
	21·25	31·7	9·79	0·00796	0·270	0·408	0·162
	21·31	37·5	11·82	0·00803	0·284	0·408	0·158

*Rotational Speed unsteady.

TABLE 2 (*continued*).

Blade Angle $\theta = 1°$.

Incidence.		V	n	L_Ω	L_V	D/L	μ
Uncorrected.	Corrected.						
4	4·13	56·4	4·94	0·01047	0·028$_5$	0·154	0·605
	4·14	83·8	8·01	0·00974	0·031$_5$	0·145	0·554$_5$
	4·15	100·5	10·00	0·00951	0·033	0·143	0·532$_5$
5	5·18	47·6	4·96	0·01008	0·039	0·155	0·507
	5·20	64·9	7·47	0·00951	0·045	0·151	0·459
	5·22	81·3	9·84	0·00926	0·048	0·150	0·437
6	6·24	41·9$_5$	5·09	0·01011	0·053	0·161	0·435
	6·28	55·8	7·54	0·00941	0·061	0·160	0·390
	6·28	55·8	7·56	0·00929	0·060$_5$	0·161	0·389
	6·30	72·0	10·15	0·00933	0·066	0·159$_5$	0·374
	6·31	82·3	11·79	0·00932	0·068	0·160	0·368
8	8·42	37·4	6·05	0·00974	0·091	0·190	0·325
	8·44	44·6	7·48	0·00957	0·096	0·189$_5$	0·313
	8·47	58·0	10·15	0·00943	0·102$_5$	0·190	0·301
	8·49	64·8	11·51	0·00946	0·106	0·190	0·293
10	10·61	38·4	7·60	0·00955	0·133	0·223	0·264
	10·64	49·6	10·09	0·00951	0·140	0·224	0·257
	10·65	55·2	11·32	0·00956	0·143	0·224	0·255
14	14·96	30·7	7·57	0·00970	0·209	0·292$_5$	0·209
	15·01	40·1	10·12	0·00965	0·218	0·295	0·204
	15·03	44·5	11·32	0·00973	0·223	0·295	0·202
18	19·32	26·1	7·53	0·00966	0·285	0·361	0·175
	19·37	34·3	10·08	0·00965	0·295	0·362	0·172
	19·40	38·7	11·46	0·00966	0·301	0·363	0·170$_5$

TABLE 2 (*continued*).

Blade Angle $\theta = 1{\cdot}8°$. *Four Blades.*

Incidence.		V	n	L_Ω	L_V	D/L	μ
Uncorrected.	Corrected.						
3	3·14	57·6	4·56	0·01353	0·030	0·146	0·670
	3·15	80·5	6·97	0·01195	0·032	0·135	0·614
	3·15	100·6	9·07	0·01150	0·033	0·134	0·590
4	4·16	41·2	3·39	0·01477	0·036	0·148	0·644
	4·18	61·4	5·89	0·01230	0·040	0·144	$0{\cdot}552_5$
	4·19	80·5	8·06	0·01197	0·043	0·142	0·529
	4·20	94·5	9·74	0·01183	0·045	0·140	0·513
5	5·21	38·4	3·69	0·01407	0·046	0·154	0·551
	5·24	60·4	6·52	0·01267	0·052	0·152	0·489
	5·29	80·3	9·88	0·01186	0·064	0·150	0·431
6	6·24	30·6	2·85	0·01666	$0{\cdot}051_5$	0·166	0·627
	6·24	30·6	2·95	0·01561	0·052	0·176	0·605
	6·26	30·6	3·02	0·01538	0·056	0·178	$0{\cdot}534_5$
	6·29	45·7	5·26	0·01343	0·063	0·161	0·461
	6·38	71·2	10·27	0·01129	0·083	0·157	0·368
7	7·25	32·7	3·82	0·01397	0·068	0·184	0·451
	7·41	45·6	6·63	0·01177	0·088	0·175	0·362
	7·49	63·4	10·48	0·01092	0·106	0·175	0·319
8	8·38	29·0	3·66	0·01448	0·082	$0{\cdot}196_5$	0·417
	8·51	40·2	6·65	0·01149	0·112	$0{\cdot}187_5$	0·317
	8·59	56·9	10·35	0·01088	0·128	0·190	0·289

TABLE 2 (*continued*).

Blade Angle $\theta = 1 \cdot 8°$. *Four Blades* (*continued*).

10	10·68	27·8	5·25	0·01161	0·147	0·224	0·277
	10·74	37·5	7·60	0·01107	0·161	$0 \cdot 223_5$	0·258
	10·78	47·2	9·80	0·01101	0·169	$0 \cdot 224_5$	0·252
12	12·80	20·1	4·05	0·01212	0·175	0·267	0·258
	12·82	20·1	4·13	0·01184	0·178	0·263	0·252
	12·97	42·6	9·74	0·01126	0·210	0·263	0·227
	12·97	44·1	10·08	0·01128	0·210	0·260	0·227
14	15·02	19·4	4·44	0·1184	0·221	0·300	0·225
	15·18	39·8	10·03	0·1132	0·256	$0 \cdot 299_5$	0·205
16	17·23	18·2	4·57	0·01185	0·265	0·344	0·203
	17·36	36·5	9·84	0·01133	0·294	0·337	0·189
18	19·43	18·5	4·98	0·01187	0·306	0·374	0·187
	19·56	33·7	9·74	0·01131	0·334	0·377	0·175

TABLE 2 (*continued*).

Blade Angle $\theta = 1 \cdot 8°$. *Four Blades* (*Repeats*).

Incidence.		V	n	L_Ω	L_V	D/L	μ
Uncorrected.	Corrected.						
2	2·10	100·6	7·08	0·01272	0·022	0·143	$0 \cdot 753_5$
3	3·13	57·6	4·32	0·01402	0·028	0·160	0·706
	3·14	80·5	6·89	0·01187	0·031	0·141	0·619
	3·15	101·2	9·04	0·01157	0·033	0·137	$0 \cdot 593_5$
4	4·18	61·4	5·97	0·01201	0·040	0·146	$0 \cdot 544_5$
	4·19	80·5	8·10	0·01183	$0 \cdot 042_5$	0·144	$0 \cdot 526_5$
	4·21	95·0	10·00	0·01148	0·045	0·142	0·503
5	5·20	38·4	3·64	0·01403	0·045	0·162	0·559
	5·25	60·4	6·78	0·01207	0·054	0·150	0·471
	5·28	80·2	9·87	0·01138	0·061	0·149	0·430
	5·30	92·2	11·87	0·01118	0·066	$0 \cdot 148_5$	0·411
6	6·28	45·7	5·20	0·01318	0·061	0·167	0·464
	6·37	71·3	10·04	0·01136	0·080	0·162	0·374
	6·39	82·4	11·98	$0 \cdot 01132_5$	0·085	0·161	0·363
8	8·50	40·2	6·59	0·01157	0·110	0·190	0·320
	8·60	56·9	10·26	0·01124	0·130	0·193	0·291
	8·61	65·9	12·12	0·01098	0·132	0·193	0·285
20*	21·65	19·0	5·45	0·01185	$0 \cdot 346_5$	0·418	$0 \cdot 173_5$
	21·72	26·1	7·74	0·01151	0·361	0·418	0·168
	21·76	32·5	9·79	0·01146	0·370	0·420	0·166

* After breakage and repair of one blade.

TABLE 2 (*continued*).

Blade Angle $\theta = 1{\cdot}8°$. *Two Blades.*

Incidence.		V	n	L_Ω	L_V	D/L	μ
Uncorrected.	Corrected.						
4	4·10	55·4	5·51	0·00608	0·021	0·134	0·533$_5$
	4·10	73·2	7·67	0·00581	0·023	0·129	0·506
	4·11	90·8	10·00	0·00574	0·025	0·127	0·481
5	5·12	45·3	5·02	0·00617	0·027	0·144	0·477
	5·14	60·1	7·40	0·00577	0·031	0·142	0·430
	5·16	74·4	9·85	0·00560	0·035	0·136	0·399
6	6·16	37·5	4·77	0·00609	0·035	0·163	0·415
	6·17	37·5	4·90	0·00605	0·037	0·155	0·404
	6·21	49·7	7·49	0·00558	0·045	0·155	0·350
	6·21	49·7	7·51	0·00567	0·045	0·152	0·350
	6·23	61·7	9·89	0·00559	0·051	0·151	0·329
	6·25	61·7	9·83	0·00598	0·054	0·147	0·331
8	8·30	29·9	5·27	0·00590	0·065	0·185$_5$	0·299
	8·34	39·8	7·61	0·00564	0·073	0·184	0·275
	8·36	49·2	9·81	0·00562	0·079	0·185	0·264
12	12·54	22·0	5·19	0·00592	0·117	0·254	0·220
	12·61	29·0	7·48	0·00569	0·134	0·254	0·202
	12·67	36·6	9·86	0·00565	0·146	0·254	0·193
16	16·92	19·5	6·03	0·00586	0·199	0·325	0·165
	16·96	23·8	7·61	0·00577	0·210	0·326	0·159$_5$
	17·03	29·5	9·74	0·00576	0·223	0·328	0·154$_5$
20	21·25	19·0	6·76	0·00577	0·269	0·405	0·138
	21·29	21·4	7·71	0·00579	0·277	0·406	0·136
	21·34	26·6	9·80	0·00571	0·286	0·407	0·133

TABLE 2 (*continued*).

Blade Angle $\theta = 2 \cdot 3°$.

Incidence. Uncorrected.	Incidence. Corrected.	V	n	L_Ω	L_V	D/L	μ
4	4·19	59·4	4·89	0·01708	0·041	0·174	0·633
	4·21	80·6	7·40	0·01502	0·045	0·159$_5$	0·577
	4·22	100·6	9·71	0·01434	0·047$_5$	0·157	0·549
5	5·23	56·3	4·95	0·01796	0·049	0·194	0·602
	5·25	75·7	7·67	0·01521	0·056	0·166$_5$	0·523
	5·27	92·7	9·86	0·01491	0·060	0·164	0·498
6	6·28	57·0	5·84	0·01658	0·062	0·189	0·514$_5$
	6·32	67·9	7·60	0·01548	0·069	0·174	0·470$_5$
	6·35	78·0	9·51	0·01437	0·076	0·168$_5$	0·432
7	7·33	49·8	5·37	0·01751	0·073	0·194$_5$	0·488
	7·49	65·9	9·90	0·01324	0·106	0·179	0·360$_5$
8	8·40	48·1	6·20	0·01483	0·088	0·206	0·407
	8·55	54·2	8·62	0·01344	0·121	0·194	0·330
	8·60	60·7	10·18	0·01303	0·130	0·195	0·313
	8·62	66·4	11·46	0·01280	0·135$_5$	0·195	0·304
10	10·75	36·1	6·90	0·01254	0·163	0·229	0·273*
	10·83	47·4	9·64	0·01223	0·180	0·229$_5$	0·257
	10·86	57·1	11·73	0·01247	0·187$_5$	0·230$_5$	0·254
14	15·01	21·0	4·58	0·01293	0·218	0·300	0·236
	15·17	30·4	7·22	0·01265	0·253	0·301	0·217
	15·23	38·3	9·32	0·01261	0·265	0·301	0·212
	15·28	48·2	11·90	0·01273	0·276	0·302	0·209
20	21·61	19·8	5·38	0·01283	0·336	0·416	0·184
	21·72	26·0	7·34	0·01268	0·359	0·418	0·177
	21·83	33·3	9·72	0·01266	0·383	0·419	0·171
	21·88	40·5	11·86	0·01286	0·392	0·421	0·170

* At V = 25·3 the model "packed up."

TABLE 2 (*continued*).

Blade Angle $\theta = 3°$.

Incidence.		V	n	L_Ω	L_V	D/L	μ
Uncorrected.	Corrected.						
12	13·09	45·6	9·95	0·01397	0·236	0·278	0·238
	13·14	54·2	11·90	0·01449	0·248	0·271	0·236
	13·16	54·2	12·06	0·01428	0·251	0·274	0·233
14	15·26	34·8	8·06	0·01360	0·273	0·313	0·222
	15·31	41·3	9·73	0·01433	0·283	0·311	0·218
	15·36	48·0	11·42	0·01466	0·294$_5$	0·303	0·217
16	17·36	26·1	6·18	0·01466	0·293	0·348	0·215
	17·47	32·5	8·03	0·01454	0·316	0·344	0·206
	17·48	32·5	8·14	0·01425	0·318	0·345	0·203
	17·51	40·5	10·18	0·01440	0·325	0·349	0·302
	17·52	40·5	10·18	0·01450	0·326	0·347	0·202
	17·55	40·4	10·33	0·01423	0·332	0·347	0·199
	17·56	44·9	11·41	0·01460	0·335	0·342	0·201
18	19·45	18·6	4·41	0·01533	0·307	0·380$_5$	0·213
	19·67	30·3	7·94	0·01451	0·353	0·383	0·193
	19·68	30·7	7·98	0·01487	0·355	0·389	0·194$_5$
	19·69	36·8	9·72	0·01428	0·358	0·384	0·191
	19·74	36·8	9·76	0·01467	0·367	0·385	0·190$_5$
	19·74	36·7	9·87	0·01439	0·369	0·388	0·188
20	21·60	18·2	4·57	0·01472	0·331	0·423	0·199
	21·82	26·6	7·20	0·01442	0·376	0·423	0·184
	21·95	39·9	11·13	0·01455	0·403	0·427	0·179

For information about speed of "packing up" *see* § 3.0.

TABLE 3.

Tests at varying rotational speed.

Blade Angle $\theta = 1°$.

	n	$\mu = \frac{V \cos i}{R\Omega}$	$Q_\Omega = \frac{Q}{\pi \varrho R^5 \Omega^2}$
	2·27	0·574	−4·33 × 10⁻⁴
	2·50	0·522	−3·66
	2·78	0·470	−3·16
	3·12	0·418	−2·94
$i = 17·2°$*	3·33	0·391	−2·83
(16°)	3·85	0·339	−2·44
	4·16	0·313	−2·39
$V = 25·3$	5·00	0·261	−2·22
	5·56	0·235	−1·53
	6·25	0·209	−0·80₅
	6·86	0·190	
	2·38	0·689	−4·60 × 10⁻⁴
	2·50	0·656	−4·60
	2·78	0·590	−4·32
	3·12	0·525	−4·05
	3·33	0·492	−3·83
$i = 17·2°$	3·85	0·427	−3·49
(16°)	4·16	0·393	−3·33
	5·00	0·328	−2·88₅
$V = 31·8$	5·56	0·295	−2·77
	6·25	0·262	−2·55
	7·14	0·230	−1·50
	7·69	0·213	−1·17
	8·84	0·185	
	3·70	0·505	−2·39 × 10⁻⁴
	4·00	0·468	−2·16
	4·35	0·431	−1·93
$i = 10·6°$	4·54	0·411₅	−1·78
(10°)	4·76	0·393	−1·61
	5·26	0·355	−1·20
$V = 34·7$	5·55	0·337	−1·10
	3·88	0·318	−0·89
	6·25	0·300	−0·68
	7·04	0·265	
	4·76	0·538₅	−3·22 × 10⁻⁴
	5·00	0·512	−3·05
	5·26	0·487	−3·00
	5·88	0·436	−2·44
$i = 10·6°$	6·67	0·384	−2·02₅
(10°)	7·14	0·359	−1·80
	7·69	0·333	−1·55
$V = 48·6$	8·33	0·308	−1·16₅
	9·09	0·282	−0·78
	10·03	0·255	0·00

* Uncorrected incidence shown in brackets.

TABLE 3 (*continued*).

Blade Angle $\theta = 1 \cdot 8°$.

	n	μ	Q_Ω
	3·22	0·463	$-0 \cdot 98 \times 10^{-4}$
	3·33	0·447	−1·09
	3·57	0·418	−1·30
	3·84	0·388	−1·37
$i = 17 \cdot 3°$	4·54	0·328	−1·57
(16°)	5·00	0·299	−1·69
	5·56	0·268	−1·76$_5$
$V = 28 \cdot 9$	6·25	0·239	−1·55
	6·67	0·224	−1·18
	7·15	0·209	−0·52
	7·74	0·193	
	3·13	0·595	$-1 \cdot 17 \times 10^{-4}$
	3·33	0·558	−1·28
	3·57	0·520$_5$	−1·31
	3·84	0·484	−1·44
	4·17	0·446	−1·47
$i = 17 \cdot 3°$	4·54	0·409	−1·63
(16°)	5·00	0·372	−1·85
	5·56	0·335	−2·10$_5$
$V = 36 \cdot 0$	6·25	0·298	−2·08
	7·14	0·260	−2·10
	7·69	0·242	−1·99
	8·33	0·223	−1·47
	9·09	0·204$_5$	−0·60$_5$
	9·94	0·187	
	4·54	0·456	$-1 \cdot 39 \times 10^{-4}$
	5·00	0·414	−1·18
$i = 10 \cdot 7°$	5·56	0·373	−1·00
(10°)	6·25	0·331	−0·90
	6·67	0·311	−0·76
$V = 39 \cdot 3$	7·14	0·290	−0·55$_5$
	8·21	0·252	
	5·56	0·445	$-1 \cdot 60 \times 10^{-4}$
	6·25	0·395$_5$	−1·27
$i = 10 \cdot 7°$	6·67	0·370$_5$	−1·26
(10°)	7·14	0·346	−1·19
	7·69	0·321	−1·02
$V = 46 \cdot 8$	8·33	0·297	−0·93
	9·09	0·272	−0·46
	9·84	0·250	

TABLE 3 (*continued*).

Blade Angle $\theta = 1{\cdot}8°$ (*continued*).

	n	μ	Q_Ω
	3·33	0·756	$-2{\cdot}56 \times 10^{-4}$
	3·57	0·706	−1·89
$i = 6{\cdot}3°$	3·85	0·656	−1·59
(6°)	4·00	0·630	−1·39
	4·17	0·605	−1·19
$V = 47{\cdot}4$	4·64	0·554	−1·02
	5·00	0·504	−0·69
	5·26	0·478	−0·44
	4·00	0·776	$-2{\cdot}57_5$
	4·17	0·745	−2·51
	4·64	0·683	−2·22
$i = 6{\cdot}3°$	5·00	0·620	−1·89
(6°)	5·26	0·592	$-1{\cdot}66_6$
	5·56	0·559	−1·28
$V = 58{\cdot}4$	5·88	0·528	−1·02
	6·25	0·496	$-0{\cdot}85_5$
	6·67	0·465	$-0{\cdot}55_5$
	7·14	0·434	−0·39
	8·22		

Blade Angle $\theta = 2{\cdot}3°$.

	n	μ	Q_Ω
	4·76	0·327	$-0{\cdot}29 \times 10^{-4}$
	5·00	0·312	−0·75
$i = 17{\cdot}4°$	5·26	0·296	−0·97
(16°)	5·56	0·281	$-1{\cdot}03_5$
	5·88	0·265	−1·07
$V = 30{\cdot}2$	6·25	0·249	−1·10
	6·67	0·234	−0·94
	7·14	0·218	
	8·01	0·201	
	5·56	0·347	−0·53
	5·71	0·337	−0·67
	5·88	0·328	−0·76
	6·25	0·308	−0·89
$i = 17{\cdot}4°$	6·67	0·289	−1·18
(16°)	7·14	0·270	−1·32
	7·69	0·251	−1·40
$V = 37{\cdot}3$	8·33	0·231	−1·38
	8·70	0·222	−1·11
	9·09	0·212	$-0{\cdot}70_5$
	10·02	0·193	0·00

TABLE 3 (*continued*).

Blade Angle $\theta = 3°$.

	n	μ	Q_Ω	$L_\Omega = \frac{L}{\pi\rho R^4\Omega^2}$
$i = 17{\cdot}5°$ (16°) V = 21·0	7·5	0·145		
	7·0	0·155		
	6·5	0·167	$1{\cdot}51 \times 10^{-4}$	
	6·0	0·182	1·26	
	5·5	0·198	0·64$_5$	
	5·3	0·205	0·48	
	5·0	0·217	0·20	
	4·8	0·226	0·19	
	4·6	0·236	0·30	
	4·4	0·247$_5$	0·46	
	4·0	0·272	0·92	
	3·5	0·310	1·72	
	3·0	0·362	2·62	
$i = 17{\cdot}5°$ (16°) V = 32·0	6·0	0·276	0·13	
	5·9	0·280$_5$	0·25$_5$	
	5·8	0·285$_5$	0·35	0·0196
	5·7	0·291	0·46	0·0200
	5·5	0·301	0·80	0·0207
	5·0	0·331	1·37	0·0226
	4·5	0·368	2·04	0·0255
	4·0	0·414	2·73	0·0295
	3·5	0·478		0·0353
$i = 17{\cdot}5°$ (16°) V = 32·0	6·5	0·255		
	6·6	0·251	−0·17	0·0173$_5$
	6·8	0·244	−0·23	0·0167
	7·0	0·236	−0·28$_5$	0·0163
	7·2	0·230	−0·32$_5$	0·0161
	7·4	0·224	−0·41	0·0157
	7·6	0·218	−0·41$_5$	0·0153
	7·8	0·213	−0·25	0·0148
	7·9	0·210	−0·15	0·0146
	8·0	0·207	−0·06	
$i = 17{\cdot}5°$ (16°) V = 32·0	12·0	0·138		
	11·5	0·144	2·44	
	11·0	0·151	1·99	
	10·4	0·159	1·40	0·0113
	10·0	0·166	1·25	0·0122
	9·5	0·174$_5$	0·90	0·0125
	9·0	0·184	0·74	0·0131
	8·8	0·189	0·54	0·0134
	8·6	0·193	0·40$_5$	0·0137
	8·4	0·197	0·27	0·0139

TABLE 3 (*continued*).

Blade Angle $\theta = 3°$ (*continued*).

	n	μ	Q_Ω	L_Ω
	7·2	0·287	$0·05 \times 10^{-4}$	
	7·1	0·291	0·16	
$i = 17·5°$	7·0	0·295	0·32	0·0206
(16°)	6·9	0·299	0·39	0·0208
	6·5	0·318	0·75	0·0221
V = 40	6·0	0·344	1·15	0·0243
	5·5	0·376	$1·56_5$	0·0272
	5·0	0·413	2·07	0·0303
	7·8	0·265	—0·35	0·0186
	8·0	0·258	—0·41	0·0180
	8·5	0·243	—0·52	0·0169
$i = 17·5°$	9·0	0·230	—0·60	0·0161
(16°)	9·5	0·217	—0·47	0·0154
	9·7	0·213	—0·31	0·0151
V = 40	9·8	$0·210_5$	—0·23	0·0149
	9·9	$0·208_5$	—0·16	0·0148
	10·0	0·206	—0·09	0·0147
	10·1	0·204		0·0145
	8·0	0·286	—0·39	
	8·5	0·269	—0·55	
	9·0	0·254	$-0·65_5$	
	9·5	0·241	—0·75	
$i = 17·5°$	10·0	0·229	—0·69	
(16°)	10·5	0·218	—0·50	
	10·8	0·210	—0·33	
V = 44·2	11·0	0·208	—0·22	
	11·1	0·206	—0·15	
	11·2	0·204	—0·05	
	11·3	0·202		

TABLE 3 (*continued*).

Blade Angle $\theta = 3°$ (*continued*).

	n	L_Ω	$\frac{D}{L}$	μ	Q_Ω	$\left(\frac{D}{L}\right)' = \frac{D}{L} + \frac{Q\Omega}{LV}$
$i = 10{\cdot}9°$ (10°) $V = 40{\cdot}0$	9·5	0·0117	0·226	0·222	$2{\cdot}48 \times 10^{-4}$	0·322$_5$
	9·2	0·0125	0·227	0·229	1·60	0·284
	9·0	0·0128	0·225	0·234	0·78	0·252
	8·5	0·0131$_5$	0·226	0·248	0·43	0·239
	8·0	0·0137	0·224$_5$	0·264	0·48	0·238
	7·0	0·0156	0·219	0·301	0·63	0·233
	6·0	0·0179	0·220	0·351	0·86	0·234
	5·0	0·0209	0·229	0·422	1·24	0·243
	4·0			0·527	1·94	
$i = 10{\cdot}9°$ (10°) $V = 47{\cdot}9$	12·0	0·0113	0·228	0·210$_5$	1·16	0·278
	11·5	0·0112	0·233	0·220	1·00	0·274
	11·0	0·0115	0·237	0·230	0·81	0·268
	10·5	0·0124	0·236	0·241	0·51	0·253
	10·0	0·0132	0·235	0·253	0·39	0·247
	9·5	0·0140	0·233	0·266	0·31	0·242
	9·0	0·0146$_5$	0·232	0·281	0·30	0·239
	8·5	0·0153	0·232	0·297	0·39	0·241
	8·0	0·0160	0·232	0·316	0·43	0·241
	7·0	0·0209	0·236	0·361	0·72$_5$	0·246
	6·0	0·0244		0·421	0·96	
$i = 10{\cdot}9°$ (10°) $V = 55{\cdot}0$	11·5	0·0132	0·236	0·252	0·235	0·243
	11·0	0·0138	0·235	0·263	0·23	0·241
	10·5	0·0143	0·234	0·276	0·26	0·240
	10·0	0·0148	0·234	0·290	0·28	0·240
	9·5	0·0158$_5$	0·234	0·305	0·36	0·242
	9·0	0·0166	0·235	0·322	0·45	0·243
	8·5	0·0174	0·236	0·341	0·56	0·246
	8·0	0·0184	0·241	0·362	0·72	0·251
	7·5	0·0195	0·246	0·387	0·95	0·259
$i = 8{\cdot}6°$ (8°) $V = 55{\cdot}0$	11·8			0·247	0·89	
	11·4			0·256	0·81	
	11·0			0·265	0·72	
	10·5	0·0140		0·277	0·60	
	10·0	0·0136		0·291$_5$	0·58	
	9·5	0·0141		0·306$_5$	0·59	
	9·0	0·0148		0·324	0·64	
	8·5	0·0155		0·343	0·71$_5$	
	7·5	0·0171		0·388	0·92	
$i = 8{\cdot}6°$ (8°) $V = 55{\cdot}0$	11·7	0·0111	0·204	0·249	0·90$_5$	0·237
	11·4	0·0115	0·202	0·256	0·77	0·230
	11·0	0·0119	0·200	0·265	0·63	0·220
	10·5	0·0125	0·197	0·277	0·59	0·214
	10·0	0·0130	0·196	0·291	0·57	0·211
	9·0	0·0142	0·195	0·324	0·64	0·209$_5$
	8·0		0·199	0·364	0·80$_5$	

TABLE 3 (*continued*).

Blade Angle $\theta = 3°$ (*continued*).

	n	L_Ω	D/L	μ	Q_Ω	(D/L)′
	11·8	0·0126	0·202	0·269	$0·63 \times 10^{-4}$	0·221
	11·4	0·0130	0·199	0·279	0·58	0·215
$i = 8·6°$	11·0	0·0134	0·197	0·289	0·55	0·211
(8°)	10·5	0·0139	0·197	0·303	0·53	$0·209_5$
V = 60·0	10·0	0·0145	0·197	0·318	0·54	0·209
	9·0	0·0156	0·200	0·353	0·66	0·212
	8·0	0·0172	0·205	0·397	0·84	0·217
	11·4	0·0093	$0·158_5$	0·233	1·71	0·238
	11·0	0·0097	0·158	0·241	1·71	$0·231_5$
	10·5	0·0102	0·157	0·253	1·60	0·220
$i = 6·3°$	10·0	0·0106	0·158	$0·265_5$	1·51	0·212
(6°)	9·5	0·0111	0·159	0·280	1·43	0·205
	9·0	0·0116	0·160	0·295	1·28	0·197
V = 49·9	8·5	0·0120	0·161	0·312	1·18	0·193
	8·0	0·0125	0·161	0·332	1·04	0·187
	7·5	0·0131	0·163	0·354	1·08	0·187
	7·0	0·0138	0·165	0·380	1·08	0·186
	11·5	0·0106	0·164	0·277	1·14	0·203
	11·0	0·0113	0·163	0·290	1·04	0·195
	10·5	0·0119	0·163	0·304	1·01	0·191
$i = 6·3°$	10·0	0·0125	0·162	0·319	0·93	0·185
(6°)	9·5	0·0131	0·162	0·336	0·92	0·183
	9·0	0·0135	0·163	0·355	$0·90_5$	0·184
V = 60·0	8·5	0·0141	0·166	0·376	0·94	0·184
	8·0	0·0145	0·172	0·399	0·93	0·188
	7·5	0·0153	0·177	0·425	0·95	0·192
	7·0	0·0162	0·183	0·456	$0·98_5$	0·197
	11·8		0·182	0·315	0·75	
	11·4		0·177	0·326	0·77	
	11·0		0·173	0·339	0·79	
$i = 6·3°$	10·5	0·0136	0·163	0·355	0·80	0·180
(6°)	10·0	$0·0140_5$	0·165	0·372	0·84	0·181
	9·5	0·0146	0·168	0·392	0·84	0·183
V = 70·0	9·0	0·0151	0·171	0·414	$0·85_5$	0·184
	8·5			0·438	0·84	
	8·0			0·466	0·85	
	7·5			0·497	0·87	

TABLE 4

Observations of the Flapping Motion.

Blade Angle $\theta = 0°$.

Incidence i (degrees).		V	n	Values of β (degrees).				Coeff. in Fourier expansion.			μ
Corrected.	Uncorrected.			$\psi = 0$	90	180	270	a_0	a_1	b_1	
5·1	5°	52·2	4·78	—4·21	0·48	3·63	—0·07	—0·04	3·92	—0·27	0·578
		63·4	6·12	—3·52	0·45	3·83	0·52	0·32	3·67	0·03	0·548
		82·8	8·38	—2·86	0·35	3·91	1·88	0·84	3·38	0·76	0·522
6·2	6°	47·9	5·30	—2·74	0·44	3·00	0·49	0·30	2·87	0·02	0·477
		63·4	7·47	—2·08	0·57	3·33	1·10	0·73	2·70	0·26	0·448
		82·0	10·10	—1·64	0·69	3·41	1·41	0·97	2·52	0·36	0·429
8·3	8°	35·6	5·16	—2·14	0·00	2·04	0·64	0·13	2·09	0·32	0·363
		47·0	7·18	—1·33	0·20	2·33	1·26	0·61	1·83	0·53	0·344
		63·5	10·10	—1·04	0·27	2·65	1·50	0·89	1·94	0·61	0·330
10·5	10°	29·2	5·12	—1·44	—0·33	1·65	0·79	0·17	1·54	0·56	0·298
		40·3	7·46	—0·99	—0·05	2·13	1·62	0·68	1·56	0·83	0·282
		53·0	9·78	—0·66	0·11	2·39	1·97	0·95	1·52	0·93	0·283
14·7	14°	18·3$_5$	4·10	—1·74	—0·98	1·16	0·50	—0·26	1·45	0·74	0·230
		31·6	7·53	—0·76	—0·35	2·03	2·00	0·73	1·39	1·18	0·215
		41·8$_5$	10·3	—0·53	—0·26	2·32	2·26	0·95	1·42	1·26	0·208$_5$
19·1	18°	19·0	5·20	—1·13	—1·03	1·22	1·38	0·11	1·17	1·20	0·184
		26·8	7·53	—0·73	—0·68	1·91	1·93	0·61	1·32	1·30	0·179
		35·7	10·30	+0·55	—0·51	2·16	2·20	0·82	1·35	1·35	0·174

TABLE 4 (*continued*).

Blade Angle $\theta = 1{\cdot}8°$.

Incidence.		V	n	Values of β (degrees).												Coeff. in Fourier Expansion.			μ
Corrected.	Uncorrected.			$\psi = 0$	30	60	90	120	150	180	210	240	270	300	330	a_0	a_1	b_1	
4·2°	4°	41·2	3·05$_5$	− 9·57	−7·01	−2·94	1·55	4·89	7·20	7·80	6·50	3·38	−1·10	−5·53	−8·89	−0·33	9·18	−1·32	0·730
		61·4	5·69	− 5·80	−4·65	−1·69	1·49	4·39	6·58	7·54	7·00	4·78	+1·64	−1·83	−4·95	+1·19	6·72	+0·07	0·571
		80·5	7·93	− 4·92	−3·95	−1·71	1·55	4·27	6·47	7·32	6·85	5·16	1·98	−1·45	−4·12	1·48	6·12	0·21	0·537
5·25	5°	38·7	3·44$_7$	− 7·86	−6·24	−2·72	0·93	4·30	6·48	7·28	6·43	3·78	0·38	−3·97	−7·06	0·18	7·57	−0·27	0·594
		60·4	6·47	− 4·78	−3·96	−1·79	1·00	3·80	5·75	6·82	6·53	4·86	2·04	−0·79	−3·65	1·27	5·80	+0·52	0·494
		80·5	9·30	− 3·77	−3·03	−1·03	1·32	3·72	5·61	6·50	6·22	4·78	2·44	−0·34	−2·79	1·62	5·13	0·56	0·457
6·3	6°	30·5$_8$	2·60$_5$	−10·33	−7·66	−3·32	0·75	4·30$_5$	6·41	6·83	5·34	1·95	−2·03	−6·59	−9·90	−1·19	8·58	−1·39	0·618
		45·7	4·42	− 5·32	−4·17	−1·75	0·77	3·65	5·54	6·31	5·76	3·86	+1·04$_5$	−2·06	−4·51	+0·70	5·81	+0·13	0·546
		45·5	5·19	− 4·66	−3·77	−1·66	0·95	3·47	5·32	6·18	5·83	4·25	1·59$_5$	−1·57	−3·70	1·01	5·42	0·32	0·463
		71·2	10·02	− 2·52	−2·01	−0·45	1·03	3·05	4·60	5·44	5·30	4·18	2·42	−0·31	−1·73	1·59	3·98	0·69	0·375
8·5	8°	28·9	3·34$_5$	− 5·81	−5·14	−2·97	0·00	2·97	5·50	6·33	5·09	3·04	0·00	−3·33	−5·09	0·13	6·07	0·00	0·453
		40·2	6·44	− 2·23	−2·13	−1·14	0·47	2·12	3·53	4·40	4·48	3·70	2·19	+0·17	−1·28	1·21	3·31	0·86	0·328
		57·9	10·19	− 1·33	−1·41	−0·72	0·54	2·10	3·41	4·37	4·53	3·96	2·72	1·16	−0·17	1·57	2·85	1·09	0·298
10·7	10°	27·8	5·22	− 2·07	−1·96	−1·08	0·17	1·68	2·92	3·69	3·75	3·04	1·69	0·00	−1·31	0·87	2·87	0·76	0·278
		37·5	7·54	− 1·38	−1·43	−0·73	0·43	1·81	3·05	3·90	4·10	3·52	2·37	0·93	−0·53	1·33	2·64	0·97	0·260
		47·1	9·74	− 1·04	−1·13	−0·53	0·63	1·89	3·13	4·03	4·25	3·75	2·65	1·23	0·00	1·57	2·53	1·01	0·252
12·9	12°	20·1	4·02	− 2·45	−2·36	−1·53	−0·20	1·01	2·18	2·96	3·04	2·34	1·00	−0·39	−1·66	0·33	2·70	0·60	0·258
		28·8	6·14	− 1·90	−1·41$_5$	−0·89	+0·10	1·33	2·54	3·45	3·69	3·28	2·31	+1·02	−0·36	1·14	2·37	1·10	0·243
		42·6	9·62	− 0·70	−1·02	−0·60	0·22	1·46	3·09	3·79	4·13	3·77	2·89	1·59	—	1·55	2·24	1·33	0·229
15·1	14°	19·4	4·22$_5$	− 1·92	−2·11	−1·63	−0·70	0·61	1·83	2·73	3·02	2·60	1·64	0·16	−0·96	0·44	2·32	1·17	0·235
		25·4	5·91	− 1·12	−1·47	−1·09	−0·24	1·07	2·27	3·29	3·73	3·43	2·51	1·26	0·00	1·11	2·20	1·37	0·220
		39·8	9·87	− 0·61	−1·04	−0·74	+0·08	1·31	2·62	3·72	4·25	4·01	3·13	1·80	0·41$_5$	1·58	2·16	1·53	0·207
17·8	16°	18·2	4·53	− 1·60	−1·98	−1·57	−0·70	0·63	1·85	2·87	3·30	3·05	2·10	0·79	−0·40	0·72	2·23	1·28	0·204
		24·0	6·23	− 1·10	−1·48	−1·12	−0·17	1·00	2·33	3·40	3·88	3·63	2·73	1·38	—	1·21	2·25	1·45	0·195
		36·5	9·84	− 0·33	−1·02	−0·93	−0·12	1·17	2·50	3·58	4·27	4·22	3·42	2·10	—	1·64	1·94	1·77	0·188

TABLE 4 (*continued*).

Blade Angle $\theta = 2{\cdot}3°$.

Incidence.		V	n	Values of β (degrees).				Coeff. in Fourier expansion.			μ
Corrected.	Uncorrected.			$\psi = 0$	90	180	270	a_0	a_1	b_1	
	6°	68·0	8·0	—4·76	0·78	7·55	3·10	1·67	6·15	1·16	0·448
		78·0	10·27	—3·78	0·67	6·75	3·03	1·67	5·26	1·18	0·402

Blade Angle $\theta = 3°$.

13·1	12°	46·0	10·10	—1·45	0·30	5·10	3·65	1·90	3·27	1·67	0·235
		53·6	11·91	—1·25	0·45	5·20	3·80	2·05	3·22	1·67	0·232
15·3	14°	35·4	8·13	—1·55	—0·25	4·70	3·30	1·65	3·12	1·77	0·223
		42·1	10·04	—1·20	+0·20	4·75	3·55	1·82	2·98	1·67	0·214
		49·6	11·95	—1·05	0·35	4·90	3·70	1·97	2·97	1·67	0·212
17·5	16°	26·1	6·22	—1·70	—0·25	4·60	3·30	1·49	3·15	1·77	0·212
		32·5	8·09	—1·25	—0·10	4·65	3·75	1·76	2·95	1·92	0·203
		39·1	9·90	—0·95	+0·05	4·75	3·90	1·98	2·85	1·92	0·200
		46·2	11·80	—0·75	0·25	4·85	4·15	2·12	2·80	1·95	0·198
21·8	20°	19·0	4·83	—1·90	—0·95	3·70	3·00	0·86	2·80	1·97	0·194
		23·3	6·20	—1·50	—0·60	4·20	3·40	1·37	2·85	2·00	0·185
		28·2	7·68	—1·20	—0·40	4·40	3·80	1·65	2·80	2·10	0·181
		36·5	10·10	—0·90	—0·20	4·50	4·00	1·85	2·70	2·10	0·180
		39·9	11·10	—0·80	—0·20	4·50	4·00	1·87	2·65	2·10	0·178

TABLE 4 (*continued*).

Blade Angle $\theta = 3°$, *starter in gear.*

Incidence.		V	n	Values of β (degrees).				Coeff. in Fourier expansion.			μ
Corrected.	Uncorrected.			$\psi = 0$	90	180	270	a_0	a_1	b_1	
	10°	27·9	8·4	—8·7	—0·17	2·92	2·41	$1·07_5$	1·89	1·31	0·173
		37·6	8·33	—1·61	+0·35	4·26	2·70	1·42	2·94	1·20	0·234
		47·3	10·2	—1·54	0·45	4·63	2·85	$1·59_5$	3·09	1·19	0·246
	10°	20·5	10·25	—0·95	—0·40	2·70	2·05	0·85	$1·82_5$	$1·22_5$	0·104
		29·0	11·05	—0·8	—0·10	2·9	2·50	1·12	1·85	1·30	0·136
		35·5	10·23	—0·9	—0·10	3·4	2·75	1·29	2·15	$1·42_5$	0·181
		41·1	10·13	—1·0	—0·10	3·95	2·95	1·45	$2·47_5$	$1·52_5$	0·210
	12°	19·5	6·46	—1·1	—0·45	2·5	2·30	0·81	1·90	$1·37_5$	0·156
		32·8	7·73	—1·5	+0·5	4·2	3·0	1·55	2·85	1·25	0·219
		27·6	6·10	—2·0	—0·5	4·3	2·70	1·12	3·15	1·60	0·233

TABLE 5.

Lateral Force Y.

Blade Angle $\theta = 1{\cdot}8°$.

Incidence i (degrees).		V	n	$Y_\Omega = \frac{Y}{\pi \rho R^4 \Omega^2}$	$\frac{Y}{L}$
Uncorrected.	Corrected.				
4°	4·2	40·9	3·055	$-6{\cdot}03 \times 10^{-4}$	−0·0387
		61·0	5·69	−3·48	−0·0281
		80·0	7·93	−3·17	−0·0264
5°	$5{\cdot}2_5$	38·5	3·447	−4·17	−0·0292
		60·0	6·47	−2·92	−0·0230
		80·0	9·30	−2·53	−0·0213
6°	6·3	30·37	2·605	−6·25	−0·0368
		45·4	4·42	−3·14	−0·0226
		70·8	10·02	−1·66	−0·0147
8°	8·5	28·77	3·345	−3·81	−0·0246
		39·9	6·44	−1·37	−0·0118
		57·5	10·19	−1·12	−0·0103
10°	10·7	27·6	5·22	−1·05	−0·0090
		37·2	7·54	−0·88	−0·0079
		46·8	9·74	−0·80	−0·0073
12°	12·9	19·93	4·02	−1·56	−0·0129
		28·55	6·14	−1·01	−0·0088
		42·23	9·62	−0·80	−0·0071
14°	15·1	19·2	4·225	−1·36	−0·0116
		25·17	5·91	−1·18	−0·0071
		39·4	9·87	−0·72	−0·0070
16°	17·3	17·96	4·53	−0·24	−0·0021
		23·7	6·23	−0·25	−0·0024
		36·05	9·84	−0·48	−0·0046

Printed by H.M.S.O. Press, Harrow.

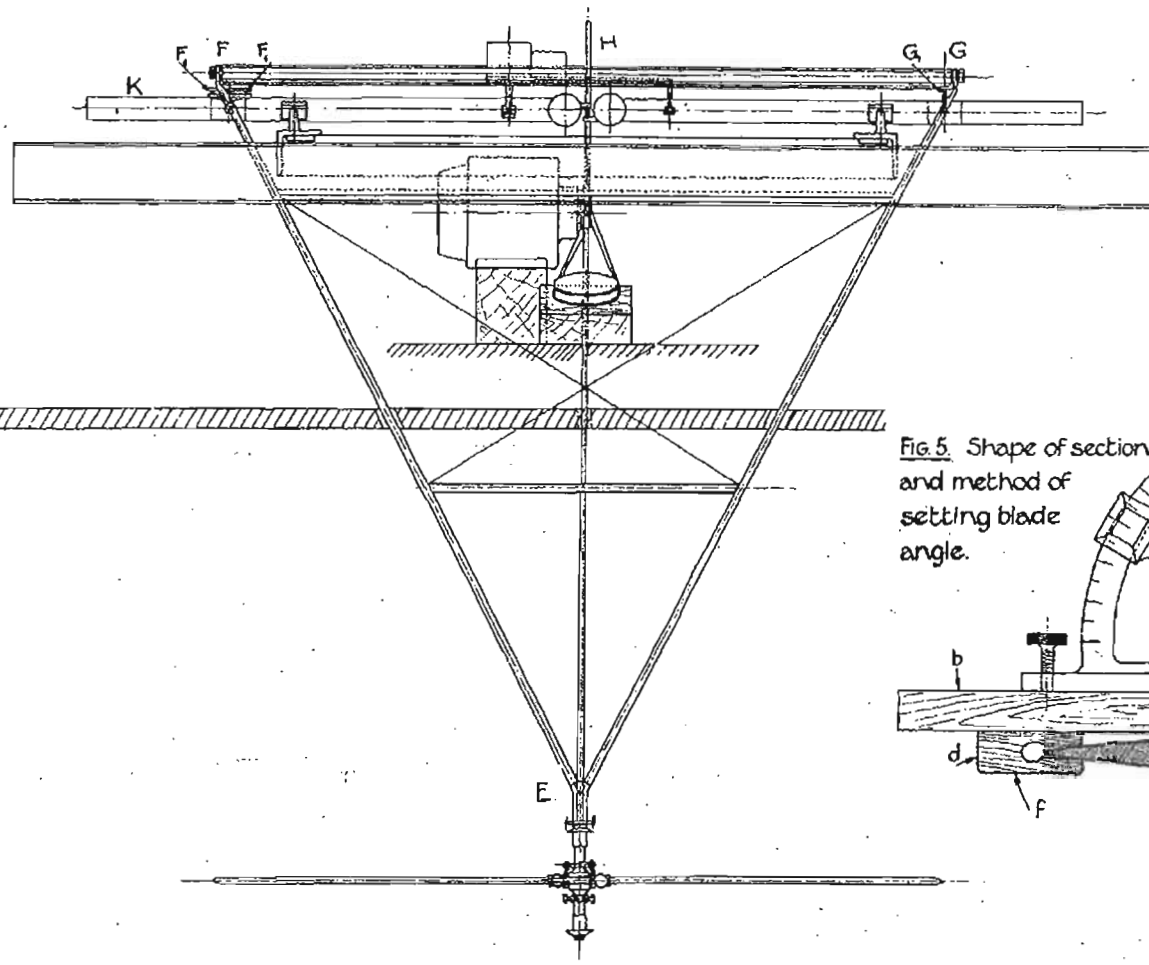

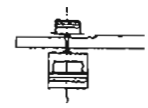

Fig.5. Shape of section and method of setting blade angle.

AUTOGYRO MODELS.

Fig.4. Elevations of Autogyro Balance with 6 ft. Model in Duplex Tunnel.

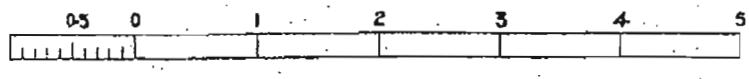

R.1154. 6/4 5007, 1607. 775, 10/28.

Figs. 4 & 5.

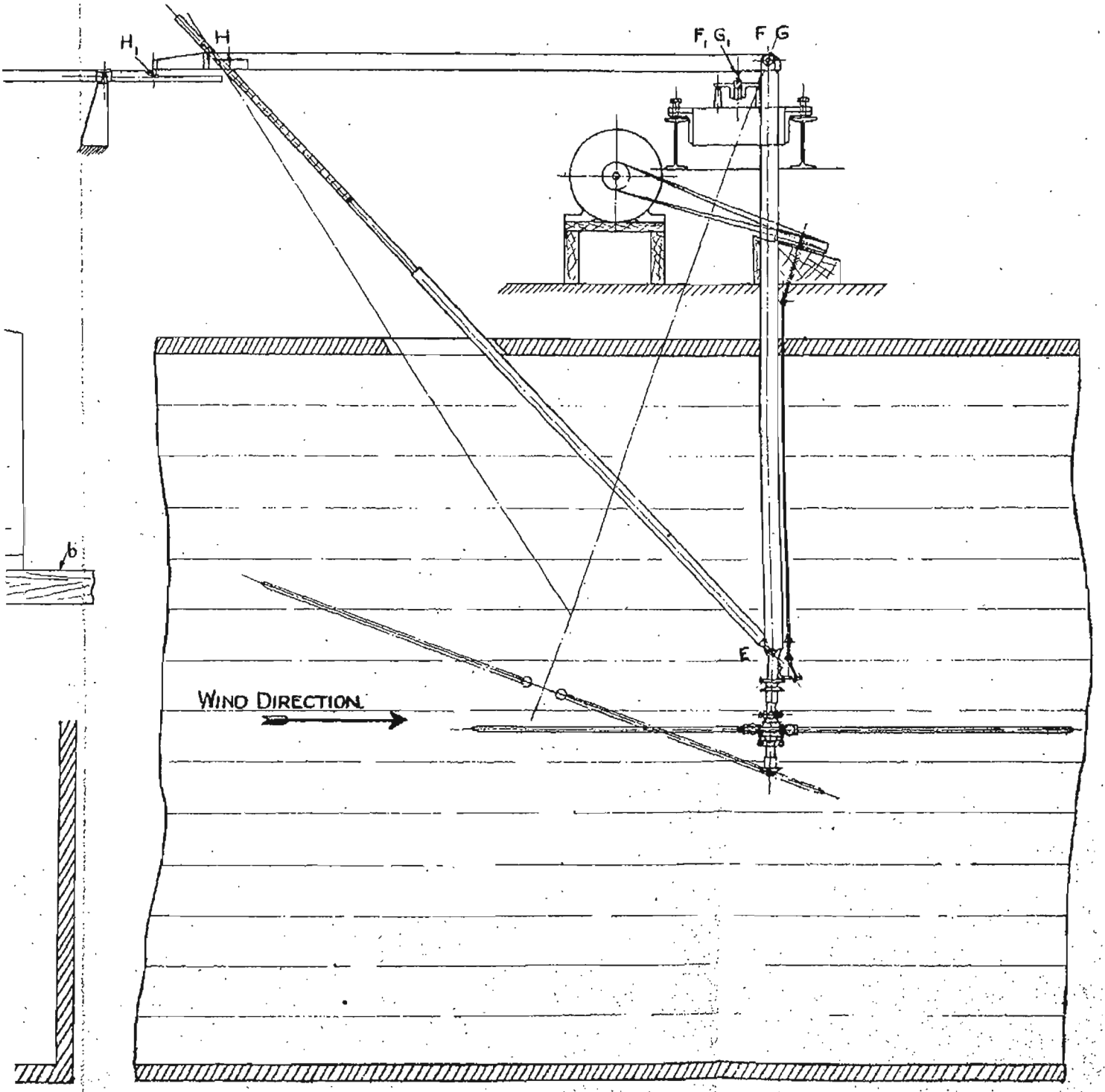

Malby & Sons Photo-Litho.

R&M.1154.

FIG. 6.

Force Measurements on 6 foot Model Autogyro.
Effect of change of blade angle.

D/L (corrected for drag of boss) plotted against $L_V = \frac{L}{\pi R^2 \rho V^2}$

4 Bladed model at 10 revolutions per second
at blade angles as marked on curves.

——— lines show values of incidence i (uncorrected).

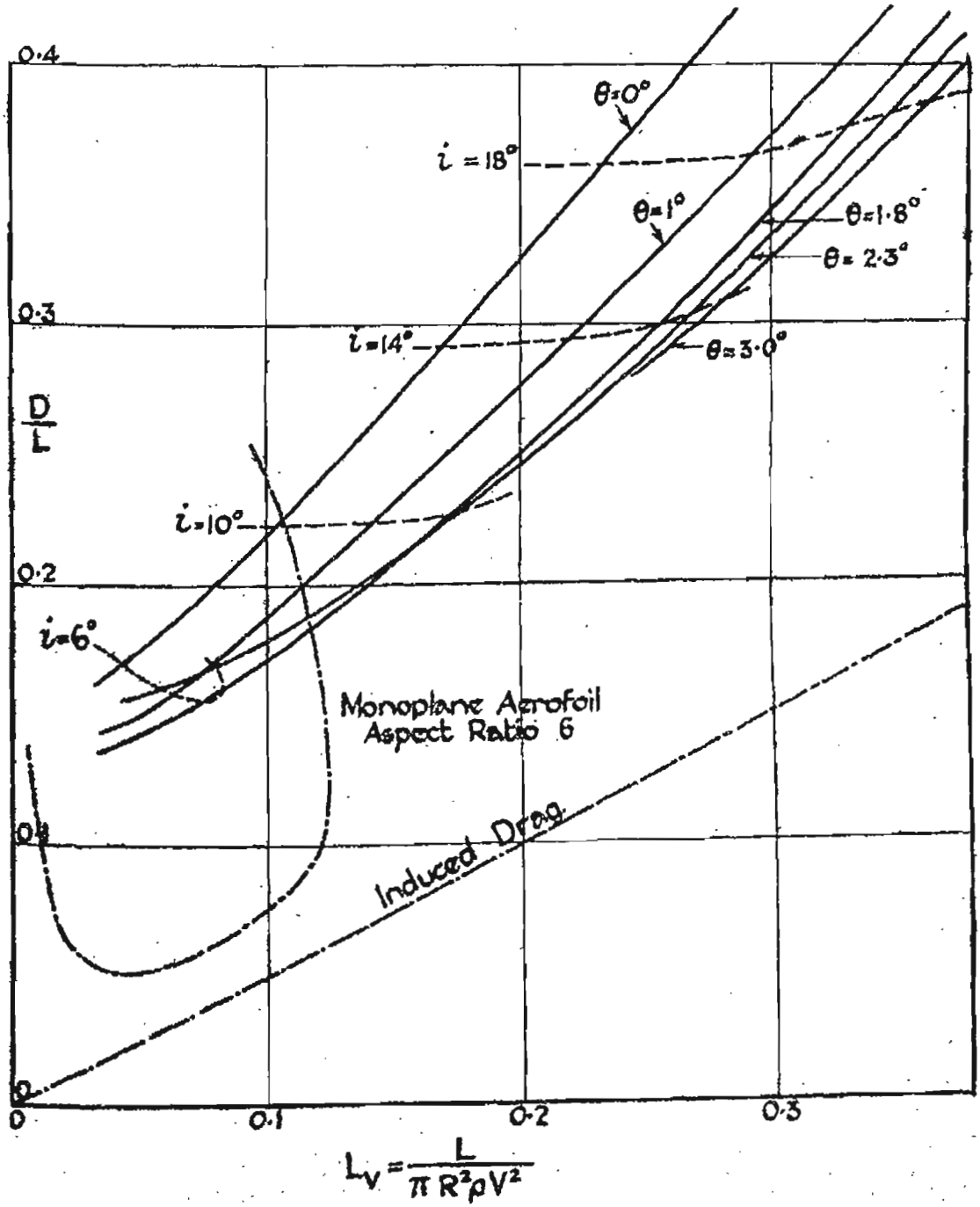

Malby & Sons, Photo-Litho.

R.&M.1154.

FIG. 7.

Force Measurements on 6 foot Model Autogyro.
Effect of change of blade angle.

$L_V = \frac{L}{\pi R^2 \rho V^2}$ against incidence i

4 Bladed model at 10 revolutions per second at blade angles as marked on curves.

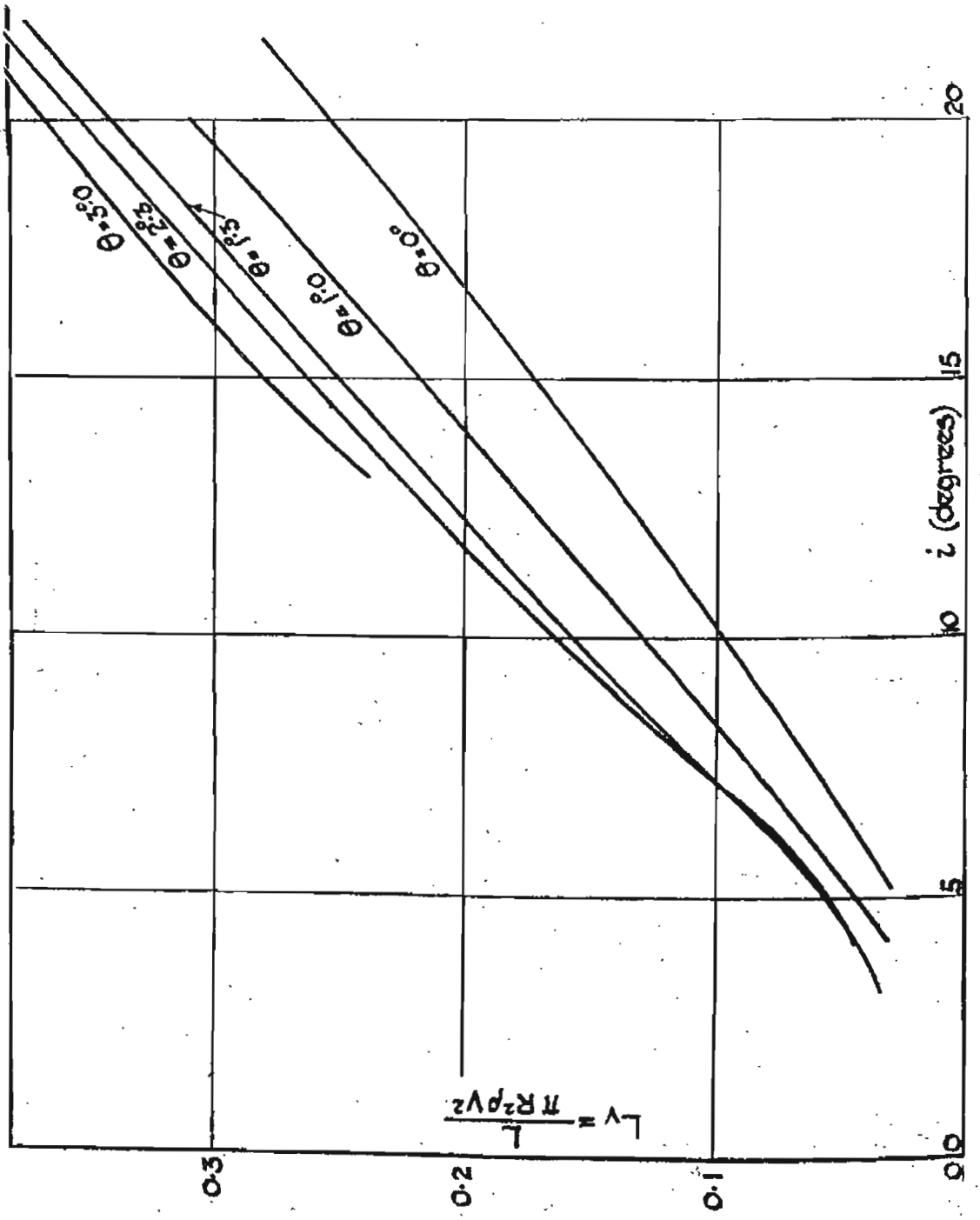

R19/4

Malby & Sons, Photo-Litho

R.&M.1154.

FIG. 8.

Force Measurement on 6 foot Model Autogyro.

Effect of change of blade angle and scale.

$L_\Omega = \frac{L}{\pi R^4 \rho \Omega^2}$ against incidence i

4 Bladed model at blade angles and rotational speeds revolutions per second as marked on curves.

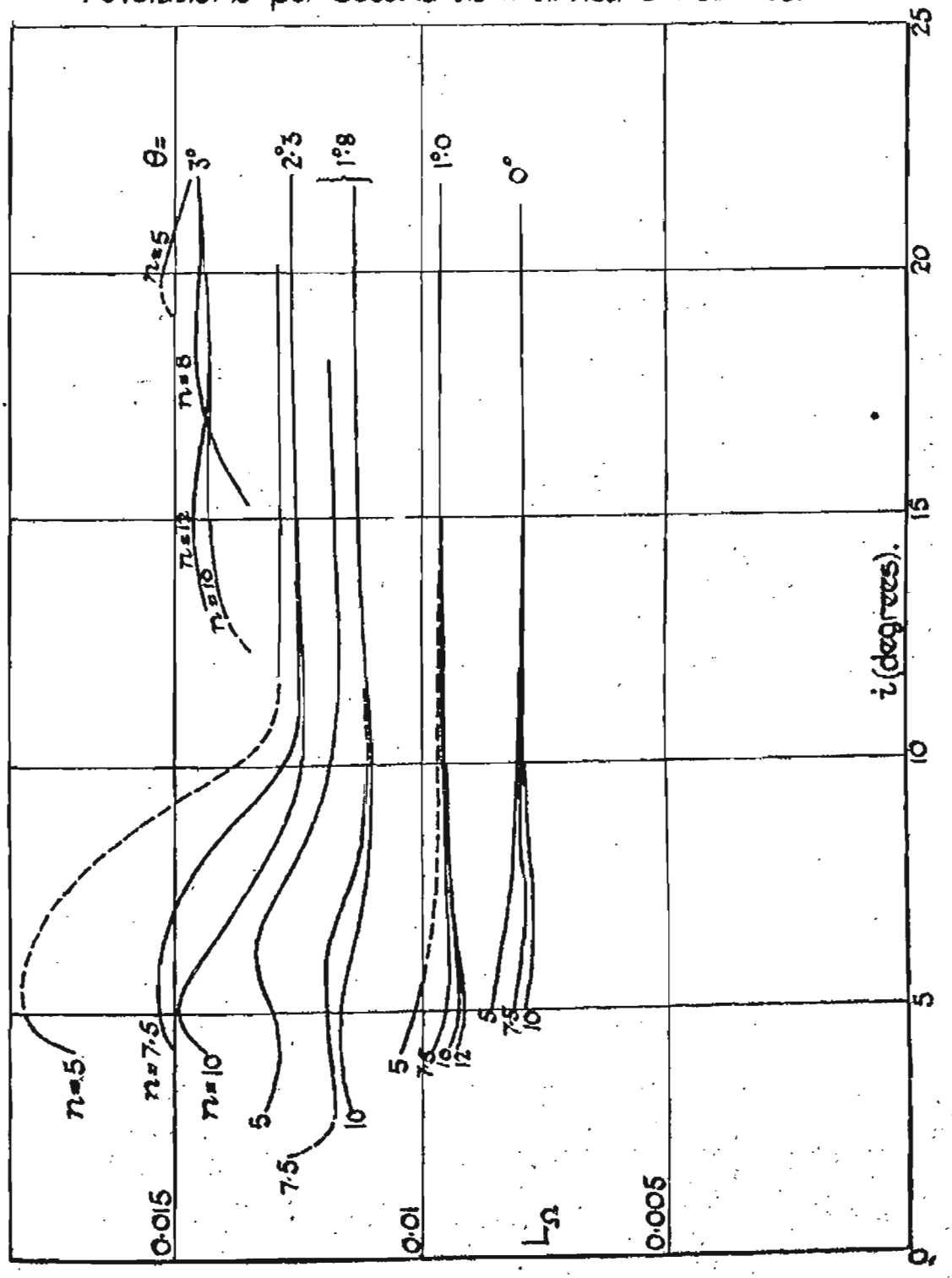

R.1914A

Malby&Sons Photo Litho

R.&M.1154.

FIG. 9.

Force Measurements on 6 Foot Model Autogyro. Effect of change of scale.

D/L (corrected for drag of boss) against n (revolutions per sec.).

4 Bladed model at blade angles 1°·8 and 2°·3 at values of incidence i (uncorrected) as marked on curves.

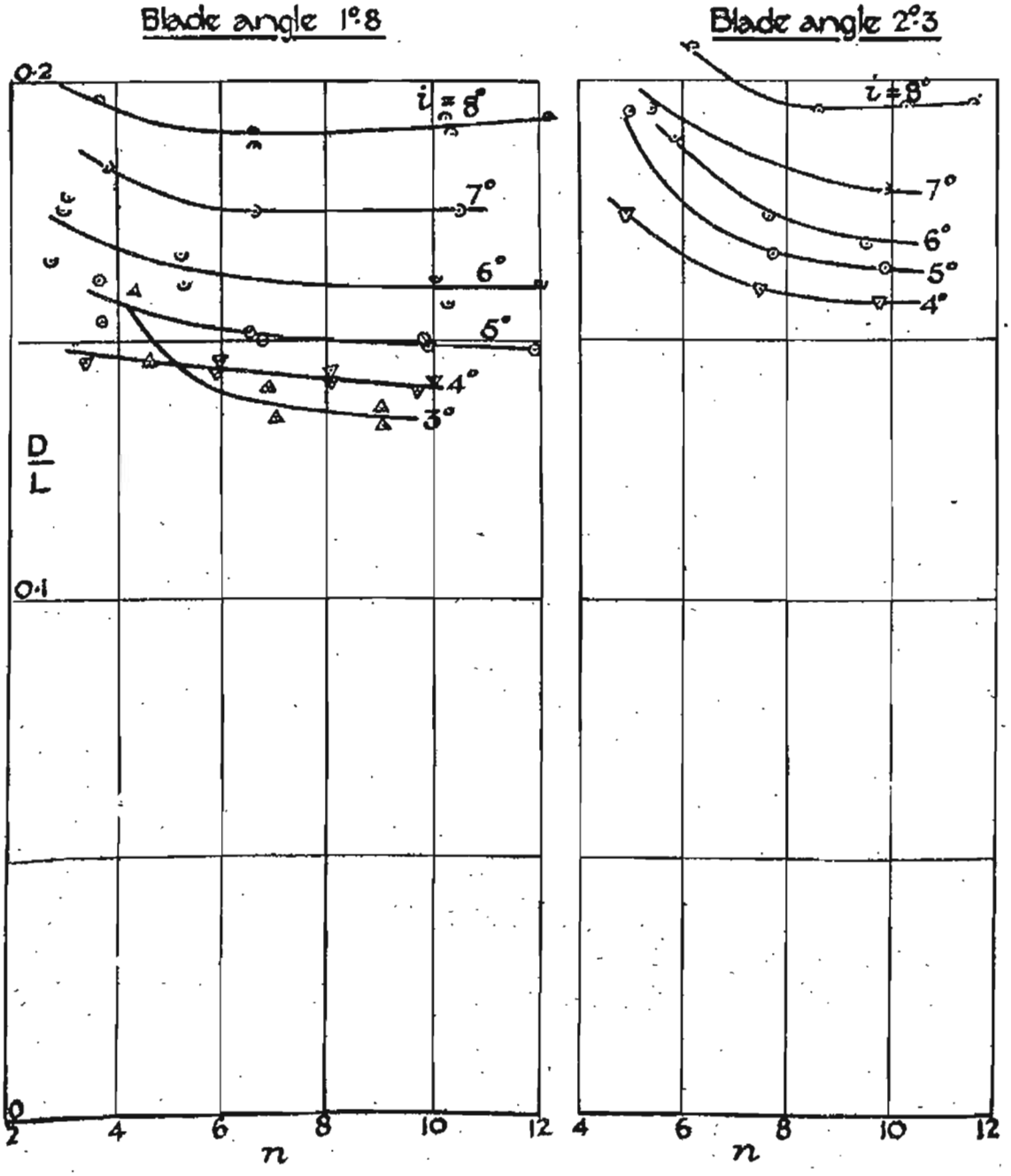

Malby & Sons, Ph

R.&M.1154.

FIG.10.

Force Measurements on 6 Foot Model Autogyro.
Effect of change of scale.

$L_V = \frac{L}{\pi R^2 \rho V^2}$ against n (revolutions per second).

4 Bladed model at blade angles θ and incidence i (uncorrected) as shown on curves.

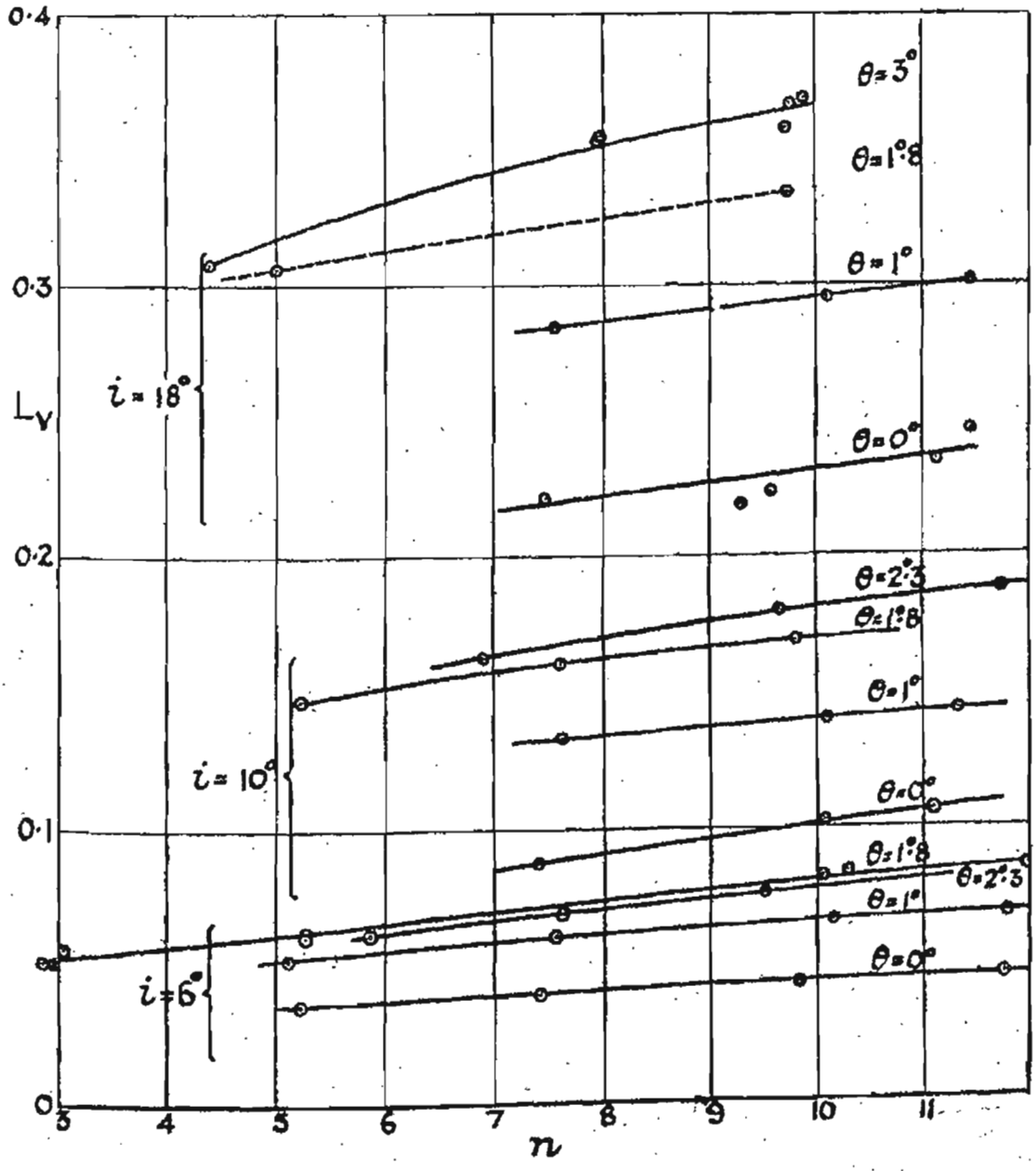

Malby & Sons Photo-Litho

R&M.1154.

Force Measurements on 6 foot Model Autogyro.

Comparison between 4 Blader and 2 Blader: FIG. 11.

$\frac{D_o}{L}$, $\frac{\sigma_4}{\sigma} L_V$, $\frac{\sigma_4}{\sigma} L_\Omega$, plotted against i_o; all reduced to zero solidity.

Blade angle 1°.8 at 10 revolutions per second.

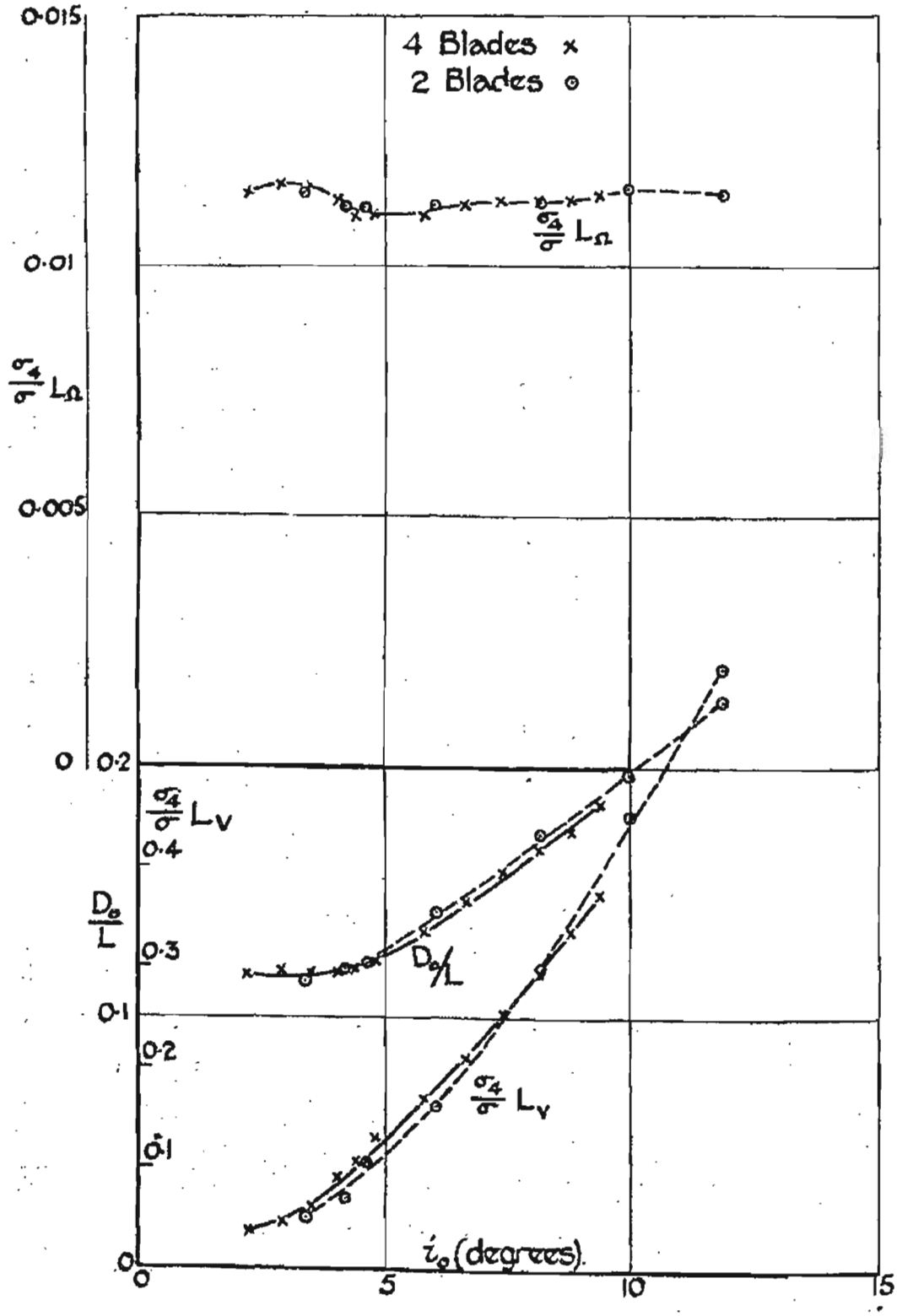

R.&M.1154.

6 Foot Model Autogyro at Varying Rotational Speed. FIG. 12.

Rotational speed plotted against time.

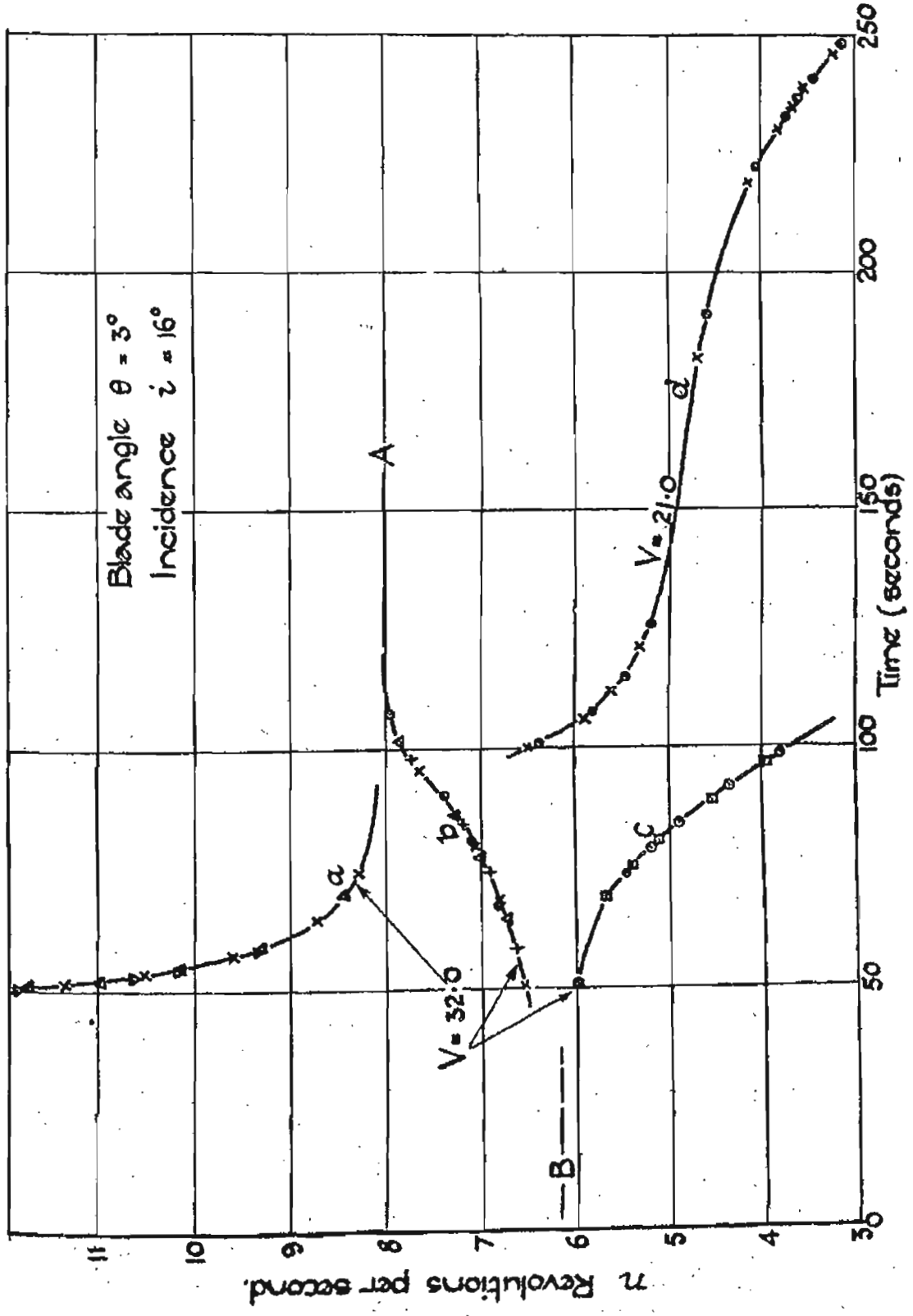

R.&M.1154.

6 Foot Model Autogyro at Varying Rotational Speed.

Torque coefficient Q_Ω against μ.

Incidence $i = 16°$

FIG. 13.

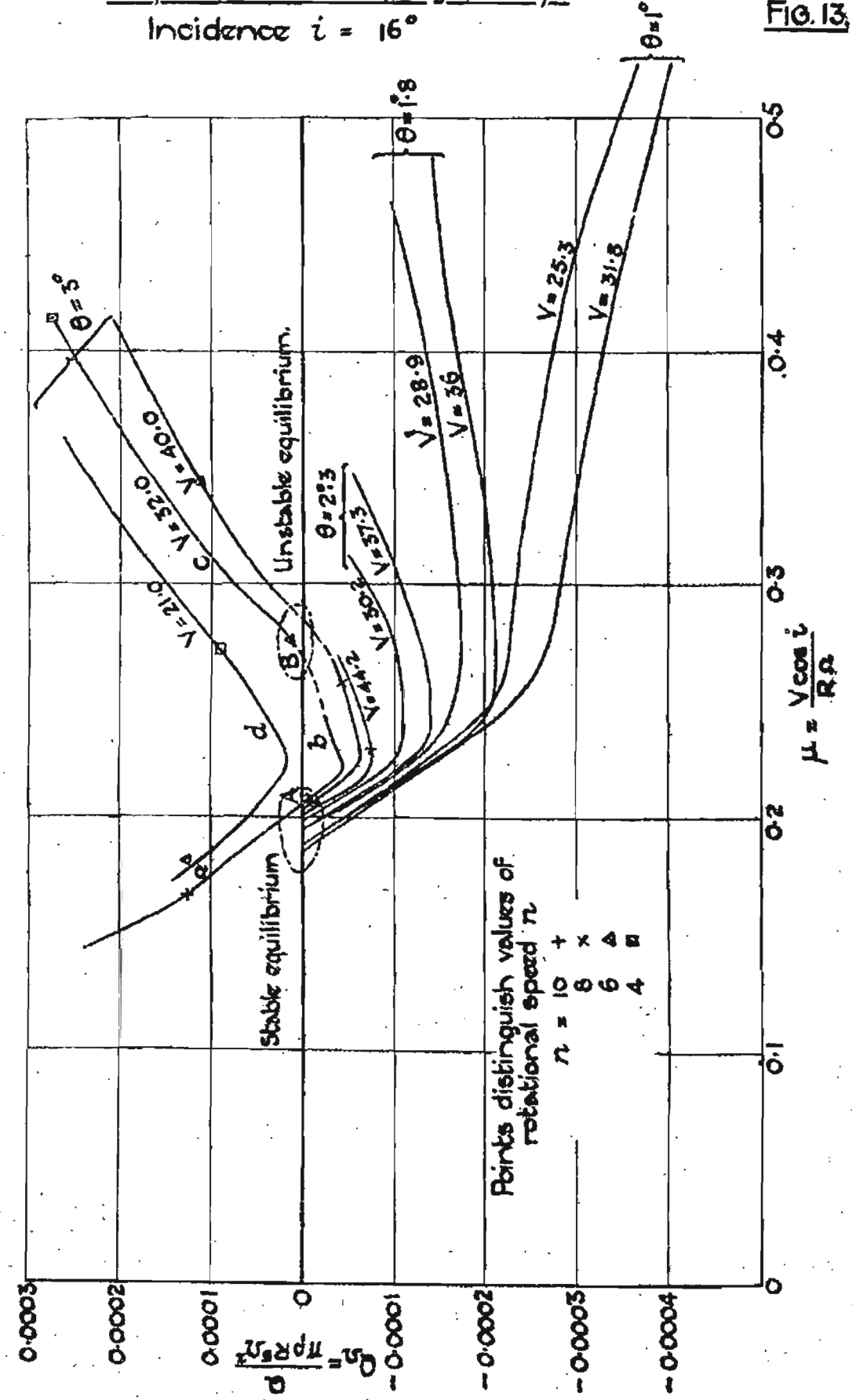

R.&M.1154.

6 Foot Model Autogyro at Varying Rotational Speed.

Torque coefficient Q_Ω against μ.

FIG.14

Incidence $i = 10°$

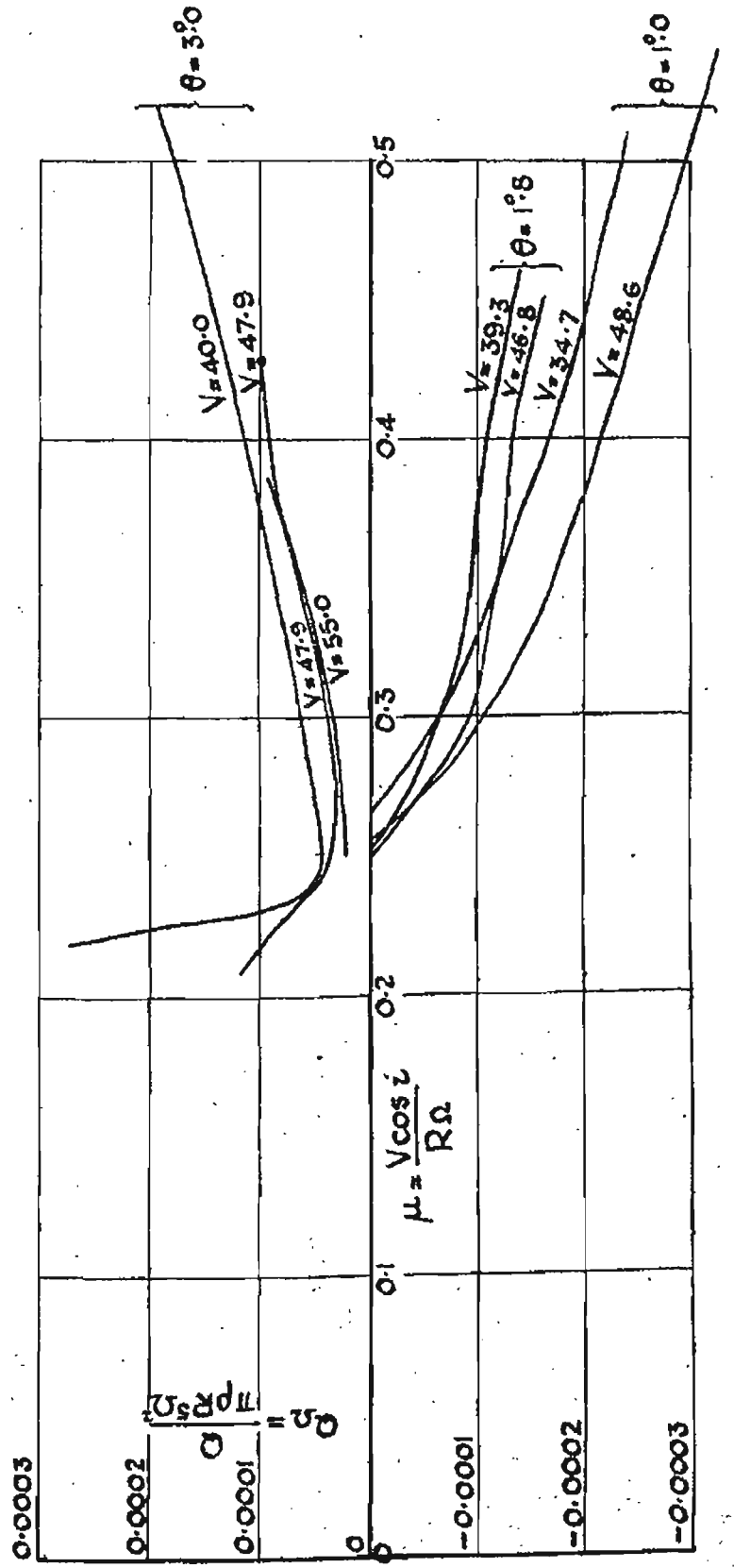

Mal by & Sons, Photo Litho

R&M 1154.

6 Foot Model Autogyro at Varying Rotational Speed.
Torque Coefficient Q_Ω against μ.

FIG. 15

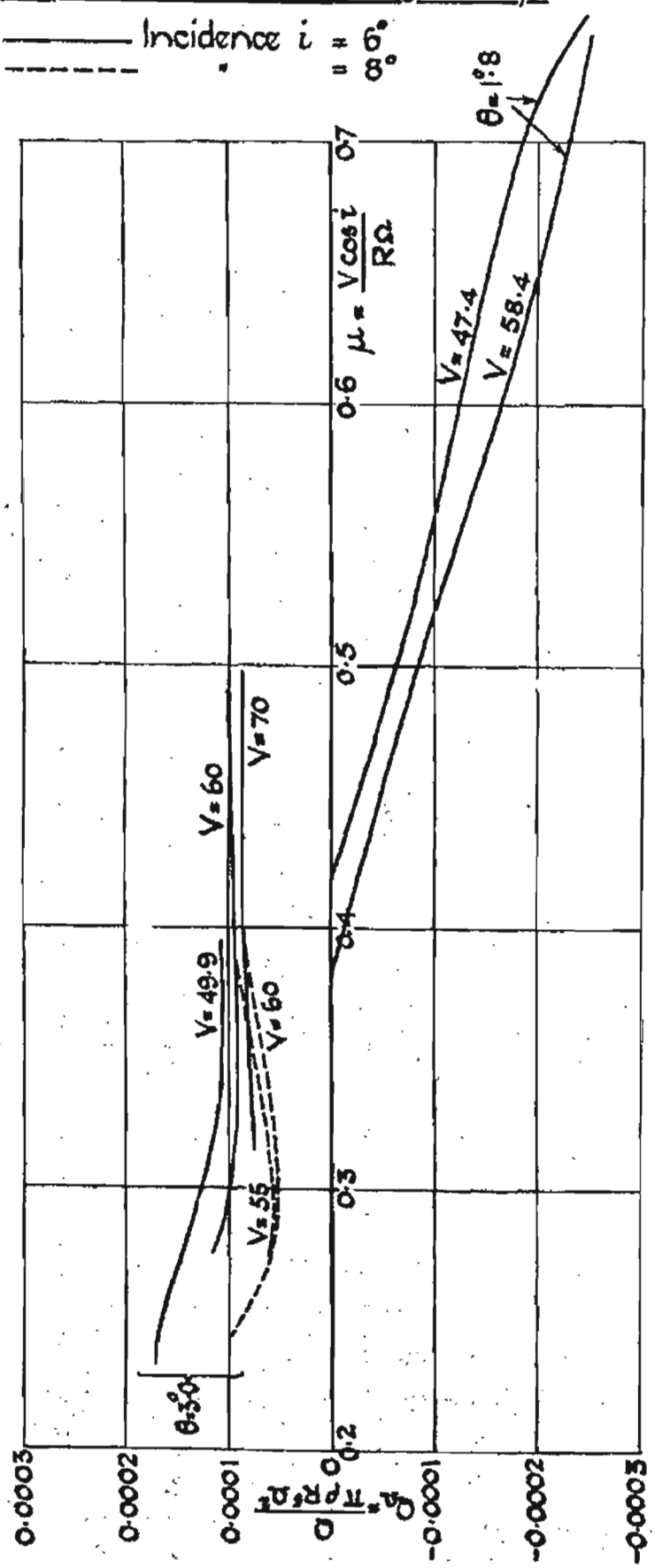

R.&M.1154.

6 Foot Model Autogyro at Varying Rotational Speed.

FIG.16

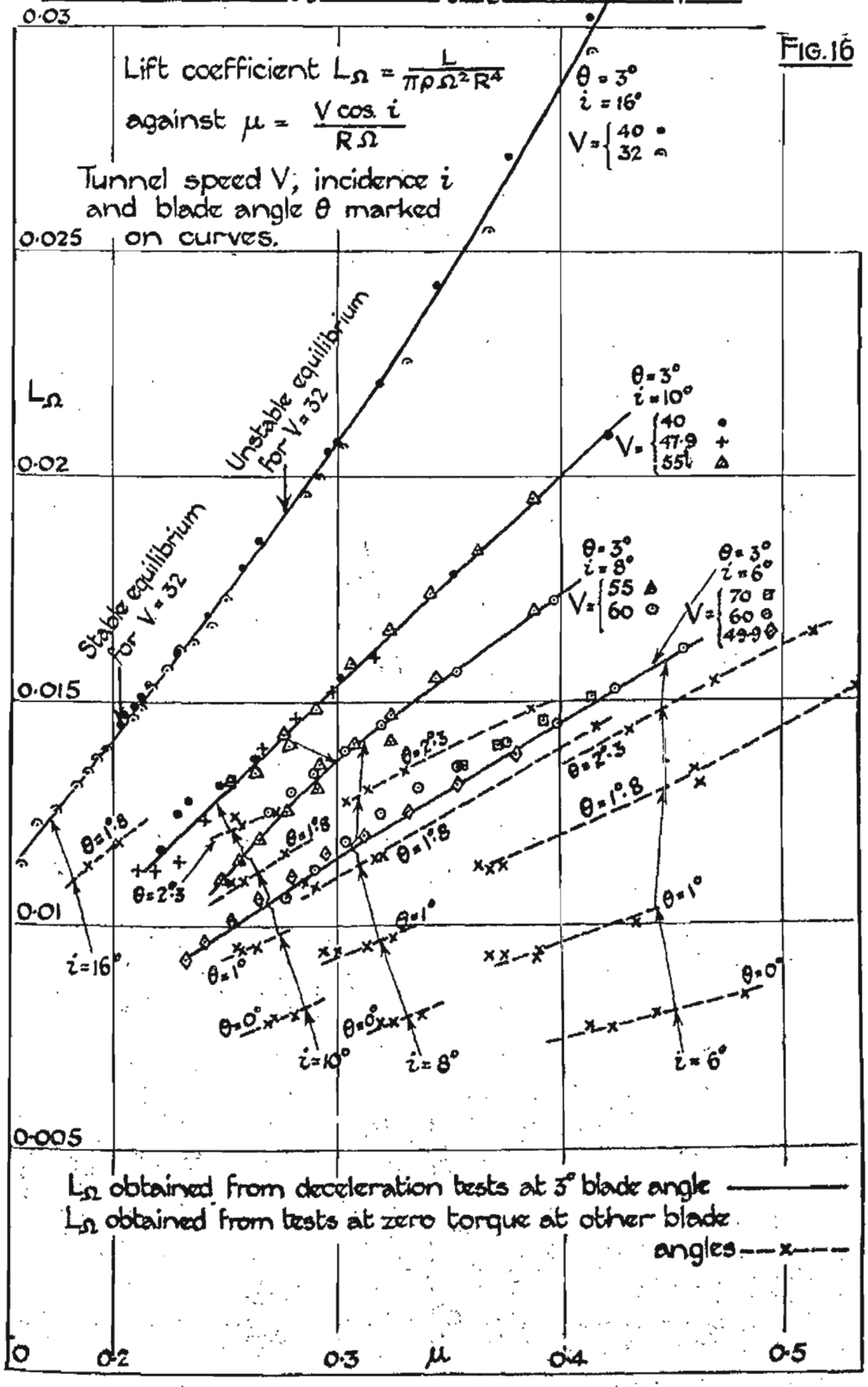

Malby&Sons Photo-Lith

R.&M.1154.

6 Foot Model Autogyro at Varying Rotational Speed.

$\left(\frac{D}{L}\right)' = \frac{D}{L} + \frac{Q\Omega}{\mu L \Omega}$ against $\mu = \frac{V \cos i}{R\Omega}$ FIG.17.

Tunnel speed V, incidence i, and blade angle θ marked on curves.

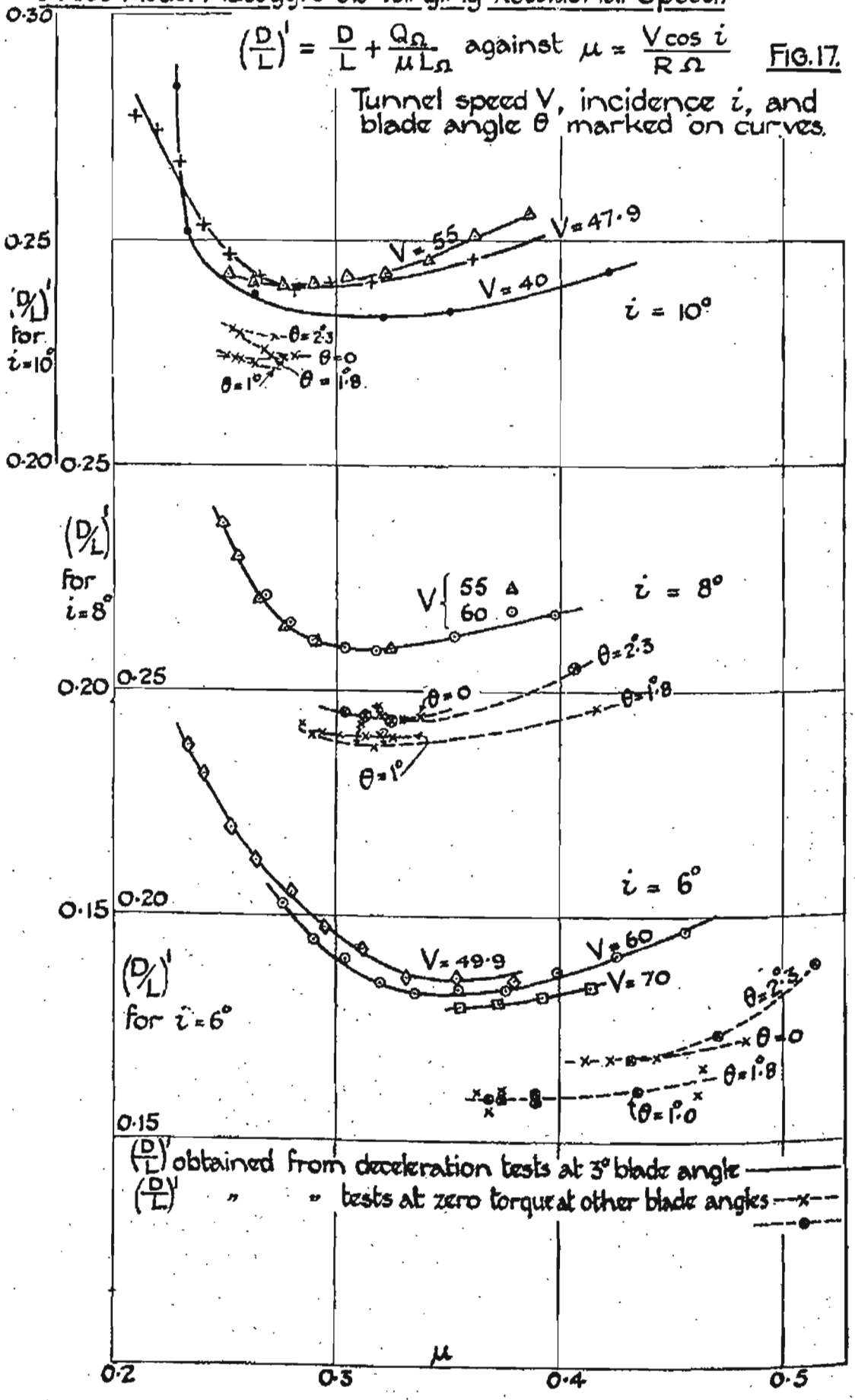

$\left(\frac{D}{L}\right)'$ obtained from deceleration tests at 3° blade angle ——

$\left(\frac{D}{L}\right)'$ " " tests at zero torque at other blade angles —x— —●—

R.814.

R.&M.1154.

FIG. 18.

6 foot Model Autogyro.

Measurement of Flapping Motion.

Specimen diagram of path of spot of light.

Blade angle θ 1°·8
Angle of incidence i (uncorrected) 14°
Rotational speed 4·23 revs. per sec.

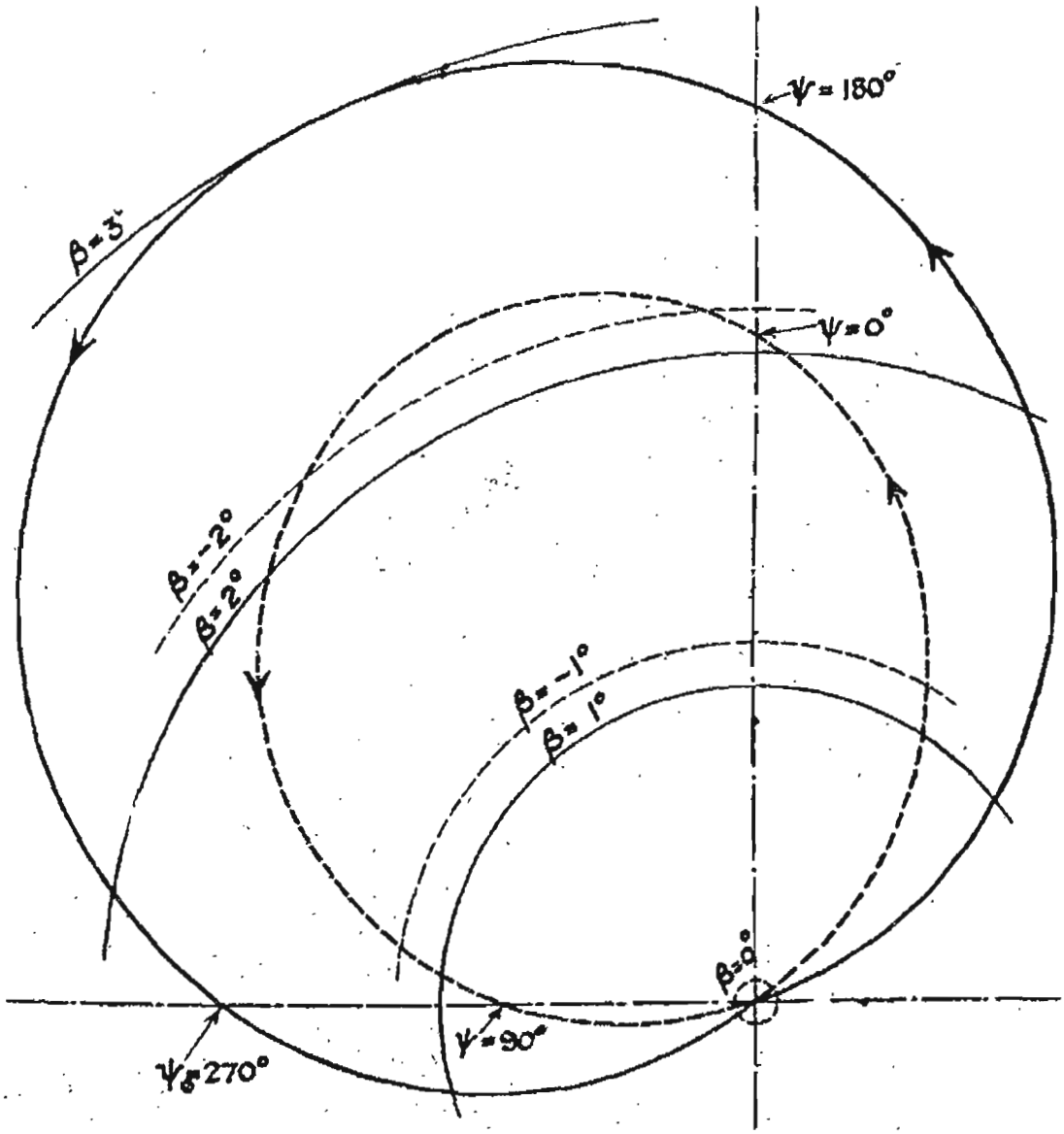

Malby & Sons Photo-lit

R.&M.1154. 6 Foot Model Autogyro.

Measurement of Flapping Motion. FIG. 19.

Specimen Curves of Flapping Angle β against Azimuth Angle ψ

Blade Angle $\theta = 1°8$

———— Observed

– – – – – – – $\beta = a_0 - a_1 \cos\psi - b_1 \sin\psi$

Incidence i (uncorrected) and rotational speed n marked on curves.

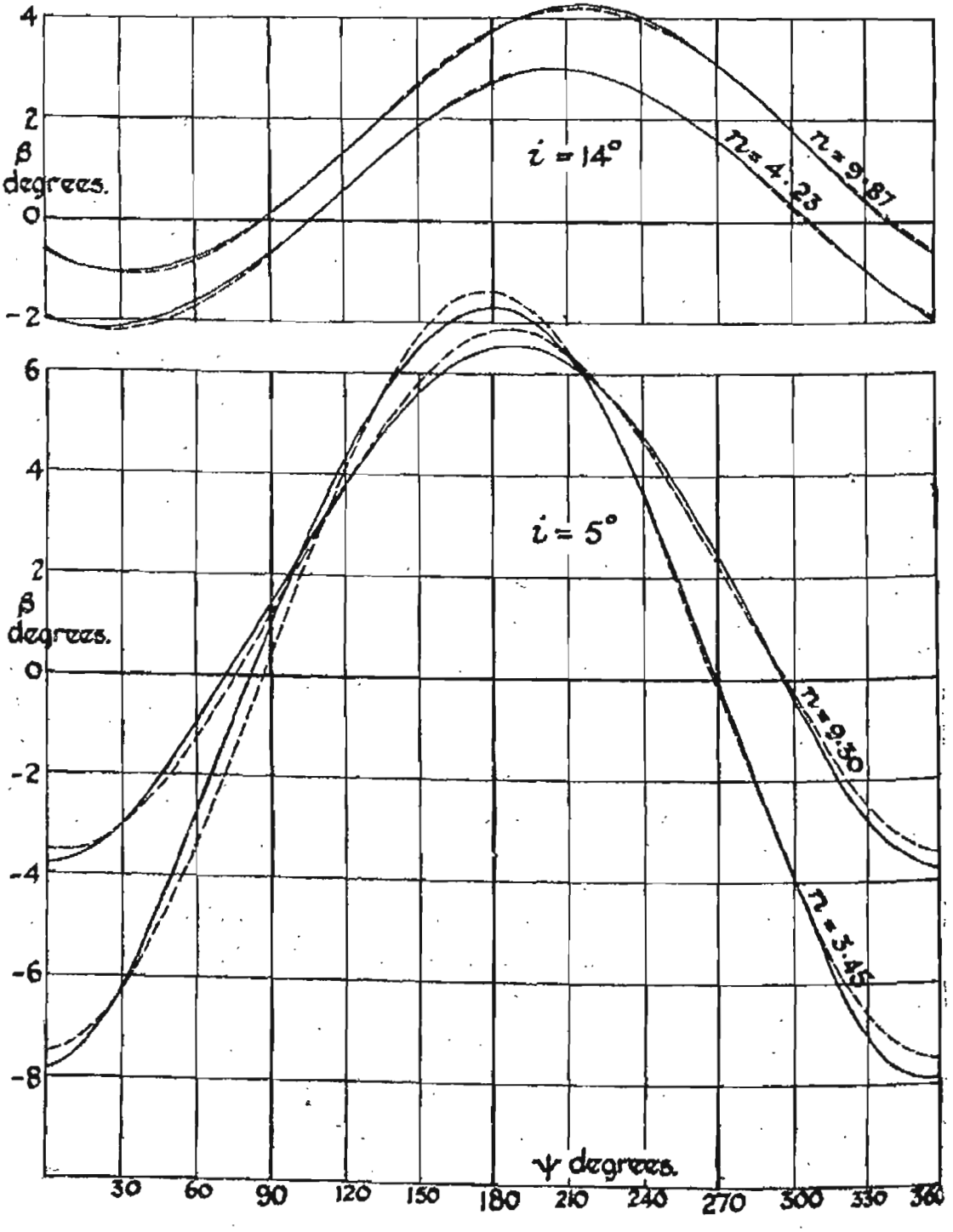

A1914

Malby&Sons. Photo-Lith

R.&M.1154.

6 Foot Model Autogyro.

Measurement of Flapping Motion.

FIG. 20.

Coefficient a_0 in the Fourier Expansion $\beta = a_0 - a_1 \cos\psi - b_1 \sin\psi$
plotted against $1/n^2$
Blade angles θ as marked.
Slope of straight lines calculated.

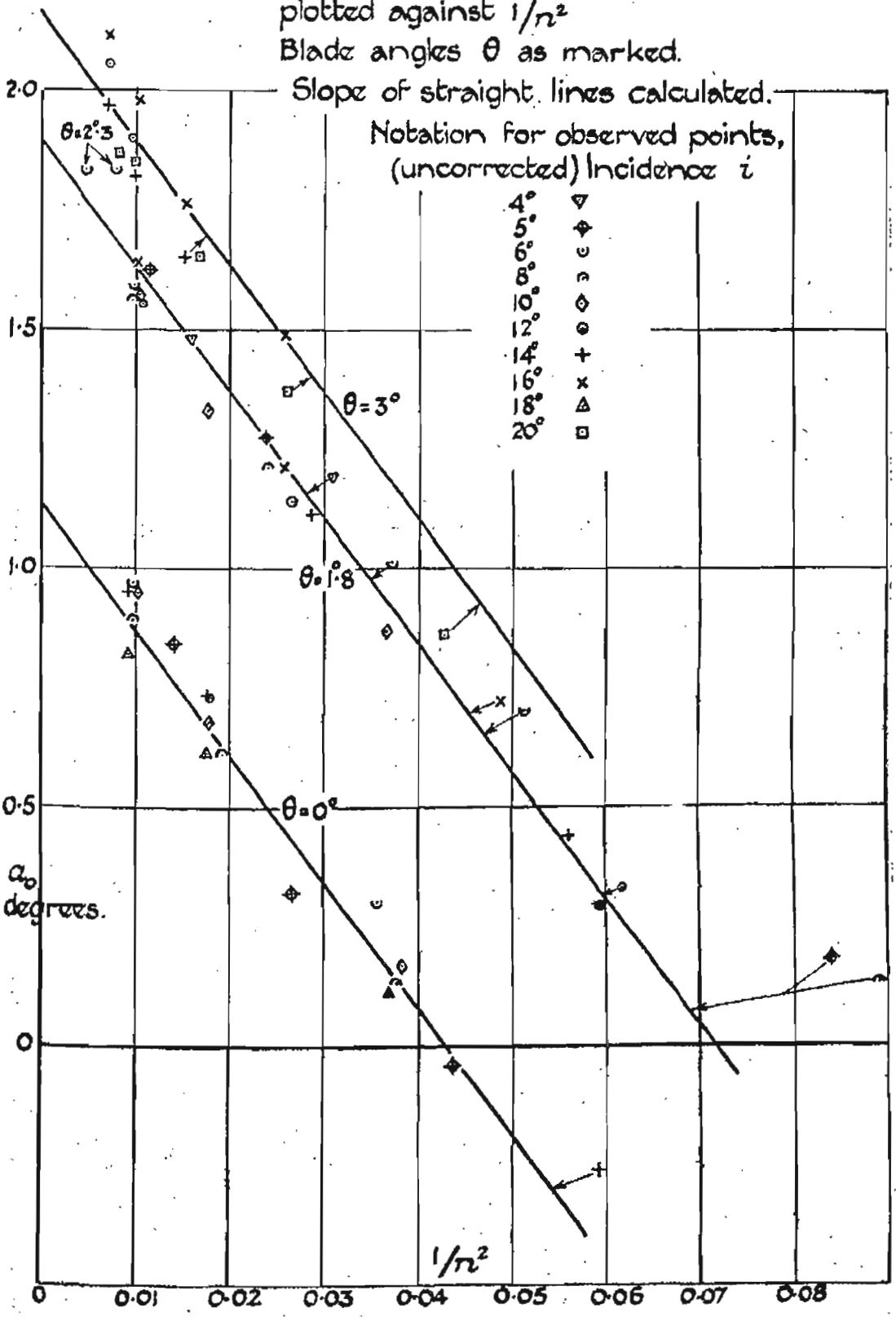

P1914A

Malby&Sons Photo-l

R.&M.1154. 6 foot Model Autogyro.

Measurement of Flapping Motion.

FIG. 21.

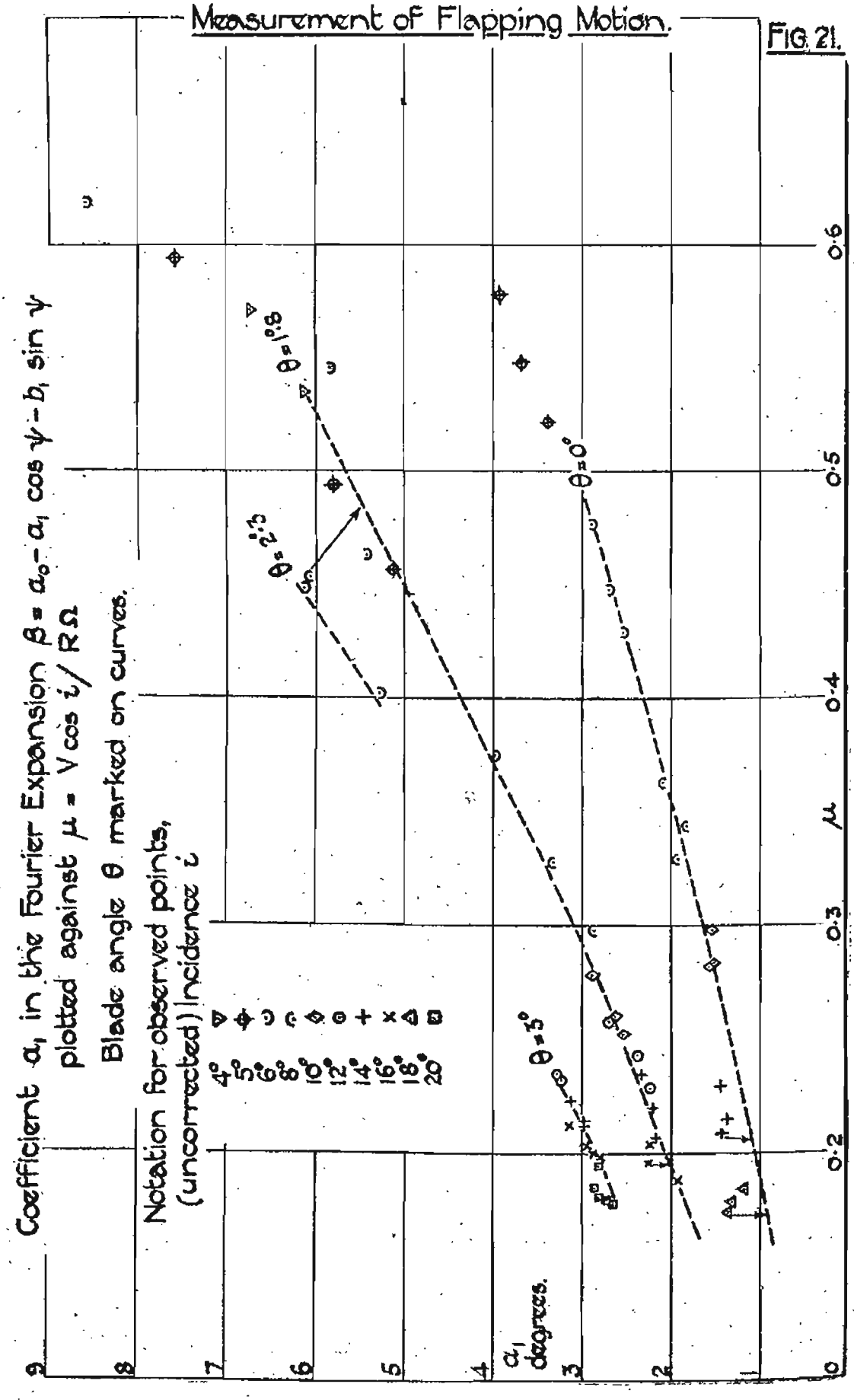

R1914

R.&M.1154.

6 foot Model Autogyro.
Measurement of Flapping Motion and Lateral Force.

Coefficient b_1 in the Fourier expansion $\beta = a_0 - a_1 \cos\psi - b_1 \sin\psi$.
and lateral force Y.

(a) $\left\{ \frac{b_1}{Y/L} \right.$ ——— and ———
expressed in degrees against a_0 for $\theta = 1°8'$,
incidence i (uncorrected) as marked on curves.

(b) slope of b_1 against a_0 } plotted against μ.
(c) slope of Y/L against a_0 }

(d) b_1 and Y/L (corrected to zero a_0) plotted against μL_V

FIG. 22.

Malby & Sons Photo-Litho

R.&M.1154.

Performance of Autogyros having different diameters of rotor.

FIG. 23.

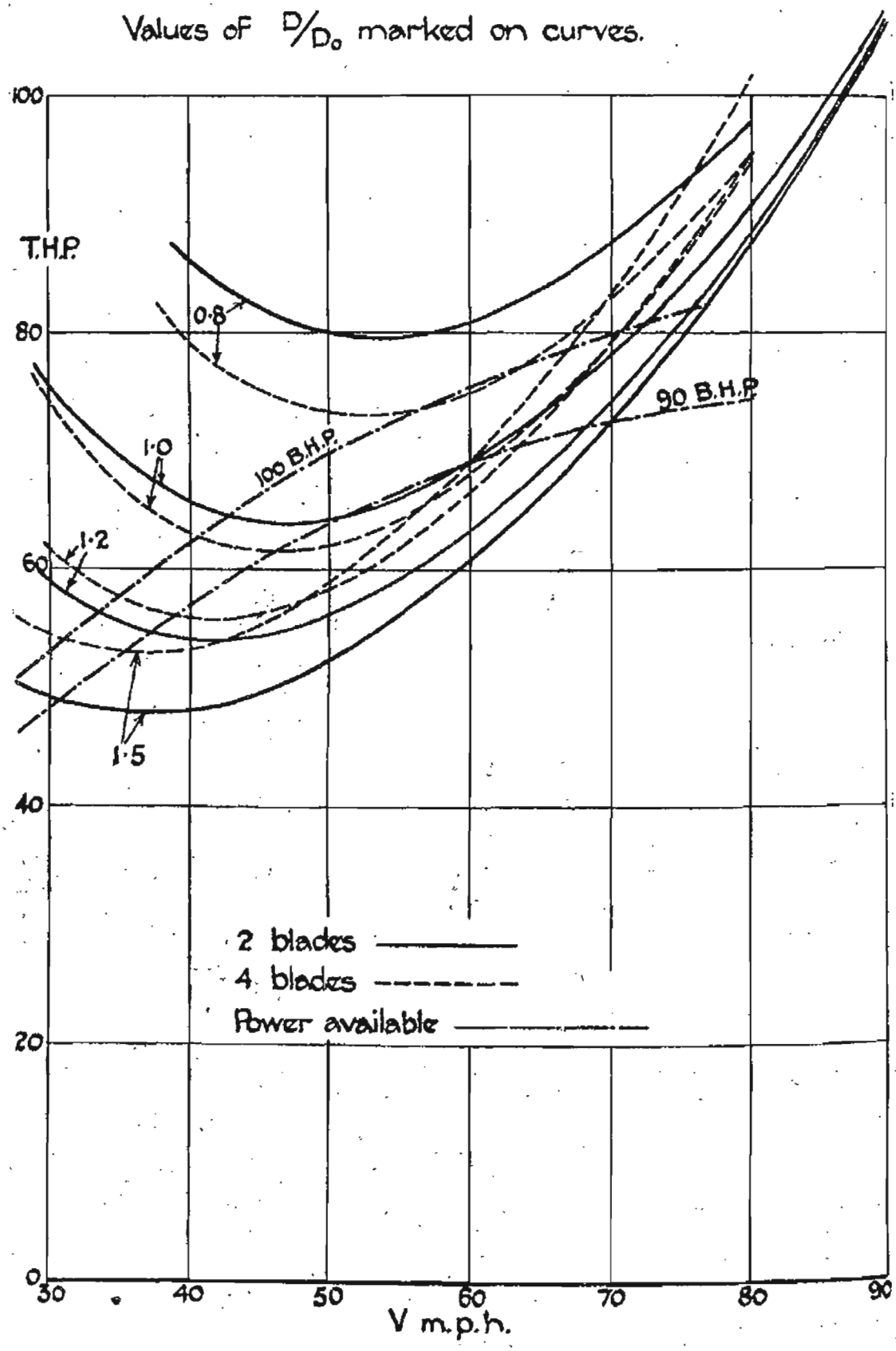

Malby & Sons, Photo-Li